UNIVERSIDADE FEDERAL DO CEARÁ
CENTRO DE CIÊNCIAS
DEPARTAMENTO DE QUÍMICA ANALÍTICA E FÍSICO-QUÍMICA
PROGRAMA DE PÓS-GRADUAÇÃO EM QUÍMICA

JOSÉ ROBERVAL CANDIDO JÚNIOR

PHENOLIC COMPOUNDS: A THEORETIC-COMPUTATION STUDY OF ANTIOXIDANT CAPACITY OF CARDANOL AND EUGENOL

FORTALEZA
2022

JOSÉ ROBERVAL CANDIDO JÚNIOR

PHENOLIC COMPOUNDS: A THEORETIC-COMPUTATION STUDY OF ANTIOXIDANT CAPACITY OF CARDANOL AND EUGENOL

Tese apresentada ao Programa de Pós-Graduação em Química da Universidade Federal do Ceará, como requisito parcial à obtenção do título de doutor em Química. Área de concentração: Físico-Química.

Orientador: Prof. Dr. Pedro de Lima Neto.

FORTALEZA

2022

Dados Internacionais de Catalogação na Publicação
Universidade Federal do Ceará
Sistema de Bibliotecas
Gerada automaticamente pelo módulo Catalog, mediante os dados fornecidos pelo(a) autor(a)

C223p Candido Júnior, José Roberval.
Phenolic compounds : a theoretic-computation study of antioxidant capacity of cardanol and eugenol / José Roberval Candido Júnior. – 2022.
102 f. : il. color.

Tese (doutorado) – Universidade Federal do Ceará, Centro de Ciências, Programa de Pós-Graduação em Química, Fortaleza, 2022.
Orientação: Prof. Dr. Pedro de Lima Neto.

1. antioxidante. 2. cardanol e cardanol. 3. DFT. 4. quantum chemical descriptors. 5. mechanism. I. Título.

CDD 540

JOSÉ ROBERVAL CANDIDO JÚNIOR

PHENOLIC COMPOUNDS: A THEORETIC-COMPUTATION STUDY OF ANTIOXIDANT CAPACITY OF CARDANOL AND EUGENOL

Tese apresentada ao Programa de Pós-Graduação em Química da Universidade Federal do Ceará, como requisito parcial à obtenção do título de Doutor em Química. Área de concentração: Físico-Química.

Aprovada em: 15/07/2022.

BANCA EXAMINADORA

_____

Prof. Dr. Pedro de Lima Neto (Orientador)
Universidade Federal do Ceará (UFC)

_____

Prof. Dr. Norberto de Kassio Vieira Monteiro
Universidade Federal do Ceará (UFC)

_____

Prof. Dr. Emmanuel Silva Marinho
Universidade Estadual do Ceará (UECE)

_____

Prof. Dra. Paula Homem de Mello
Universidade Federal do ABC (UFABC)

_____

Prof. Dr. Jair Mafezoli
Universidade Federal do Ceará (UFC)

To God.

... to my parents, my brother Luiz and my wife Adelaide for all support.

ACKNOWLEDGMENT

To CNPQ for the financial support at the beginning of the doctorate.

To CENAPAD for the structure provided to perform the calculations.

To the IFCE Campus Iguatu for granting leave to work on the thesis for a period of 1 year, which allowed for more robust results. A special thanks to my friends Adilson, Hermeson, Aparecida and Renata, for their support.

To the IFCE Campus Quixadá directors Alexandre Praxedes and Marcus Lopes, for being comprehensive and releasing me from some activities for the writing of the thesis and articles.

I would like to express my sincere gratitude to Prof. PhD. Professor Pedro de Lima Neto for his guidance, investment in structure and machines in the Theoretical Chemistry Group (GQT). A special thanks to professors Norberto and Emmanuel for their help with the articles.

I would also like to thank the Prof. PhD., and my brother, Luiz Antônio Soares Romeiro, for the teachings and support that always helped me to better understand the theory of systems beyond calculations.

To the Professors participating in the examining board Professor Doctor Norberto de Kássio Viera Monteiro, Professor Doctor Emmanuel Silva Marinho, Professor Doctor Paula Homem de Mello; Professor Doctor Jair Mafezoli for their time and valuable contributions and suggestions.

To my laboratory colleagues of Theoretical Chemistry Group, especially Leandro and Rufino, I would like to thank both of you for the exchange of knowledge and their support and help throughout this journey.

To my wife Adelaide, for her understanding and companionship, who stayed with our children so that I could complete this stage.

O sucesso nasce do querer, da determinação e persistência em se chegar a um objetivo. Mesmo não atingindo o alvo, quem busca e vence obstáculos, no mínimo fará coisas admiráveis. (José de Alencar)

RESUMO

O estudo e desenvolvimento de antioxidantes tem um importante papel nas áreas tecnológica e da saúde. O óleo mineral naftênico e o biodiesel mudam suas propriedades físicas e química ao longo do tempo devido à ação de espécies reativas de oxigênio (ERO), afetando suas performances. Nosso corpo tende a manter o balanço entre espécies antioxidantes e radicalares. Todavia, quando envelhecemos, a quantidade de radicais se torna maior, levando a uma condição conhecida como estresse oxidativo. Essa condição está associada com trombose, ataque cardíaco, depressão e câncer. Por isso, é importante o estudo de antioxidantes e o desenvolvimento de novos compostos com atividade antiradicalar para aumentar o tempo de armazenamento de óleo mineral naftênico, bem como evitar condições associadas a presença excessiva de radicais no organismo. Neste contexto, neste trabalho foram desenvolvidos dois estudos. No primeiro, foi avaliada computacionalmente a atividade antioxidante dos cardanois saturado, monoeno, dieno e trieno, com o funcional híbrido B3LYP e conjunto de bases 6-31G(d,p). Usando descritores químico quânticos, os mecanismos HAT, SPLET e SET-PT foram avaliados. Os dados obtidos sugerem que o mecanismo de HAT é a principal forma de ação para essas moléculas. A análise dos índices de Fukui confirmou os dados experimentais, mostrando o cardanol monoeno com o melhor perfil antioxidante. A análise da reatividade global mostrou que quanto maior o número de insaturações na cadeia lateral do cardanol, maior a reatividade global. No segundo estudo, foram avaliados os efeitos da acetilação e da nitração no perfil antioxidante do cardanol e seus derivados. Para este estudo, foi utilizado o funcional M06-2X com conjunto de bases 6-31+G(d,p) para simular o mecanismo de HAT com os radicais HO, HOO, CH_3O e DPPH. Os dados termodinâmicos mostraram a dependência da formação de *p*-quinometanos (27, 28 e 29) porá fazerem a reação se tornar espontânea com o DPPH, revelando a necessidade de duas etapas de HAT. Os dados cinéticos mostraram que a preferência pelo sítio doador de hidrogênio depende da instabilidade do radical atacante. Os dados computacionais corroboraram com os dados experimentais, confirmando o perfil antioxidante de (1, 4-alil-2,-metóxifenol), e o nitro derivado 7 (5-alil-3-nitrobenzeno-1,2-diol) no teste de DPPH. Por último, esse estudo mostrou que o nitro composto 6 (4-alil-2-metóxi-6-nitrofenol) apresenta atividade antiradicalar com radicais HO, HOO e CH_3O, mas devido à repulsão dos grupos nitros com o DPPH, a reação se torna lenta e indetectável experimentalmente.

Palavras-chave: antioxidante; cardanol e eugenol; DFT; descritores químico quânticos; mecanismo.

ABSTRACT

The study and development of antioxidants has an important role in technological and health areas. Naphthenic mineral oil and biodiesel modifies its physical and chemical properties due to action of reactive oxygen species (ROS) over time, affecting their performance. Our body tends to maintain a balance between antioxidant and radical species. However, as we age, the number of radicals increases, the balance is broken resulting in a condition known as oxidative stress. This condition is associated with thrombosis, heart attack, depression and cancer. Therefore, it is important the study of antioxidants and the development of new compounds with antiradical activity to increase storage time of naphthenic mineral oil and biodiesel, and avoid conditions associated with excess radicals in the body. In this context, in this work we carried out two studies. In the first, the antioxidant activity of saturated cardanol, monoene, diene and triene was computationally evaluated, with the functional hybrid B3LYP with the base set 6-31G(d,p). Using chemical quantum descriptors, the HAT, SPLET and SET-PT mechanisms were evaluated. The data obtained suggest that the HAT mechanism is the main form of action of these molecules. The analysis of the Fukui index confirms the experimental data of the best antioxidant profile of cardanol monoene. The global reactivity analysis shows that the greater the number of unsaturations in the cardanol side chain, the greater its overall reactivity. In the second study, the effect of acetylation and nitration on the antioxidant potential of eugenol and its results were evaluated. For this study, the hybrid functional M06-2X with a set of bases 6-31+G(d,p) was used to simulate the mechanism of HAT with the HO, HOO, CH_3O, DPPH radicals. The thermodynamic data showed a dependence of the formation of *p*-quinomethanes (27, 28 and 29) to make the reaction spontaneous with DPPH, revealing the need for two steps of HAT. The kinetic data that showed the preferred site for hydrogen transfer depends on the instability of the attacking radical. The computational data corroborated the experimental data, confirming the antioxidant profile of (1, 4-allyl-2-methoxyphenol), and nitro-derivative 7 (5-allyl-3-nitrobenzene-1,2-diol) in the DPPH assay. Finally, this study showed that the nitro compound 6 (4-allyl-2-methoxy-6-nitrophenol) has antiradical activity with HO, HOO and CH_3O radicals, but the repulsion between the nitro groups with DPPH makes it difficult to approach the DPPH molecule making the reaction be slow and undetectable experimentally.

Keywords: antioxidant; cardanol and eugenol; DFT; quantum chemical descriptors;· mechanism

SUMMARY

1 INTRODUCTION

1.1 Oxidation and Radicals

Oxidation is a fundamental part of aerobic life and our metabolism, and in this process, it can produce oxidizing agents such as radicals naturally, or due to some biological dysfunction or external factors. Chemically, radicals are defined as species that have one or more unpaired electrons and are associated with processes of energy production, phagocytosis, regulation of cell growth, intercellular signaling and synthesis of substances of biological importance [1].

When this unpaired electron is located on atoms with high electronegativity values, such as oxygen and nitrogen, it ends up making these species highly reactive and, therefore, called Reactive Oxygen Species (ROS) and Reactive Nitrogen Species (RNS). Among the ROS, the hydroxyl radical ($HO^{\bullet}$) is the most reactive, with a standard reduction potential of 2.31 V [2].

The production of $HO^{\bullet}$ can occurs through three basic processes: decomposition of hydrogen peroxide catalyzed by transition metals such as Cu^{+} and Fe^{2+}, heterolytic water cleavage into hydrogen ($H^{\bullet}$) and hydroxyl radicals or by the decomposition of hydrogen peroxide by ultraviolet radiation [3].

1.2. Antioxidants

Antioxidants are substances that, even at low concentrations in relation to the substrate, can to inhibit its oxidation. [3] Antioxidants are subdivided into two classes: endogenous and exogenous. The endogenous are those produced by the organism itself, in general, they are enzymes such as Se-glutathione Peroxidase (GPx), Catalase (CAT), and Superoxide Dismutase (SOD^{2}). [1]

Exogenous antioxidants are those acquired through food, such as ascorbic acid (Vitamin C), α-tocopherol, carotenes and phenolic compounds. [1]. Phenolic compounds can act as hydrogen donor, thus forming a phenoxyl radical, which is stabilized by mesomeric effect by conjugation of unpaired electron with aromatic ring.

1.3 Oxidative Stress

The human body maintains a balance between the concentrations of antioxidants and oxidation initiators, such radicals. Over time, there is a natural tendency to have an imbalance between these concentrations, where there is a predominance of antioxidant species. This condition is called *oxidative stress*. This phenomenon is believed to play a significant role in the natural aging process and in the emergence of some pathological conditions such as atherosclerosis and rheumatism. [4]

1.4 Reactivity of Radicals

Radicals can react in four different ways. [2] In a first reaction, two radicals can unite to form a single molecule. For example, two hydroxyl radicals can join together to form hydrogen peroxide (Eq. 1):

$$2\,HO^{\bullet} \rightleftharpoons H_2O_2 \quad (1)$$

A second possibility is that the free radical $R^{\bullet}$ acts as a reducing agent. In this case, it transfers its unpaired electron to a molecule M, converting itself into a cation R^{+}, while it converts the molecule into a radical anion $M^{\bullet -}$ (Eq. 2)

$$R^{\bullet} + M \rightleftharpoons R^{+} + M^{\bullet -} \quad (2)$$

The third reaction path, like the second, also consists of an electron transfer process. The difference is that the radical $R^{\bullet}$ withdraw a single electron, by converting to an anion R^{-}, while the substrate M where it acts converts into a radical cation $M^{\bullet +}$ (Eq. 3):

$$R^{\bullet} + M \rightleftharpoons R- + M^{\bullet +} \quad (3)$$

The fourth possibility is for the free radical $R^{\bullet}$ to abstract a hydrogen radical from an H–M molecule, producing a new H–R molecule and a new radical $M^{\bullet}$ (Eq. 4):

$$R^{\bullet} + H-M \rightleftharpoons H-R + M^{\bullet} \quad (4)$$

In all possibilities, the drive force that will make the reaction spontaneous is the formation of a more stable radical. There are three factors that stabilize a radical: scavenging inductive effect (+I), scavenging mesomeric effect (–M), and hyperconjugation.

These three effects can act by spreading the charge density over the unpaired electron or through the interaction of the higher energy singly occuped molecular orbital (SOMO) with non occupped orbitals. In both cases the energy of SOMO decreases, making the radical less reactive. [5]

It is through these reactional principles that the effectiveness of antioxidants is

tested. There are several tests for determining antioxidant activity, such as the DPPH and ABTS test. In this work, we will focus on the DPPH test.

1.5 Antioxidant Mechanisms

Antioxidants could react in three different forms: electron transfer, hydrogen atom transfer (HAT), and act as acting as a chelating agent for pro-oxidizing metal ions. In this work, we will address mechanisms involving hydrogen transfer.

Hydrogen transfer can occur in three ways. The first way is direct, also called Hydrogen Atomic Transfer (HAT) [6-7], where the radical ($R^{\bullet}$) withdraws an electron from the antioxidant AOH, generating a less reactive radical ($AO^{\bullet}$), as described in Equation 4. This form is more common in nonpolar solvents since it does not form ionic species. (Eq. 5).

$$AOH + R^{\bullet} \rightarrow AO^{\bullet} + RH \qquad (5)$$

The second way is called Sequential Proton Less Electron Transfer (SPLET) [6-7]. This pathway involves two steps. In the first step, the antioxidant molecule ionizes releasing H^+ to the medium and forming an anion (AO^-), (Eq. 6). In the second step occurs the electron transfer from AO^- to radical $R^{\bullet}$, in presence of H+, producing RH molecule, Eq (7):

$$AOH \rightarrow AO^- + H^+ \qquad (6)$$

$$AO^- + H^+ + R^{\bullet} \rightarrow AO^{\bullet} + R-H \qquad (7)$$

The third way is called Single Electron Transfer followed by Proton Transfer (SET-PT) [6-7]. This pathway alson involves two steps. Unlike SPLET, the first step of SET-PT mechanism is the electron transference from antioxidant to radical. This process produces an anion (R^-) and a radical cation ($AOH^{\bullet+}$), (Eq. 8). In the second step, $AOH^{\bullet+}$ releases a proton (H^+), producing a more stable radical ($AO^{\bullet}$), (Eq. 9).

$$AOH + R^{\bullet} \rightarrow AOH^{\bullet+} + R^- \qquad (8)$$

$$AOH^{\bullet+} \rightarrow AO^{\bullet} + H^+ \qquad (9)$$

Due to involve the formation of charged species, both SPLET and SET-PT are more likely to occur in protic solvents.

1.6 The DPPH Assay

The 1,1-diphenyl-2-picrylhydrazyl (DPPH) assay can determine the antioxidant potential of a substance. Among the substances analyzed by this test, there are phenolic compounds isolated or present in foods and other biological samples. This test is based on the

ability of the stable free radical, 1,1-diphenyl-2-picrylhydrazyl, to react with H-donor compounds, which can interrupt the oxidative chain reactions [8].

Figure 1 presents the two-dimensional structure of the DPPH radical. The DPPH radical is stabilized by mesomeric effect between SOMO and π* orbitals of aromatic rings and nitro groups. During the reaction of DPPH with an antioxidant, the process of scavenging hydrogen radical takes place. The conjugation of the unpaired electron with the 2,4,6-trinitrophenyl group on the DPPH radical causes strong absorption of radiation at 517 nm.

Figure 1 – Structure of DPPH radical.

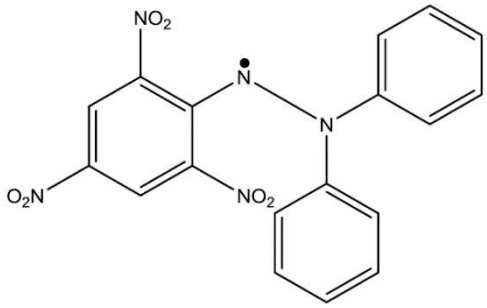

Source: by authors (2022)

The reaction of DPPH with an antioxidant can occurs by two different ways: single electron transfer (SET) or hydrogen atomic transfer (HAT). In both cases, there is a shift in the absorption band, decreasing absorption at 517 nm, which indicates the presence of antioxidant activity for a given substance [9].

The mechanism of action that will occur between DPPH and the antioxidant depends on factors such as solvent polarity, pH and temperature. Protic solvents tend to hinder HAT and facilitate SET. Values of pH greater than 10 make the compounds mostly deprotonated, facilitating electron transfer, while pH intervals lower than 10 favor hydrogen transfer [9].

DPPH• can react with some phenolic compounds as well as aromatic acids. The stability of the DPPH radical is attributed to conjugation effects with the aromatic ring and nitro groups, in addition to inductive effects that help to spread the unpaired electron from nitrogen to entire molecule, which contribute to the spin density distribution [8].

1.7 Cashew Nut Liquid Antioxidant

Antioxidantes from biomass are generally secondary products of industrial processes and therefore have low commercial value. Among these, there is cashew nut liquid (CNL). The

CNL represents about 25% of the nut weight [10] and has the following chemical composition: anacardic acid (1.09 to 1.75%), cardanol (67.82 to 94.60%), cardol (3.80 to 18.86%) and 2-methylcardol (3.05 to 4.00%) [11].

Among these, the carboxylic group of anacardic acid does not make it an interesting compound, since its acidity could accelerate the oxidation process instead of slowing it down. Due to the better reducing profile and the higher percentage by weight, the use of cardanols as an antioxidant becomes interesting.

Figure 2 shows the basic structure of cardanol. The structure is composed of a phenol *meta*-substituted by a chain of 15 carbon atoms [12]. This chain can be saturated (2-A) or present unsaturations, as shown in the structures: monoene (2-B) with one double bonds, diene (2-C) with two double bonds; and triene (2-D) with three double bonds.

Figure 2 – Structure of Cardanols

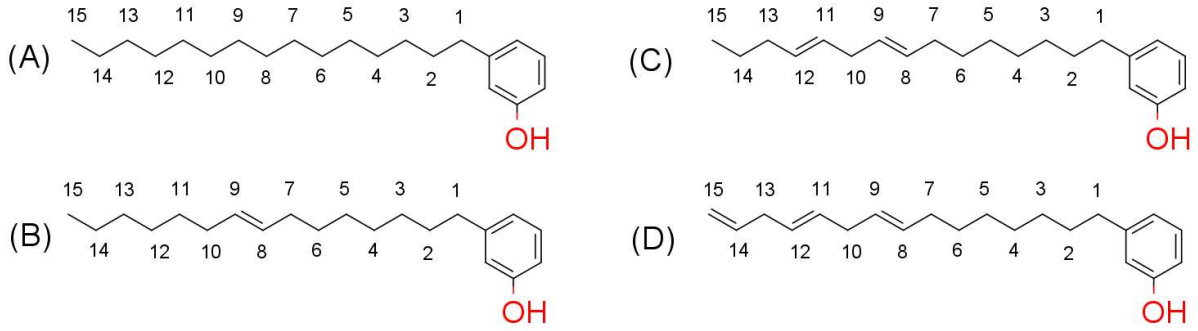

Source: by authors (2022). (A) Saturated, (B) Monoene, (C) Diene and (D) Triene.

The presence of unsaturations can improve antioxidant activity. Abstraction of hydrogen atoms on carbon atoms adjacent to unsaturations leads to the formation of allyl radicals that are stabilized by mesomeric effect. Thus, increasing the number of unsaturations could increases the number of sites able to act as hydrogen donors in hydrogen atomic transfer reactions.

1.8 Application of Cardanol and Derivatives as Additives.

Santos *et al*. (2013) studied the antioxidant activity of commercial additives (ionol and BHT) and additives from biomass (hydrogenated cardanol and alkylated cardanol) in soybean biodiesel [13]. The results of antioxidant activity through the Rancimat test showed tha alkylation improves the antiradical activity of cardanol, however the performance of cardanol and its derivatives is not as good as that of commercial antioxidants.

Database searches showed the existence of two patents on the use of cardanol

derivatives as fuel additives and lubricating oils. The BR 102014032181—0 reports the synthesis of alkylderivatives of saturated cardanol [14] and US2571092 (A) the synthesis of 4-aminocardanol derivatives for this purpose [15].

Due to this, it becomes interesting to better understand the antioxidant sites of this molecule through computational studies to change rationally the structures of cardanols to improve antioxidant activity, attributing added value.

1.9 Eugenol

Eugenol, or 4-allyl-2-methoxyphenol, is a phenolic compound and the major constituent of clove (*Syzygium aromaticum*) essential oil, as well. Eugenol has its structure represented in Figure 3. Like capsaicin, Eugenol is also a vanilloid, presenting a vanillyl group, if differentiating by the presence of an allyl group in the para position to the phenol.

Figure 3 – Structural formula of Eugenol

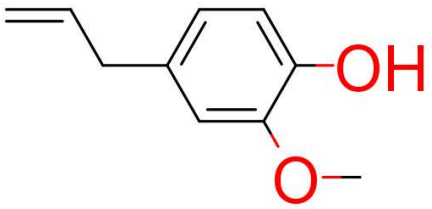

Source: by authors (2022).

Eugenol has analgesic, protective and anesthetic activities. It has very significant antioxidant activity, suppressing LDL and lipid oxidation. It has activity to scavenge reactive oxygen species. It has activity similar to BHA and BHT in the action of scavenging the DPPH$^{\bullet}$ radical and activity superior to quercetin in the scavenging of hydroxyl radicals [16].

Its pharmacological profile involves gastroprotective, antibacterial, antifungal, antiviral, anti-inflammatory, vasodilatory, vasoconstrictor and anticancer activities. Its phenyl, benzyl and phenylethyl derivatives have anticonvulsant activity, with the first two having the highest therapeutic index [17].

Due to the presence of a methylene (-CH_2-), in the *para*-position to phenol group, eugenol can generate a quinone-methide as an oxidation product [17]. Figure 4 shows the oxidation of eugenol to its metabolite *p*-quinomethane via double radical hydrogen abstraction.

Figure 4 – Production of *p*-quinomethane from eugenol oxidation.

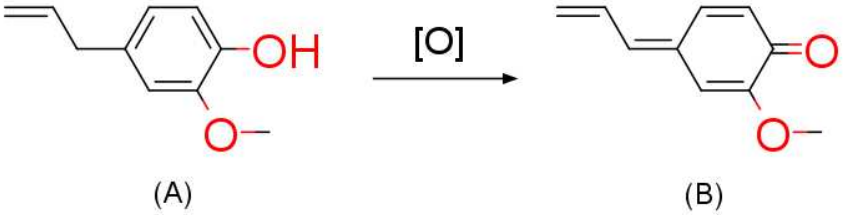

Source: by authors (2022).

The *p*-quinomethanes (*p*QM) are hepatotoxic species and can act as acceptors in the Michael reaction with reduced glutathione (GSH). GSH is a tripeptide formed by the cysteine, glycine and glutamate amino acids. It represents the main natural fat-soluble antioxidant in our body.

The presence of excess of pQM can lead to an excessive consumption of GSH in the liver. After the complete depletion of GSH, *p*QM begins to add to the cysteine residues of proteins, initiating the process of damage to liver tissue. Without the GSH in the tissue, liver cells are exposed to the reactive species, which leads to cell destruction and liver cancer [18].

An example of this process is the intoxication caused by the excessive use of paracetamol, that is converted into N-acetyl-p-benzoquinone imine (NAPBQI), initiating the process of consumption of GSH via addition of Michael [19]. Figure 5 shows the Michael addition between NAPBQI and GSH, as well as the reaction between NAPBQI and the protein.

Figure 5 – *In vivo* metabolismo of paracetamol.

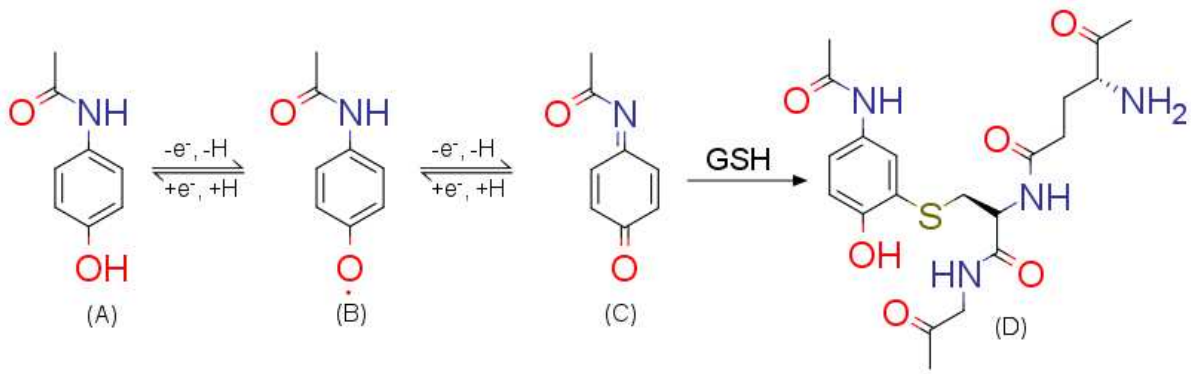

Source: adaptaded from Álvarez-Lueje. (2012).

Paracetamol (8A) can undergoes two consecutive HAT reactions producing N-acetyl-p-benzoquinone imine or NAPBQI (8C) which reacts with the antioxidant GSH via Michael addition forming (8D). For the same reason, pQM produced from Eugenol oxidation,

turns it a hepatotoxic substance [20].

1.10 The Capsaicin-Eugenol Paradox

Capsaicin (CAP) was the subject of a computational study in gas phase to determine the antioxidant site by Kogure *et al*. (2002). This study reveals that the benzyl radical is 3.3 kcal more stable than phenoxyl radical [21].

The structural similarity between CAP and EUG suggests that the benzylic site must be the main atomic hydrogen donor of eugenol, forming a radical stabilized by mesomeric effects with the aromatic ring and the unsaturation of the aliphatic chain.

However, experimental studies by Hidalgo *et al* (2009) showed that Eugenol derivatives without phenol group did not show antiradicalar activity in the DPPH test [22]. This leads to an inconsistency with Kogure's results [21]. This conflict of computational data with experimental data will be called in this work the Eugenol – Capsaicin paradox.

This paradox made us revisit the work of Hidalgo *et al*. (2009) using computational chemistry to identify the main antioxidant sites, obtain structural, thermodynamic, and kinetic data that could elucidate this paradox.

1.11 The Use of Computational Chemistry

Computational chemistry is an important tool for the clarification of chemical phenomena. With the evolution of programs and computers, computer simulations are becoming more and more realistic, predicting experimental results with greater precision [23].

From an economic point of view, computational chemistry simulations have the potential to reduce the expense of reagents, being able to work as a screening of syntheses before going to the bench. However, computational chemistry is not stilself-sufficient, needing to be associated with experimental data.

Simulations can be used in three different ways:

a) ***Post facto.*** In this case, the simulation would be done after experimental assay, to clarify some ambiguity in the experimental results.

b) **Optimization of design and progress of an experimental program.** The simulation can, for example, simulate spectra in the infrared, uv-visible, nuclear magnetic resonance region to predict which experimental technique is better to identify a mixture of some substances.

c) **Prediction of properties that are difficult to be obtained experimentally.** The simulation allows predicting properties in reactions that are too fast to identify thermodynamic data or intermediaries of reaction, or when the experiment is too dangerous to be performed.

Reactions involving radicals uses to fall into the third type. In general, these are reactions with high values of rate constant, which makes it difficult to assign a mechanism, as well as the identification of intermediates, due to the chemical species presentes in the system being unstable.

1.12 DFT – Simulating Chemical Systems

Density Functional Theory (DFT) is a useful tool that uses quantum mechanics to simulate chemical systems. The advantage of working with electron density is that while wave functions become increasingly complex as the number of electrons in the system increases, the use of density functions always maintains three variables regardless of the size of the system [24].

One of the biggest problems of DFT is inaccuracy of exchange probability and correlation separately. This imprecision can lead to unrealistic results for some study systems. Therefore, it is interesting to look for a functional one that better the working system.

Functionals are methods of calculation used to transform functions into numbers and can be considered as "the function of a function". For the DFT, the electron densities of the atoms are the functions and the functionals are the calculation methods applied on the electronic densities, which will obtain the properties of interest, such electronic, thermodynamic, and kinetic properties.

For several years and until today, B3LYP [25] , a hybrid functional that uses the Becke exchange functional and the Lee-Yang-Parr correlation functional, is one of the most used. Despite that, in the last decades new functionals were created such as the Minnesota functionals (M05, M05-2X, M06, M06-2X) [26] and the inclusion of functionals with correction for dispersion forces that was a limitation for the DFT.

1.13 Applying DFT in Antioxidant Systems

In this work, the antioxidant activity of the studied structures was evaluated using DFT. However, the approach used in each chapter is different.

In the first chapter, the analysis of quantum chemical descriptors was used. This method is usually faster. Basically, the structure of antioxidants has its structures optimized and then, from a simple point, electronic data are obtained that will be used to obtain the descriptors.

Reactivity can be associated with the energy levels of their frontier orbitals. The energy of Highest-energy Occupied Molecular Orbital (E_{HOMO}) can be associated with the facility of a molecule to donate electrons. Thus, the higher the E_{HOMO}, the easier for an antioxidant to undergoes the SET-PT mechanism.

The energy of Lowest-energy Unoccupied Molecular Orbital (E_{LUMO}) is the orbitals with lowest energy that can receive electrons. For example, along the HAT mechanism, the SOMO of the free radical must overlap the antibonding orbital of the antioxidant. In a simplified way, the lower the energy of the LUMO, the easier the hydrogen transfer.

The energy difference between HOMO and LUMO ($\Delta E_{LUMO-HOMO}$) is associated with molecular reactivity. The greater this energy difference, the less reactive the molecule will be. From the energy values of the frontier orbitals, other quantum chemical descriptors can be obtained [27-28].

The Ionization Potential (I) can be described as the energy required to remove the outermost electron. The electrons least held by the nucleus are those that occupy the HOMO. $\mathbf{I_{vertical}}$, when there is no change of molecular geometry, can be described as Eq. 10:

$$I = - E_{HOMO} \quad (10)$$

The electron affinity (A) can be described as the energy released with adding one electron to a neutral molecule or system. Once captured by the molecule, electronic transitions will occur, and the new ground state is when the new electron occupies the old LUMO. For this reason, when we do not consider the structural relaxation coming from the interaction with other molecular orbitals, **A** could be described as Eq. 11:

$$A = - E_{LUMO} \quad (11)$$

The electronegativity is a property attributed to the tendency for electron attraction by the molecule. In Mulliken scale, electronegativity (χ) can be described as arithmetic mean of I and A. Therefore χ could be defined as (Eq.12):

$$\chi = - (E_{HOMO} + E_{LUMO})/2 \quad (12)$$

The chemical hardness (η) is defined as the difficult to a chemical specie to change its electronic configuration. It is defined mathematically as being approximately half the value of $\Delta E_{LUMO-HOMO}$ (Eq. 13):

$$\eta = (E_{LUMO} - E_{HOMO})/2 \quad (13)$$

The greater the difference in energy of the boundary orbitals, the greater the

difficulty of the electronic transition [27-28].

The nucleophilic index ω determines the degree of reduction of energy when a system (atom or molecule) gains electrons and is defined as described in Equation 14.

$$\omega = \chi^2/2\,\eta \qquad (14)$$

The higher the omega value, the greater the electrophilic power of the species.

Fukui functions stand out among the second order quantum chemistry descriptors to measure antioxidant activity. The Fukui functions (f) can be defined as the change in electron density ρ(r) as a function of the number of electrons (N) after the system gains or loses electrons.

The function f+(r) measures which regions of the molecule have a greater tendency to act as an electrophile, through the variation of ρ(r) after the system receives an electron. The function f– (r) can predict which regions of the molecule are more susceptible to nucleophilic attack, being calculated by the variation of ρ(r) after the system receives an electron. The arithmetic mean between $f^{+}(r)$ and f^{-} (r) is called $f^{0}(r)$ and the higher its value, the greater the vulnerability of that site to radical attack. [27-28]

In the Chapter 1 of this thesis, for better comprehension of this work, is showed the complete study of antioxidant potential of structures 2 (A-D). However, concerns to this thesis only computational study, because experimental data belongs to master degree dissertation of Nelly Vanessa Pérez Rangel of Pos-Graduation Program of Mechanical Engineering of Universidade Federal do Ceará. [29]

Despite being quick data to obtain, the quantum descriptors do not consider steric factors of the radical that will attack. Another problem is that the energy values of the frontier orbitals are conformationally dependent. If the molecule suddenly changes conformation, it can affect the energy value of HOMO and LUMO and consequently the value of the quantum descriptors.

For this reason, in Chapter 2, we use another approach, the reactional simulation. In this case, the antioxidants are placed to react with radicals, and kinetic and thermodynamic data are obtained. The way how this is calculated will be better described in Chapter 2. The disadvantage of this method is the high computational cost. However, the molecules can change their conformation during the process, allowing a better analysis of the system during the reaction evolution.

CHAPTER 1. A POTENTIAL BIO-ANTIOXIDANT FOR MINERAL OIL FROM CASHEW NUTSHELL LIQUID: AN EXPERIMENTAL AND THEORETICAL APPROACH[1]

RESUMO DO ARTIGO

O objetivo do presente trabalho foi avaliar o potencial antioxidante de uma misturas de cardanois saturado, monoeno, dieno e trieno obtidos a partir do líquido da castanha de caju em óleo mineral naftênico. Uma amostra de óleo mineral naftênico foi dopada com a mistura de cardanóis nas concentrações de 500, 2000 e 5000 mg/kg e avaliada por calorimetria exploratória diferencial (DSC) e pelo método oxidativo acelerado (PetroOXY), seguindo as normas ASTM (E2041-18, E1970 -16, E537-12 e E698-18). A adição de cardanóis aumentou a estabilidade oxidativa do óleo mineral por um fator de 4 a 5. Para avaliar o potencial antioxidante de cada cardanol particular presente na mistura, a análise estrutural e os mecanismos antioxidantes específicos foram investigados pela teoria do funcional da densidade (DFT). Cada estrutura molecular foi otimizada com o funcional híbrido B3LYP com um conjunto de bases 6-31G(d, p), e os mecanismos antirradicalar (HAT, SPLET e SET-PT) foram avaliados. A HAT foi o mecanismo melhor observado, destacando-se o cardanol monoeno que apresentou melhor atividade antirradicalar. No que diz respeito ao estudo da reatividade global, concluiu-se que o aumento das insaturações na cadeia lateral das moléculas contribui significativamente para o aumento da sua reatividade geral. Ao avaliar o índice de Fukui, confirmou-se que, para o cardanol monoeno, a reatividade prevalece no anel aromático com ênfase no oxigênio.

Palavras-chave: Energia de ativação · Antioxidante · Cinética de degradação · Estudo DFT · Óleo mineral naftênico.

[1] Article published in the Brazilian Journal of Chemical Engineering entitled "A potential bio-antioxidant for mineral oil from cashew nutshell liquid: an experimental and theoretical approach," available at DOI: https://doi.org/10.1007/s43153-020-00031-z

ABSTRACT

The objective of the present work was to evaluate the antioxidant potential of a mixture of saturated, monoene, diene, and triene cardanols derived from the cashew nutshell liquid in naphthenic mineral oil. A mineral naphthenic oil sample was doped with the cardanols mixture at concentrations of 500, 2000, and 5000 mg/kg and evaluated using differential scanning calorimetry (DSC) and the accelerated oxidative method (PetroOXY), following ASTM standards (E2041-18, E1970-16, E537-12, and E698-18). The addition of cardanols increased the oxidative stability of the mineral oil by a factor of 4 to 5. To evaluate the antioxidant potential of each particular cardanol present in the mixture, structural analysis and specific antioxidant mechanisms were investigated by density functional theory (DFT). Each molecular structure was optimized with the hybrid functional B3LYP with a basis set 6-31G (d, p), and the antiradical mechanisms (HAT, SPLET, and SET-PT) were evaluated. The HAT was the best observed mechanism, standing out for the cardanol monoene that showed presented better antiradical activity. Concerning the global reactivity study, it was concluded that the increase of the unsaturations in the side chain of the molecules contributes significantly to their increased general reactivity. When evaluating the Fukui index, it was confirmed that, for the cardanol monoene, the reactivity prevails in the aromatic ring with an emphasis on oxygen.

Keywords: Activation energy · Antioxidant · Degradation kinetic · DFT study · Naphthenic mineral oil.

INTRODUCTION

Thermo-oxidative degradation is a recurrent problem in several organic products and processes, primarily in the fuel and lubricant industry (Rios et al. 2013; Lopes et al. 2008; Syahir et al. 2017; Sousa Rios and Mazzetto 2013). Thus, antioxidant additives have been used in these sectors to add or enhance desirable physicochemical properties or suppress the nonconformities resulting from the oxidation of those products. Currently, there is an increasing research focus on the evaluation and development of antioxidants derived from biomass and industrial residues, aiming to develop less expensive and environmental friendly antioxidants (Esmaeili et al. 2018; Kleinberg et al. 2017; Maia et al. 2015).

According to the Food and Agriculture Organization (FAO 2020), about 4.1 million tons of cashew nuts were produced worldwide in 2016, mostly in Africa and Asia. In the world, 5.7 million hectares are used for this production. The main destination of the cashew nut shells in industry is currently as fuel for boilers. However, a residue of the cashew nut processing industry is a viscous oil present in the shell entitled cashew nutshell liquid (CNSL) that shows great potential to be used as resin, paint, additive, and intermediates for the chemical industry (Cashol Resibras 2020; Lopes et al. 2008).

Cardanols are the major constituents of cashew nutshell liquid (CNSL). Since it is a mixture of phenolic compounds (Fig. 1), it exhibits antioxidant activity inherent to phenols; therefore, it is a possible antioxidant additive for the petrochemical industry (Rios et al. 2007; Lopes et al. 2008; Paiva et al. 2015). Examples include radical sequestration, decomposition of hydroperoxides, and metal deactivation that result in the retardation of the thermal and oxidative degradation of materials (Kleinberg et al. 2017; Lomonaco et al. 2013; Mothé et al. 2013).

Fig. 1 Chemical structures of cardanol's molecules. Saturated: $C_{21}H_{36}O$, Monoene: $C_{21}H_{34}O$, Diene: $C_{21}H_{32}O$, Triene: $C_{21}H_{30}O$

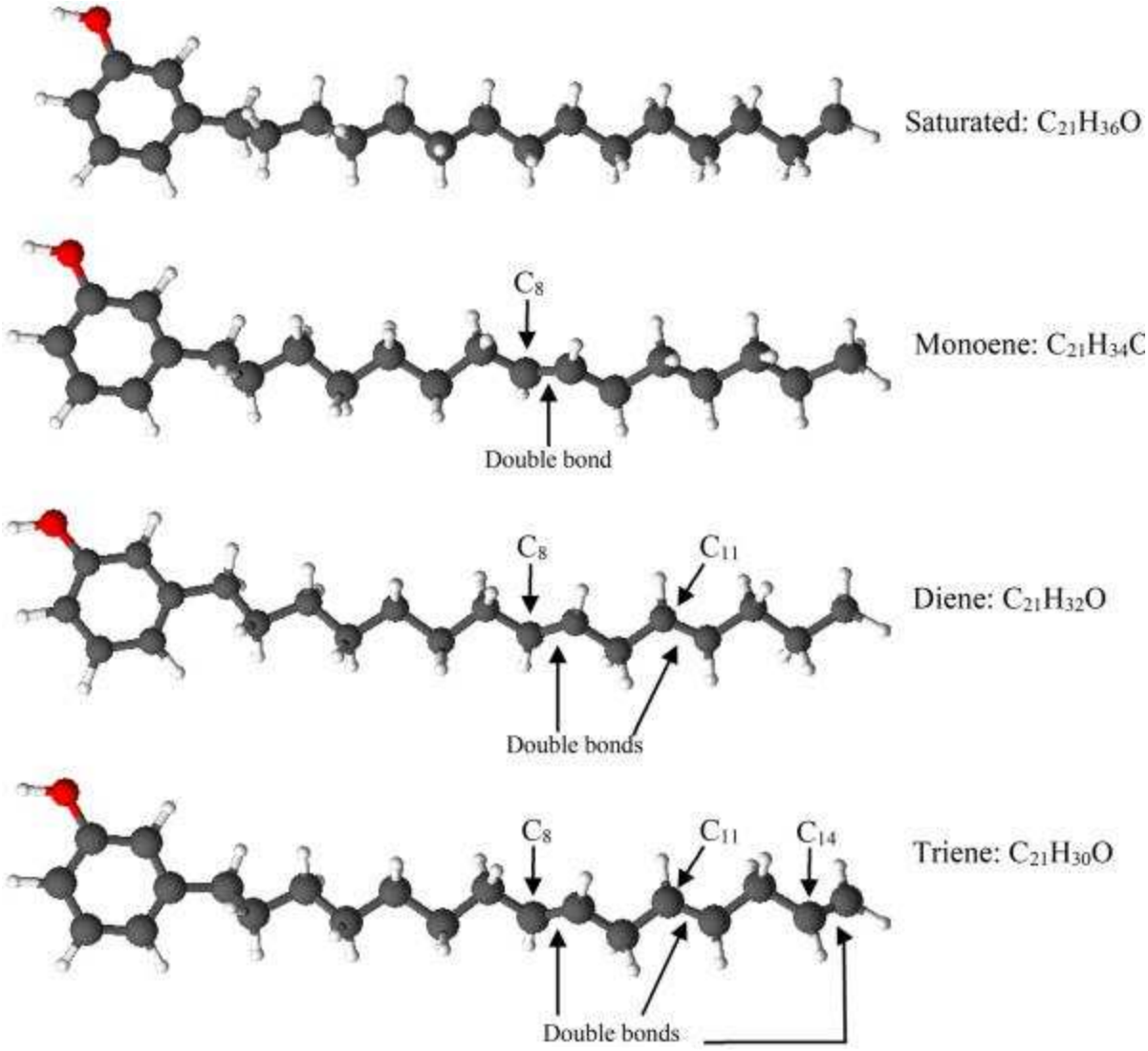

Source: Prepared by authors

Thermal analysis techniques, specifically thermogravimetry (TG) and differential scanning calorimetry (DSC), are promising experimental methods for studying the thermooxidative stability of organic compounds. These techniques provide information on the thermal properties of materials, purity, stability, decomposition of compounds, degradation kinetics, enthalpy variations, and other properties (Oliveira *et al.* 2011; Moreira *et al.* 2017; Silva *et al.* 2012). They monitor a physical or chemical property of a substance under a controlled temperature program as a function of time or temperature in specific atmosphere conditions (Zhao et al. 2020; Ilyas *et al.* 2017). The enthalpy, heat capacity, total thermal resistance, and thermal or thermo-oxidative decomposition curves are examples of properties

that may be determined through thermal analysis (Attia *et al.* 2017; Masoud *et al.* 2017; Kök *et al.* 2017). DSC is applied for the characterization, development, and quality control of new products (Zhao *et al.* 2020). DSC, the method used in this therefore, it is a possible antioxidant additive for the petrochemical industry (Rios et al. 2007; Lopes et al. 2008; Paiva et al. 2015). Examples include radical sequestration, decomposition of hydroperoxides, and metal deactivation that result in the retardation of the thermal and oxidative degradation of materials (Kleinberg et al. 2017; Lomonaco et al. 2013; Mothé et al. 2013).

Thermal analysis techniques, specifically thermogravimetry (TG) and differential scanning calorimetry (DSC), are promising experimental methods for studying the thermooxidative stability of organic compounds. These techniques provide information on the thermal properties of materials, purity, stability, decomposition of compounds, degradation kinetics, enthalpy variations, and other properties (Oliveira et al. 2011; Moreira et al. 2017; Silva et al. 2012). They monitor a physical or chemical property of a substance under a controlled temperature program as a function of time or temperature in specific atmosphere conditions (Zhao et al. 2020; Ilyas et al. 2017). The enthalpy, heat capacity, total thermal resistance, and thermal or thermo-oxidative decomposition curves are examples of properties that may be determined through thermal analysis (Attia et al. 2017; Masoud et al. 2017; Kök et al. 2017). DSC is applied for the characterization, development, and quality control of new products (Zhao et al. 2020). DSC, the method used in this investigation, has several advantages with regard to the use of reduced sample amounts (5–10 mg), short experimental time, and it also supplies information on kinetic parameters (Silva et al. 2008).

The cardanol mixture is constituted of four class of compounds: saturated, monoene, diene and triene. Since the fractionation of the cardanol mixture is not feasible experimentally, it is not possible to individually evaluate the antioxidant potential of each cardanol molecule present in the mixture, DFT theoretical studies can collaborate in the elucidation of the antioxidant mechanism and the potential antioxidant ranking of each molecule. Therefore DFT calculations were performed, implying three possible mechanisms for hydrogen abstraction: Hydrogen Atom Transfer (HAT), Sequential Electron Transfer-Proton Transfer (SET-PT), and Sequential Proton Loss Electron Transfer (SPLET) to allow comparison between the different molecules (Osorio *et al.* 2013; Wright *et al.* 2001; Galano and Alvarez-Idaboy 2013). Besides, an analysis to observe the variation of the reactivity of cardanol with the increase of the degree of unsaturation, and a Fukui analysis aiming to observe the preferential reactive sites of the molecules were realized (Eddy and Ita 2011; Parr and Yang 1984). Thus, this work focused on

evaluating the thermo-oxidative stability of cardanol and investigating its antioxidant potential in mineral oil. The model of Borchardt and Daniels was used to determine kinetic parameters and reaction order, and the PetroOXY method for the accelerated oxidative study.

MATERIALS AND METHODS

Materials

The cardanol sample was obtained from cashew nutshell liquid (CNSL) by separation/purification in column chromatography employing silica gel as solid phase and hexane as eluant (Freitas et al. 2015). The CNSL sample was supplied by Companhia Industrial de Óleos do Nordeste (CIONE), Fortaleza-Brazil. Samples of mineral naphthenic oil were provided by PETROBRAS (Brazil). The main physicochemical properties of mineral naphthenic oil are presented in Table 1.

Table 1. Physicochemical properties of mineral naphthenic oil

Properties	Value	Method
Density at 20 °C, kg/m^3	0.895	ASTM D1298
Total acid number, mg OH/g	0.001	ASTM D664
Pour point, °C	− 33	ASTM D97
Flash point, °C	164	ASTM D 93
Kinematic viscosity at 40 °C, cSt	20.1	ASTM D445
Kinematic viscosity at 100 °C, cSt	4.7	ASTM D445
Viscosity index	160.9	ASTM D2270

Measurements

Experiments were performed with a differential scanning calorimetry (DSC 1— Mettler Toledo, Columbus, OH, USA), using aluminum crucibles, and under synthetic air atmosphere with a flow rate of 50 mL min^{-1}. The sample size was 5.0 ± 0.1 mg with heating rates of 2.5, 5.0, 7.5, and 10.0 °C min^{-1} applied at temperatures between 30 and 500 °C. The equipment was calibrated with indium (melting point = 156.6 °C; ΔHm = 28.54 J g^{-1}) and zinc (melting point = 419.6 °C; ΔHm = 108.40 J g^{-1}). Data treatment was performed with the STARe Evaluation Software 13.00 by Mettler Toledo (Columbus, OH, USA).

The gas-chromatography coupled to mass spectrometry (GC/MS) analysis was performed in a GCMS-QP2010 ultra spectrometer (Shimadzu, Kyoto, Japan) equipped with a DB-5 column (0.25 mm, 30 m, 0.25 μm film) (Agilent, USA). The initial column temperature of 100 °C was linearly increased to 300 °C at a rate of 10 °C min^{-1} and the column temperature was held at the upper temperature until the end of detection. The injection temperature was set to 250 °C, while interface and ion source temperatures were set to 280 °C. Samples were ionized

by an electron impact (EI) ionization method.

The accelerated oxidation experiments were performed using a PetroOXY method (Petrotest, Germany).

Methods

Differential scanning calorimetry

The enthalpy changes, the onset temperature (*To*), the extrapolated onset temperature (*Ts*), and the peak temperature (*Tp*) of the degradation reaction were obtained according to ASTM E537-12 (ASTM 2012). To determine the beginning of the enthalpy effect, i.e. the point at which the curve moves away from the baseline, *Ts* was obtained by crossing the line tangent to the side of the peak and the tangent to the baseline. *Tp* corresponds to the maximum deflection of the DSC curve. These parameters are shown in Figure S1.

The DSC curve as a function of time was used to obtain the enthalpy of reaction (ΔH). Some DSC curve evaluation software programs provide abscissa, time or temperature, and independent information. The integration of the interval corresponding to the peak provides an area numerically proportional to ΔH.

Kinetic parameters and reaction order

Method 1 The estimation of the order of the reaction (*n*), the activation energy (*E*), and the Arrhenius pre-exponential factor (*Z*) in the first method was based on method ASTM E2041-18 (ASTM 2018a). Equation 1 is based on the model of Borchardt and Daniels, which assumes that the reaction rate is dependent on the amount of material present.

$$\frac{d\alpha}{dt} = k(T) \cdot (1 - \alpha)^n \quad (1)$$

where dα/dt is the reaction rate (min^{-1}), α is the reacted fraction (dimensionless), n is the reaction order (dimensionless), and k(T) is the rate constant at temperature T (min^{-1}). The reaction order follows the Arrhenius equation, Eq. 2.

$$E = Z \cdot e^{-E/RT} \quad (2)$$

Thus, by plotting ln k versus 1/T and optimizing the repeatability and reproducibility factors through the trial and error method of the reaction order, the values of the activation energy and the Arrhenius pre-exponential factor are obtained as shown in Eqs. 3 and 4.

$$E = m \cdot R \tag{3}$$

$$Z = e^{b} \tag{4}$$

where m is the angular coefficient, b is the linear coefficient, and R is the gas constant 8.314 J mol^{-1} K^{-1}.

The values of the unreacted fraction (1 − α) and the reaction rate (dα/dt) are obtained as shown in Figure S2 with at least 10 experimental points. Thus, the values of k(T) are determined from the corresponding temperatures using Eq. 5.

$$\ln(k) = \ln\left(\frac{d\alpha}{dt}\right) - n \cdot \ln\,(1 - \alpha) \tag{5}$$

The angular and linear coefficients, with their respective standard deviations, are obtained in accordance with ASTM E1970-16 (ASTM 2016).

Method 2 In the second method, the order of the reaction (n = 1) is defined a priori. Thus, higher-order reactions are not accurately described. The activation energy and the Arrhenius pre-exponential factor are determined based on an alternative model by Kissinger, described in ASTM E698-18 (ASTM 2018b), where Eq. 6 provides the activation energy.

$$E = R\,\frac{d[-\ln\,(\beta/Tp^{2})}{d(1/Tp)} \tag{6}$$

where β is the heating rate in K min^{-1}, and *Tp* is the peak temperature in K.

This method assumes that the complete reaction can be summarized by the peak temperature and the heating rate. Thus, the values of − ln (β/Tp2) are plotted against the respective inverse of the obtained peak temperatures. The angular coefficient of the line can be determined through linear regression. The activation energy is calculated as the product of the angular coefficient (m) with the gas constant (R), as shown in Eq. 6. The Arrhenius pre-exponential factor is obtained from Eq. 7.

$$Z = \frac{E \cdot e^{b}}{R} \tag{7}$$

where b corresponds to the line intercept (s^{-1}).

Accelerated oxidative experiments using the PetroOXY method

The PetroOXY method (Neumann *et al*. 2008; Araújo *et al*. 2009; Luna *et al*. 2011) estimates the induction period from the measurement of pressure drop in a hermetically sealed test chamber. The induction period is the elapsed time between starting the test and the breaking point, which is defined as a pressure drop of 10% below the maximum pressure as detected in the pressure versus time curve.

In this method, a sample of 5 mL is placed into a sealed chamber and a pressure of 700 kPa is reached by the injection of oxygen. To assure the complete elimination of air, the chamber is purged 3 times with oxygen. After reaching a pressure of 700 kPa, the temperature of the chamber is increased to 140 °C. The breaking point is noted when a pressure drop of 14 kPa is reached once or twice within 15 min in the pressure profile of oxidation, according to Luna et al. (2011).

Computational methods

Optimized geometry In this work, the geometrical optimization of the cardanol molecules has been carried out using density functional theory (DFT), because of its good compromise between computational time and description of electronic correlation (Nenadis and Tsimidou 2012). The calculations were performed with the ORCA 4.1.1 molecular package (Neese 2017), the molecular structures were optimized with the hybrid functional B3LYP (Becke 1993) with basis set 6-31G (d, p). All the calculations were performed in the gas phase at 298.15 K (Hehre et al. 1972).

The B3LYP optimized structures were confirmed to be real minima by frequency calculations (no imaginary frequency) and to obtain zero-point vibrational energy (ZPVE) corrections. The molecules were drawn in MarvinSketch 18.30 version using a calculation plugin for achieving the lowest energy conformer. Only the most stable conformation (with the lowest electronic energy) of each compound was used in this work (Chemaxon 2019).

Mechanism of antiradical activity The antioxidation process can be elucidated by three mechanisms: (HAT); (SPLET) and (SET-PT) (Wright *et al.* 2001; Nwankwo *et al.* 2017). The first numerical parameter that characterizes the antioxidant potential for cardanol-based molecules is bonddissociation enthalpy (BDE), which was calculated by using

thermodynamical data from DFT calculations of neutral and radical structures of cardanol molecules.

In this case, the HAT mechanism was applied to the O–H bonding, the radical was formed on the phenolic oxygen of the molecule. The chemical equations for the HAT mechanism consist on a direct homolytic rupture of O–H bonding, having a –O• and H• as products, and the enthalpy from each product is calculated and used for the BDE calculation, Eq. 8.

$$BDE = H(ArO\bullet) + H(H\bullet) - H(ArOH) \quad (8)$$

where H is the total enthalpy of the studied species at a temperature of 298.15 K and estimated from Eq. 9.

$$H = E_0 + H_{rot} + H_{trans} + H_{vib} + ZPE + RT \quad (9)$$

The E_0 is the total energy at 0 K, H_{rot} , H_{trans} , and H_{vib} are the rotational, translational and vibrational contributions to the enthalpy respectively, and ZPE is the zero-point vibrational energy. The enthalpy value for the hydrogen atom in the solvent was calculated at the same level of theory, while this value in the gas phase was taken at its exact energy of 0.5 Hartree at 0 K, and thermal correction at the given temperature was added by the value of 2.5 RT. The calculated enthalpies of the proton (H^+), ($H^\bullet$) and electron (e^-) were taken from the literature (Bartmess 1994; Rimarˇcík et al. 2010; Parker 1992).

The BDE parameter, a tool for evaluating the antioxidant activity of organic compounds, gives the binding dissociation energy showing that a low BDE value indicates higher antioxidant activity for the molecule. To make this value as small as possible, part of the contribution was attributed to the energetic stability of the formed phenol radical in the reaction (Zhang 1999).

The SET-PT is performed in two steps, the first step is governed by the electron affinity (IP) parameter where the formation of the cation-radical occurs (Eq. 10). Then the phenolic radical formation occurs, calculated by PDE, Eq. 11.

$$IP = H(ArOH^{+\bullet}) + H(e^-) - H(ArOH) \quad (10)$$

$$PDE = H(ArO^\bullet) + H(H^+) - H(ArOH^{+\bullet}) \quad (11)$$

The SPLET mechanism, also performed in two steps, is initiated by the electronic affinity (PA) (Eq. 12) occurring anion formation, followed by the second step, generating the output of an electron for the formation of the radical associated with the parameter ETE, Eq. 13.

$$PA = H(ArO^-) + H(H^+) - H(ArOH) \quad (12)$$

$$ETE = H(ArO^\bullet) + H(e^-) - H(ArO^-) \quad (13)$$

Frontiers orbitals The frontier orbitals HOMO (highest occupied molecular orbital) and LUMO (lowest unoccupied molecular orbital) of a chemical species are very important orbitals, that play a key role in the understanding of the chemical reactivity (Hehre et al. 1972). The HOMO is the outermost orbital containing donor electrons and LUMO is the innermost orbital containing free places to accept electrons. The chemical behavior of monoene cardanol can be predicted by the following parameters, HOMO energy, LUMO energy, and energy gap (ΔE), emphasizing that the energy gap is an important parameter, as it reveals the stability of the molecular structure that can be calculated using the Eq. (14) (Eddy and Ita 2011).

$$\Delta E(gap) = E_{LUMO} - E_{HOMO} \quad (14)$$

To describe the reactivity relationship of cardanols, the Koopman's theorem was used (Koopmans 1934), associating the energy of boundary orbitals to describe the overall reactivity of the molecule: Electron affinity (A) is the energy required to add an electron to the molecule; ionization potential (I) being the energy required to remove the electron from the boundary orbital; electronegativity (χ) attributed to the tendency for electron attraction by the molecule; chemical hardness (η) is defined by the resistance of the molecule to electron distortion (Parr), and the index that measures the electrophilicity of the compound (ω). Therefore Eqs. 15–19 are used to obtain the reactivity parameters.

$$Ionizationpotential : (I) = -E_{HOMO} \quad (15)$$

$$Electronaffinity : (A) = -E_{LUMO} \quad (16)$$

$$Electronegativity : (\chi) = -(E_{HOMO} + E_{LUMO})/2 \quad (17)$$

$$Chemicalhardness(\eta) = (E_{LUMO} - E_{HOMO})/2 \quad (18)$$

$$Electrophilicity(\omega) = \chi^2/2\eta \quad (19)$$

Fukui index Fukui functions are indices that give information about the tendency of a molecule to lose or gain an electron. Thus, to predict which atom in the molecule would be more prone

to a nucleophilic or electrophilic attack. The Fukui function for a given molecule has been defined as the derivative of electron density with respect to the change of the number of electrons, keeping the positions of nuclei unchanged (Eddy and Ita 2011; Parr and Yang 1984).

The local reactivity of cardanol molecules was analyzed through an evaluation of the Fukui indices (Eddy and Ita 2011; Parr and Yang 1984). These are measures of the chemical reactivity, as well as an indication of the reactive regions and the nucleophilic and electrophilic behavior of the molecule. Fukui condensate helps understand local reactivity, which can be interpreted by varying electron density $\partial\rho(r)$ as a function of the variation of the number of electrons in a constant external potential (Eq. 20, see Supplementary material) (Parr and Yang 1984).

The obtained condensed Fukui functions helped understand the nucleophilic $f^{+}(r)$ and electrophilic $f^{-}(r)$ attack of the molecule. The Fukui function is given by Eqs. 21–23, see Supplementary material.

With Hirshfeld charges, the contribution of each atom to local reactivity can be obtained by Eqs. 24–26 (see Supplementary material) being qk the atom in study and N the number of electrons in the atom. To calculate the total variation of the atom's charge the index $\Delta f = (f_k^{+} - f_k^{-})$ was used; when the index is positive, there is a predisposition for nucleophilic attacks and a negative index, for electrophilic attacks. The electron density surfaces of the electrophilic Fukui function were obtained by MultiWFN software (Lu and Chen 2012a, b).

RESULTS AND DISCUSSIONS

Characterization of cardanol mixture

Physical state and color: viscous yellow oil. The GC/MS analysis showed the molecular ion peaks at m/z 302 [$C_{21}H_{34}O$, M +], m/z 300 [$C_{21}H_{32}O$, M +], and m/z 304 [$C_{21}H_{36}O$, M +] for the monoene, diene, and saturated cardanols, respectively. Other fragments compatible with a mass spectrum of monoene, diene, and saturated cardanols were observed.

Fig. 2 GC/MS of cardanol mixture

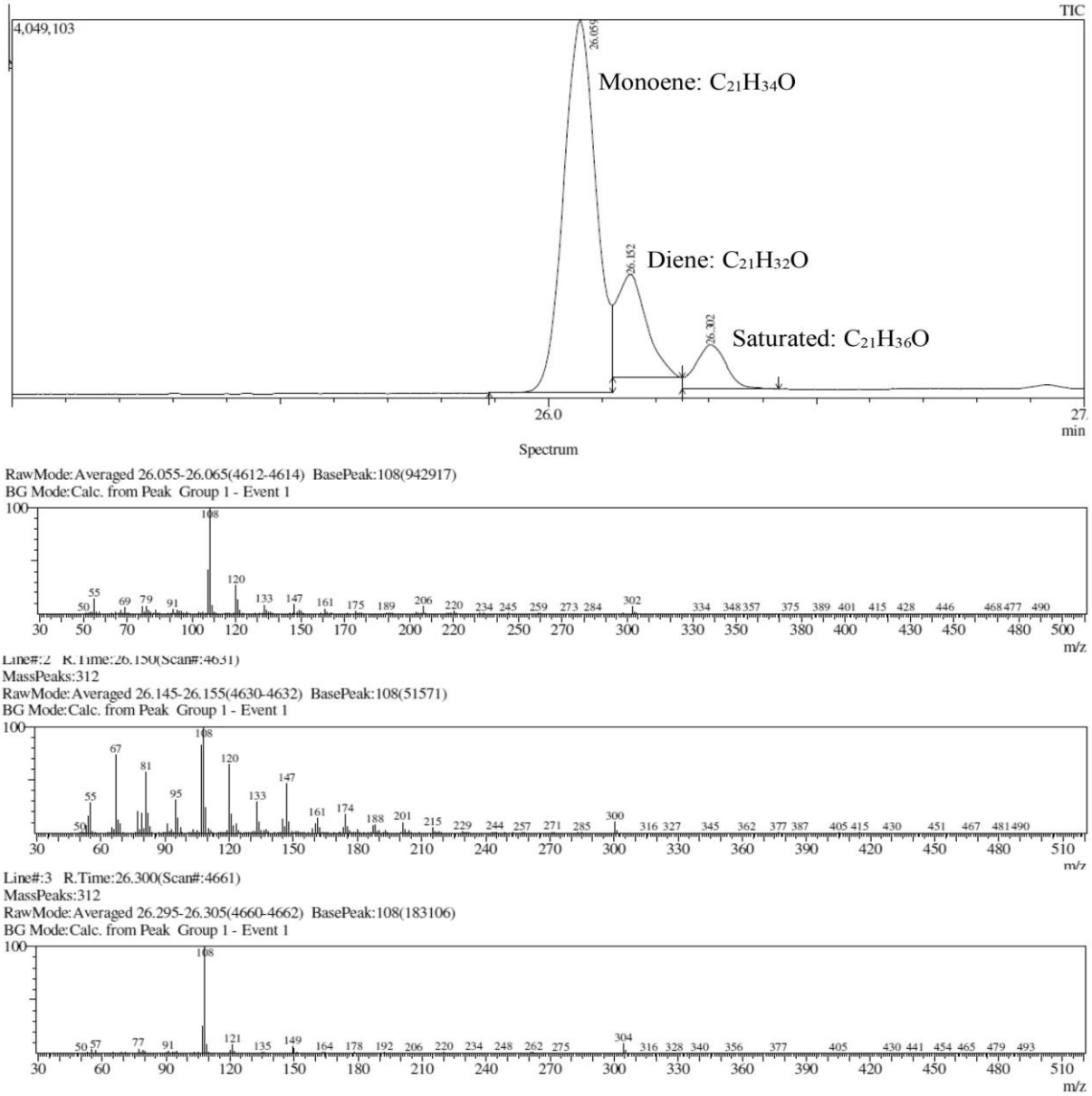

Source: Prepared by authors

The cardanol monoene showed fragments at m/z 55, 79, 108, 120, 133, 147, 161 and 206; cardanol diene presented fragments at m/z 55, 67, 81, 95, 108, 120, 133, 147, 174, 201 and 215; and cardanol saturated at m/z 108, 121 and 149 (see Fig. 2).

Thermal parameters

In alkylphenols, a characteristic base peak facilitates their identification. The base peak at m/z 108, the main characteristic of alkylbenzenes, is attributed to the β cleavage of the lateral aliphatic chain. In derivatives with a longer alkyl chain, benzylic cleavage and alkene elimination (McLafferty rearrangement) are the dominant primary fragmentation processes (Pretsch et al. 2009).

Figure 3 shows the DSC curves of the cardanol mixture at four heating rates (β = 2.5, 5.0, 7.5, and 10.0 K min^{-1}). Exothermic peaks, typical of the thermal and oxidative degradation processes of organic molecules can be observed (Micić et al. 2015; Martínez-Monteagudo et al. 2012; Mohammed et al. 2018).

Fig. 3 DSC curves of cardanol at four heating rates: β = 2.5, 5, 7.5 e 10 K/min

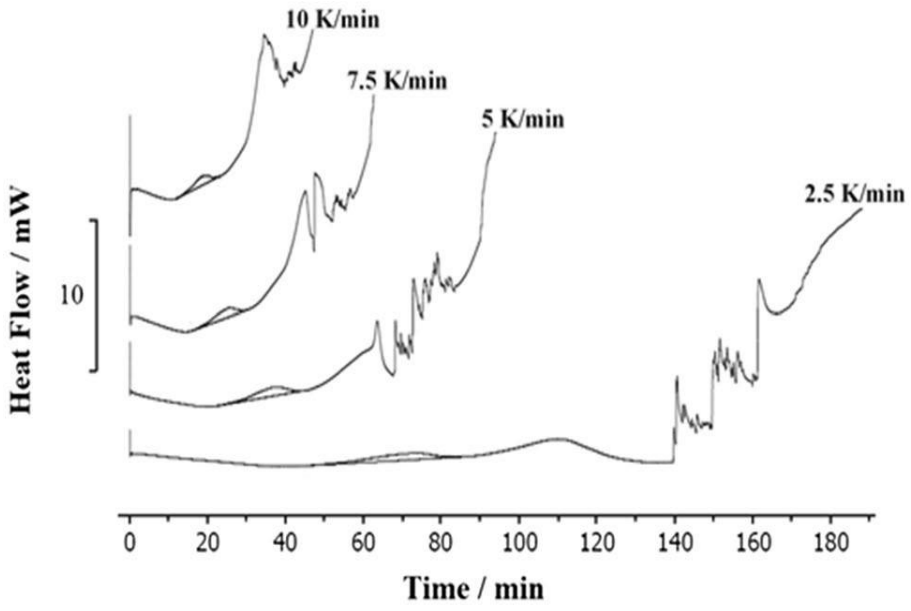

Source: Prepared by authors

Based on the thermogravimetric results obtained by Paiva *et al*. (2015), it can be inferred that the first thermal event observed in the DSC curves is the beginning of the thermooxidative degradation of the compound. This is consistent with the mass loss range in TG of cardanol with degradation beginning between 141 and 153 °C. Therefore, since the

alkylphenol degradation starts at this stage, the first thermal event was used to characterize the thermal and oxidative stability and determine the kinetic parameters of oxidation. This stage is also likely the start of the reduction of its antioxidant potential (Micić et al. 2015; Reda 2011).

Figure 4 shows the first events for each evaluated heating rate and Table 2 includes the thermal stability characterization parameters according to ASTM E537-12. As can be seen, the first thermal event of each test (β = 2.5, 5.0, 7.5, and 10.0 K min^{-1}), unlike the other events, shows similar behavior in the gradual increase of the degradation onset temperatures (T_o), the peak temperature (T_p), and decrease of the enthalpic variation (ΔH) with increasing heating rate.

Table 2 Thermal parameters of cardanol at different heating rates (β), ASTM E537-12

β (K/min)	To (K)	Ts (K)	Tp (K)	ΔH (J g^{-1})
10	152.95	178.02	216.20	34.906
7.5	150.54	170.34	215.81	45.328
5	143.55	169.51	213.18	65.882
2.5	141.01	163.53	207.02	99.726

Source: Prepared by authors

Fig. 4 First thermal event of cardanol at four heating rates: β = 2.5, 5, 7.5 e 10 K/min

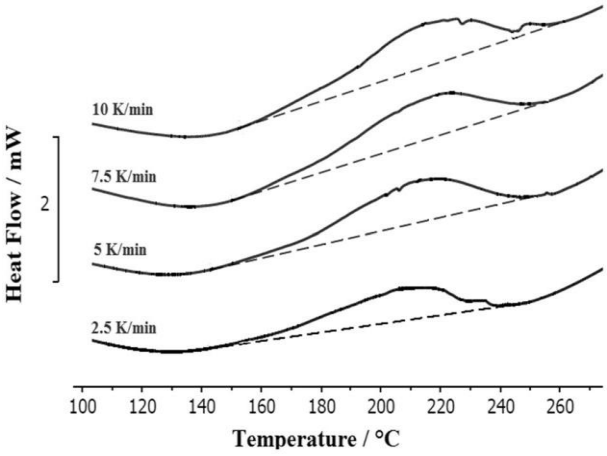

Source: Prepared by authors

According to Speyer (1993), the relationship between the increase of the degradation onset temperature (*To*) and the increase of the heating rate is associated with a heat diffusion delay between the sample and the thermocouples because the sample undergoes a

more pronounced temperature variation in a given time interval at higher heating rates. With regard to the enthalpy variation, the increase of ΔH in an exothermic process indicates a decrease in the heat released by the system. Herein ΔH values of 34.906 and 99.726 J g^{-1} were obtained at heating rates of 10.0 and 2.5 K min^{-1}, respectively.

Kinetics parameters

After obtaining the enthalpy variation for the performed experiments, the $T_{10\%}$ and $T_{90\%}$ temperatures were defined as the temperatures at which 10% and 90% of the peak area are obtained, respectively. This interval was divided into 20 equal sub-intervals, where the values of the reaction rate (dH/dt) in mW, the temperature (T) in °C, and the residual heat of reaction (ΔH_T) in mJ were determined. The value of ln k was then calculated from Eq. 5. The data for the experiment at the heating rate of 5 K min^{-1} is shown in Table 3.

The statistical procedure defined in ASTM E1970-16 (Standard Practice for Statistical Treatment of Thermoanalytical Data) was used to determine the activation energy and the Arrhenius pre-exponential factor. Values for the reproducibility and repeatability factors of the order of $R^2 > 0.99$ were obtained. Table 4 shows the Arrhenius pre-exponential factor and the activation energy for all evaluated heating rates. As can be observed, these parameters did not show a significant variation for the assessed heating rates.

Table 3 Kinetic parameters of degradation of cardanol, β = 5 K/min, ASTM E2041-18

	d*H*/d*t* (mW)	Δ*Ht* (mJ)	*T* (°C)	*T* (K)	*1/T* (K^{-1})	*dα/dt* (s−1)	ln(*dα/dt*)	*1 − α*	*N*	*n*·ln(*1 − α*)	ln *k*
1	0.21	297.15	181.75	454.90	0.0021983	0.00063750	− 7.3580	0.90207	1	− 0.10307	− 7.25488
2	0.25	289.70	184.39	457.54	0.0021856	0.00075893	− 7.1836	0.87945		− 0.12846	− 7.05514
3	0.29	282.12	186.91	460.06	0.0021736	0.00088036	− 7.0352	0.85644		− 0.15497	− 6.88021
4	0.31	272.49	189.55	462.70	0.0021612	0.00094108	− 6.9685	0.82721		− 0.18970	− 6.77878
5	0.36	260.93	192.19	465.34	0.0021490	0.00109286	− 6.8190	0.79211		− 0.23305	− 6.58590
6	0.4	248.68	194.71	467.86	0.0021374	0.00121429	− 6.7136	0.75493		− 0.28114	− 6.43246
7	0.43	237.33	197.35	470.50	0.0021254	0.00130536	− 6.6413	0.72047		− 0.32785	− 6.31342
8	0.46	223.91	199.87	473.02	0.0021141	0.00139644	− 6.5738	0.67973		− 0.38606	− 6.18777
9	0.48	208.08	202.39	475.54	0.0021029	0.00145715	− 6.5313	0.63167		− 0.45938	− 6.07189
10	0.53	192.8	204.91	478.06	0.0020918	0.00160894	− 6.4322	0.58529		− 0.53565	− 5.89653
11	0.54	177.01	207.55	480.70	0.0020803	0.00163929	− 6.4135	0.53735		− 0.62110	− 5.79239
12	0.57	159.20	210.19	483.34	0.0020689	0.00173037	− 6.3594	0.48329		− 0.72714	− 5.63228
13	0.58	140.96	212.71	485.86	0.0020582	0.00176072	− 6.3420	0.42792		− 0.84883	− 5.49320
14	0.57	123.70	215.23	488.38	0.0020476	0.00173037	− 6.3594	0.37552		− 0.97944	− 5.37998
15	0.55	105.90	217.74	490.89	0.0020371	0.00166965	− 6.3951	0.32148		− 1.13481	− 5.26033
16	0.53	87.87	220.39	493.54	0.0020262	0.00160894	− 6.4322	0.26675		− 1.32144	− 5.11074
17	0.5	72.35	222.91	496.06	0.0020159	0.00151787	− 6.4905	0.21964		− 1.51579	− 4.97466
18	0.45	58.73	225.42	498.57	0.0020057	0.00136608	− 6.5958	0.17829		− 1.72435	− 4.87146
19	0.4	45.18	227.94	501.09	0.0019956	0.00121429	− 6.7136	0.13715		− 1.98665	− 4.72695
20	0.33	32.98	230.71	503.86	0.0019847	0.00100179	− 6.9060	0.10012		− 2.30140	− 4.60456

Source: Prepared by authors

Table 4. Kinetic parameters of the cardanol degradation at four heating rates, ASTM E2041-18

β (K/min)	*n*	*E* (kJ/mol)	ln *Z* ($Z\ s^{-1}$)	*R2*
10	1	99.93 ± 1.34	19.699 ± 0.333	0.99680
7.5		98.65 ± 0.57	19.146 ± 0.142	0.99940
5		101.50 ± 0.57	19.627 ± 0.144	0.99942
2.5		100.99 ± 1.42	22.167 ± 0.362	0.99645

Source: Prepared by authors

In the Kissinger model, the reaction is considered to be characterized by the peak temperature (T_p) and the analysis of the plot of ln (β/T_p^2) versus $1/T_p$. Thus, using this model with $R^2 > 0.95$, values of 262.690 kJ mol^{-1} and 64.687 s^{-1} were determined for the activation energy and the Arrhenius pre-exponential factor, respectively. These values differ significantly from the values obtained using the method of Borchardt and Daniels. This difference is likely because the characteristics at the peak of the reaction do not represent the magnitude of the entire thermal event (ASTM 2018b; Neumann et al. 2008).

Performance experiments

A comparison of the pressure profiles of mineral oil doped with cardanol mixture is shown in Fig. 5. It may be observed that increasing the cardanol concentration the induction period increased. The induction period obtained for the mineral oil without additive was approximately 22 min. These results indicate that the mineral oil doped with cardanol mixture had oxidative stability significantly higher than the original mineral oil.

This behavior occurs probably due to the action of the cardanol in the thermodegradation process of oil. The cardanol is an alkylphenol and this additive can trap peroxy radicals formed during autoxidation of organic molecules to stop the chain reaction (Kajiyama and Ohkatsu 2002; Rios et al. 2010). These peroxy radicals-trapping reactions include electron transfer and hydrogen abstraction processes.

Fig. 5 Pressure profiles of oxidation tests at 140 °C of mineral oil doped with cardanol at different concentrations.

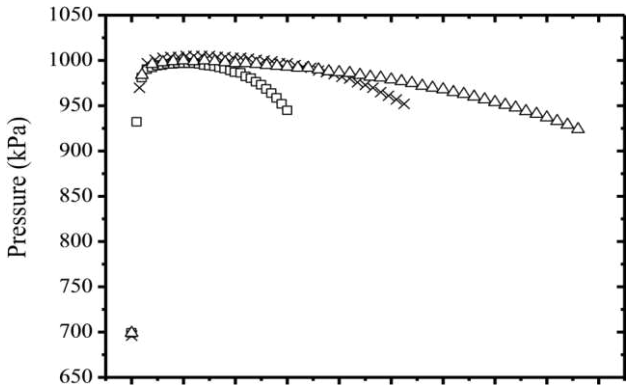

Unfilled square: 500 mg/kg; cross: 2000 mg/kg; unfilled triangle: 5000 mg/kg
Source: Prepared by authors

Mineral oil oxidation is initiated by the formation of free radicals. These species can easily be formed from the removal of a hydrogen atom from the organic molecule (Fox and Stachowiak 2007; Dwivedi et al. 2018), and they can react rapidly with the oxygen of the air to form a peroxy radical, which is the most important oxidation product of lubricant oil. According to results, the cardanol probably acted by a radical chain-breaking mechanism removing species that accelerate the chain propagating steps, for example, alkyl-peroxy and alkyl radicals and consequently, the oxidative stability of the mineral oil increased (Rios and Mazzetto 2012).

Antioxidant mechanism analysis

Currently, computational studies have promoted the elucidation of the antioxidant activity of phenolic compounds (Leopoldini *et al*. 2011; Stepanic *et al*. 2013). The BDE values are shown in Table 5.

Table 5. Enthalpies (kcal mol^{-1}) of mechanisms calculations for cardanol molecules in vacum

Molecule (Cardanol)	HAT	SET-PT			SPLET		
	BDE	IP	PDE	Total	PA	ETE	Total
Saturated	81.33	172.52	222.41	394.93	359.36	35.57	394.93
Monoene	81.32	174.21	220.71	394.93	359.27	35.65	394.92
Diene	81.37	163.61	231.36	394.97	359.15	35.82	394.97
Triene	81.36	164.82	230.13	394.95	359.05	35.90	394.95

Source: Prepared by authors

As the BDE represents the calculation of the difference between the radical plus atomic hydrogen and the neutral enthalpies, the saturated and monoene cardanols performed more effectively for the radical reaction since their BDE parameters showed lower values when compared to the other molecules in the mixture. This result can be associated with the experimental finding of the antioxidant potential of the cardanol mixture since the major component is the cardanol monoene. The monoene and saturated compounds presented the lower BDE values. This contribution can be explained by the stability of the radicals formed by the homolytic rupture of the phenol O–H bond (Table S1).

For HAT, the antioxidant (ArOH) reacts with the free radical (R), by transferring a hydrogen atom to R. through homolytic rupture of the O–H bond. The ArOH reactivity can be estimated by O–H BDE, the lower the BDE value, the weaker the O–H bond, and the greater the expected antiradical activity. In the SET-PT, the first step (IP) is more favored for the diene and triene cardanols, as a consequence of the greater number of π–π bonds than double bonds. However, the second step (ETE) favored the monoene cardanol. Therefore, saturated and

monoene cardanols favored the complete mechanism. For SPLET, the first stage proved to be more viable for the triene cardanol, in the second stage it favored the saturated cardanol, while in the complete mechanism, monoene and saturated cardanols presented the lowest values (Table 5).

Reactivity analysis

The energies of frontiers orbitals (E_{HOMO} and E_{LUMO}) allow the understanding of the way electron transfer affects the stability of a molecule during a chemical reaction. HOMO is the orbital that primarily acts as the electron donor and LUMO is the orbital that largely acts as the electron acceptor, and the gap (E_{LUMO}–E_{HOMO}) characterizes the molecular chemical stability (Eddy and Ita 2011; Parr and Yang 1984).

In the monoene cardanol the energy of the order of 0.172 eV for the HOMO was calculated and it is located in the phenolic ring having symmetry between the positive and negative phases, characteristic also found in the orbital LUMO, which has an energy of the order of − 5.755 eV, allowing to calculate a gap of 5.927 eV (Fig. 6).

Fig. 6 Isodensity plots of frontier orbitals and gap to cardanol monoene

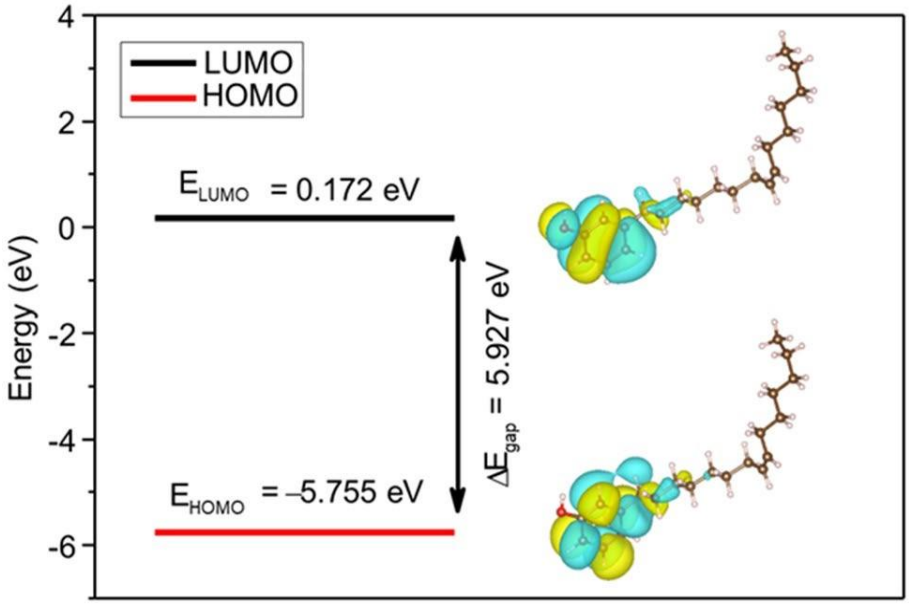

Source: Prepared by authors

Therefore, the global reactivity of all cardanols was very similar (Table 6), however, chain unsaturation significantly influences the increased reactivity of cardanol, where the values for Gap Energy, Electron affinity, Electronegativity and Hardness had changed.

Table 6. Selected quantum chemical parameters for the cardanols mixture.

Molecule	E_{HOMO}/eV	E_{LUMO}/eV	I/eV	A/eV	ΔE/eV	χ/eV	η/eV	ω/eV
Saturated	− 5.75	0.19	5.75	− 0.19	5.94	2.78	5.94	0.17
Monoene	− 5.76	0.17	5.76	− 0.17	5.93	2.80	5.93	0.17
Diene	− 5.76	0.16	5.76	− 0.16	5.92	2.80	5.92	0.17
Triene	− 5.76	0.15	5.76	− 0.15	5.91	2.81	5.91	0.17

Source: Prepared by authors

The Fukui index shows the obtained data about the tendency of the atom for the local reactivity of the molecule (Parr and Yang 1984; Srivastava et al. 2016; Stepanic et al. 2013). In this case, the focus is the Fukui function Δf and $f°$. Therefore, the atoms with the greatest potential for the radical and nucleophilic reactions are located in the phenolic ring, atoms from 0 to 6 (Table S2). In this perspective, quantum studies for the monoene cardanol have shown reactivity in the phenolic ring due to the boundary orbitals that are located in this molecular region. Besides, the ΔF indices showed the highest absolute values. Thus, the phenolic region tends to be favored by reactivity, which can have a radical formation since the oxygen can remove the electronic charge of the hydrogen and consequently generate the radical on the oxygen atom.

Figure 7 shows how the Fukui index is placed upon this molecule where there is a highlight for oxygen and carbon 4 as nucleophilic site and carbon 2, 3, 4, 5 and oxygen for radical attack (Figure S3) where carbon 1 has the lowest value which may be explained by a steric impediment.

Fig. 7 Electrophilic Fukui function over cardanol monoene

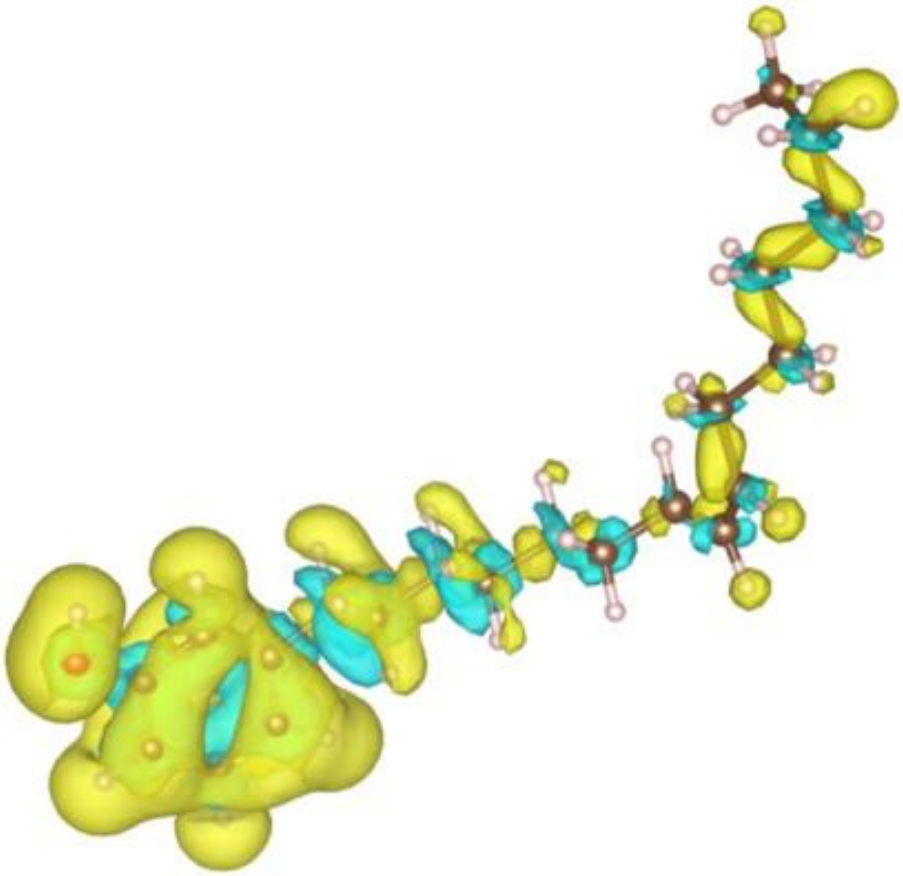

Source: Prepared by authors

CONCLUSIONS

Based on these results, it may be concluded that cardanol has good thermo-oxidative stability, with To ranging from 141.01 to 152.95 °C for β = 2.5 and 10 K min−1, respectively. These degradation onset temperatures are important in the evaluation of antioxidants because the organic substrates (fuels and lubricants) to which the additives will be added generally function in the temperature range between 90 and 120 °C.

The activation energy for the degradation process also represents an important parameter in the evaluation of the antioxidant potential of chemical compounds because a high value of E indicates a lower susceptibility to the thermo-oxidative degradation. With respect to the investigation of thermo-oxidative stability by means of the DSC technique, it is important to note that thermal analysis represents a significant time-saving technique compared to other oxidative degradation testing techniques for organic materials.

The mineral naphthenic oil induction period increased after the oil was doped with the cardanols mixture. In the DFT study, the antiradical mechanisms (HAT, SPLET, and SET-PT) for the molecules were evaluated. The HAT was the best presented mechanism, standing out for the monoene cardanol that showed better antiradical activity.

Concerning the global reactivity study, it was concluded that the increase of the unsaturations in the side chain contributes significantly to the increased of the reactivity general. In the analysis of Fukui index, it is confirmed that in cardanol monoene, the reactivity prevails in the aromatic ring with an emphasis on oxygen and carbon 4, without the interference of the carbonic chain.

The results showed that the cardanol mixture, extracted from the cashew nutshell liquid, has potential for application as an antioxidant in mineral oil. Thus, within the principles of sustainability, it adds both financial and environmental value to the cashew nut industry waste.

REFERENCES

[1] American Society for Testing and Materials, ASTM E537-12 (2012) Standard test method for the thermal stability of chemicals by differential scanning calorimetry, ASTM International.

[2] American Society for Testing and Materials, ASTM E1970-16 (2016) Standard test method for statistical treatment of thermoanalytical data, ASTM International.

[3] Araújo SV, Luna FMT, Rola EM Jr, Azevedo DCS, Cavalcante CL Jr (2009) A rapid method for evaluation of the oxidation stability of castor oil FAME: influence of antioxidant type and concentration. Fuel Process Technol 90(10):1272–1277

[4] American Society for Testing and Materials, ASTM E2041-18 (2018) Standard test method for estimating kinetic parameters by differential scanning calorimeter using the Borchardt and Daniels, ASTM International.

[5] American Society for Testing and Materials, ASTM E698-18 (2018) Standard test method for arrhenius kinetic constants for thermally unstable materials using differential scanning calorimetry and the Flynn/Wall/Ozawa Method, ASTM International.

[6] Attia AK, Abdel-Moety MM, Abdel-Hamid SG (2017) Thermal analysis study of antihypertensive drug doxazosin mesylate. Arab J Chem 10(1):S334–S338

[7] Bartmess JE (1994) Thermodynamics of the electron and the proton. J Chem Phys 98(25):6420–6424

[8] Becke AD (1993) Density-functional thermochemistry. III. The role of exact exchange. J Chem Phys 98(7):5648–5652

[9] Cashol Resibras. https ://casho l.com.br/2017/#mater iais. Accessed 19 Apr 2020

[10] Dwivedi G, Verma P, Sharma MP (2018) Optimization of storage stability for Karanja biodiesel using Box-Behnken design. Waste Biomass Valoriz 9(4):645–655

[11] Eddy NO, Ita BI (2011) QSAR, DFT and quantum chemical studies on the inhibition potentials of some carbozones for the corrosion of mild steel in HCl. J Mol Model 17(2):359–376

[12] Esmaeili H, Karami A, Maggi F (2018) Essential oil composition, total phenolic and flavonoids contents, and antioxidant activity of *Oliveria decumbens* Vent. (Apiaceae) at different phenological stages. J Clean Prod 198(10):91–95

[13] Food and Agriculture Organization (FAO). https ://www.fao.org/faost at/en/#data/QC. Accessed 19 Apr 2020

[14] Fox NJ, Stachowiak G (2007) Vegetable oil based lubricants: a review of oxidation. Tribol Int 40(7):1035–1046

[15] Freitas AR, Almeida LR, Sales FAM, Rios MAS (2015) Green methodology for synthesis of alkylated cardanol based on the green chemical principles. Prog Ind Ecol Int J 9(3):312–325

[15] Galano A, Alvarez-Idaboy JR (2013) A computational methodology for accurate predictions of rate constants in solution: application to the assessment of primary antioxidant activity. J Comput Chem 34(28):2430–2445

[16] Hehre WJ, Ditchfield R, Pople JA (1972) Self—consistent molecular orbital methods. XII. Further extensions of Gaussian—type basis sets for use in molecular orbital studies of organic molecules. J Chem Phys 56(5):2257–2261

[17] https://www.chemaxon.com. Accessed 2 Dec 2019.

[18] https://www.fiesp.com.br/mobile/noticia/?id=239879. Accessed 2 Dec 2019.

[19] Ilyas SU, Pendyala R, Narahari M (2017) Stability and thermal analysis of MWCNT-thermal oil-based nanofluids. Colloids Surf A 527(20):11–22

[20] Kajiyama T, Ohkatsu Y (2002) Effect of meta-substituents of phenolic antioxidants—proposal of secondary substituent effect. Polym Degrad Stab 75(3):535–542

[21] Kleinberg MN, Rios MAS, Buarque HLB, Parente MMV, Cavalcante CL Jr, Luna FMT (2017) Influence of synthetic and natural antioxidants on the oxidation stability of beef tallow before biodiesel production. Waste Biomass Valoriz 10(4):797–803

[22] Kök MV, Varfolomeev MA, Nurgaliev DK (2017) Crude oil characterization using TGA-DTA, TGA-FTIR and TGA-MS techniques. J Petrol Sci Eng 154:537–542

[23] Koopmans T (1934) Über die Zuordnung von Wellenfunktionen und Eigenwerten zu den Einzelnen Elektronen Eines atoms. Physica 1(1–6):104–113

[24] Leopoldini M, Russo N, Toscano M (2011) The molecular basis of working mechanisms of natural polyphenolic antioxidants. Food Chem 125(2):288–306

[25] Lomonaco D, Maia FJN, Mazzetto SE (2013) Thermal evaluation of cashew nutshell liquid as new bioadditives for poly(methyl methacrylate). J Therm Anal Calorim 111:619–626

[26] Lopes AAS, Carneiro EA, Rios MAS, Hiluy Filho JJ, Carioca JOB, Barros GG, Mazzetto SE (2008) Study of antioxidant property of a thiosphorated compound derived from cashew nut shell liquid in hydrogenated naphthenics oils. Braz J Chem Eng 25(1):119–127

[27] Lu T, Chen F (2012a) Multiwfn: a multifunctional wavefunction analyzer. J Comput Chem 33(5):580–592

[28] Lu T, Chen F (2012b) Quantitative analysis of molecular surface based on improved

Marching Tetrahedra algorithm. J Mol Graph Model 38:314–322

[29] Luna FMT, Rocha BS, Rola EM Jr, Albuquerque MCG, Azevedo DCS, Cavalcante CL Jr (2011) Assessment of biodegradability and oxidation stability of mineral, vegetable and synthetic oil samples. Ind Crops Prod 33(3):579–583

[30] Maia FJN, Ribeiro FWP, Rangel JHG, Lomonaco D, Luna FMT, Lima Neto P, Correia AN, Mazzetto SE (2015) Evaluation of antioxidant action by electrochemical and accelerated oxidation experiments of phenolic compounds derived from cashew nut shell liquid. Ind Crops Prod 67:281–286

[31] Martínez-Monteagudo SI, Saldaña MDA, Kennelly JJ (2012) Kinetics of non-isothermal oxidation of anhydrous milk fat rich in conjugated linoleic acid using differential scanning calorimetry. J Therm Anal Calorim 107(3):973–981

[32] Masoud MS, Ghareeb DA, Ahmed SS (2017) Synthesis, characterization, spectral, thermal analysis and computational studies of thiamine complexes. J Mol Struct 1137(5):634–648

[33] Micić DM, Ostojić SB, Simonović MB, Krstić G, Pezo LL, Simonović BR (2015) Kinetics of blackberry and raspberry seed oils oxidation by DSC. Thermochim Acta 601(10):39–44

[34] Mohammed MN, Atabani AE, Uguz G, Lay CH, Kumar G, AlSamaraae RR (2018) Characterization of Hemp (*Cannabis sativa* L.) biodiesel blends with euro diesel, butanol and diethyl ether using FT-IR, UV–Vis, TGA and DSC techniques. Waste Biomass Valoriz 2018:1–17

[35] Moreira R, Orsini RR, Vaz JM, Penteado JC (2017) Production of biochar bio-oil and synthesis gas from cashew nut shell by slow pyrolysis. Waste Biomass Valoriz 8(1):217–224

[36] Mothé CG, Vieira CR, Mothé MG (2013) Thermal and surface study of phenolic resin from cashew nut shell liquid cured by plasma treatment. J Therm Anal Calorim 114(2):821–826

[37] Neese F (2017) Software update: the ORCA program system, version 4.0, WIREs Computational Molecular Science, 8 (1)

[38] Nenadis N, Tsimidou MZ (2012) Contribution of DFT computed molecular descriptors in the study of radical scavenging activity trend of natural hydroxybenzaldehydes and corresponding acids. Food Res Int 48(2):538–543

[39] Neumann A, Jebens T, Wierzbicki V (2008) A method for determining oxidation stability of petrodiesel biodiesel, and blended fuels. Am Lab 40(4):22–26

[40] Nwankwo HU, Olasunkanmi LO, Ebenso EE (2017) Experimental, quantum chemical and molecular dynamic simulations studies on the corrosion inhibition of mild steel by some carbazole derivatives. Sci Rep 7:1–18

[41] Oliveira MA, Yoshida MI, Gomes ECL (2011) Análise térmica aplicada a fármacos e formulações farmacêuticas na indústria farmacêutica. Quím Nova 34:1224–1230

[42] Osorio E, Pérez EG, Areche C, Ruiz LM, Cassels BK, Flórez E, Tiznado W (2013) Why is quercetin a better antioxidant than taxifolin? Theoretical study of mechanisms involving activated forms. J Mol Model 19:2165–2172

[43] Paiva GMS, Freitas AR, Nobre FX, Leite CMS, Matos JME, Rios MAS (2015) Kinetic and thermal stability study of hydrogenated cardanol and alkylated hydrogenated cardanol. J Therm Anal Calorim 120(3):1617–1625

[44] Parker VD (1992) Homolytic bond (H–A) dissociation free energies in solution. Applications of the standard potential of the (H+/H. bul.) couple. J Am Chem Soc 114(19):7458–7462

[45] Parr RG, Yang W (1984) Density functional approach to the frontier-electron theory of chemical reactivity. J Am Chem Soc 106(14):4049–4050

[46] Pretsch E, Bühlmann P, Badertscher M (2009) Structure determination of organic compounds: tables of spectral data, 4th edn. Springer, Heidelberg

[47] Reda SY (2011) Avaliação da estabilidade de antioxidantes por análise térmica e seu efeito protetor em óleo vegetal aquecido. Food Sci Technol 31(2):475–480

[48] Rimarˇcík J, Lukeš V, Klein E, Ilˇcin M (2010) Study of the solvent effect on the enthalpies of homolytic and heterolytic N–H bond cleavage in p-phenylenediamine and tetracyano- p-phenylenediamine. J Mol Struct (Thoechem) 952(30):25–30

[49] Rios MAS, Mazzetto SE (2012) Thermal behavior of phosphorus derivatives of hydrogenated cardanol. Fuel Process Technol 96:1–8

[50] Rios MAF, Mazzetto SE, Carioca JOB, Barros GG (2007) Evaluation of antioxidant properties of a phosphorated cardanol compound on mineral oils (NH10 and NH20). Fuel 86(15):2416–2421

[51] Rios MAS, Santiago SN, Lopes AAS, Mazzetto SE (2010) Antioxidative activity of 5-*n*-pentadecyl-2-*tert*-butylphenol stabilizers in mineral lubricant oil. Energy Fuels 24(5):3285–3291

[52] Rios MAS, Santos FFP, Maia FJN, Mazzetto SE (2013) Evaluation of antioxidants on the thermo-oxidative stability of soybean biodiesel. J Therm Anal Calorim 112:921–927

[53] Silva G, Nakamura NM, Ilha K (2008) Estudo cinético da decomposição térmica do

pentaeretritol-tetranitrado (PETN). Quím Nova 31:2060–2064

[54] Silva GAM, Da Rós PCM, Souza LTA, Costa APO, Castro HF (2012) Physico-chemical, spectroscopical and thermal characterization of biodiesel obtained by enzymatic route as a tool to select the most efficient immobilized lipase. Braz J Chem Eng 29(1):39–47

[55] Sousa Rios MA, Mazzetto SE (2013) Effect of organophosphate antioxidant on the thermo-oxidative degradation of a mineral oil. J Therm Anal Calorim 111:553–559

[56] Speyer RF (1993) Thermal analysis of materials. CRC Press, New York

[57] Srivastava S, Gupta P, Sethi A, Singh RP (2016) One pot synthesis of Curcumin-NSAIDs prodrug, spectroscopic characterization, conformational analysis, chemical reactivity, intramolecular interactions and first order hyperpolarizability by DFT method. J Mol Struct 117(5):173–180

[58] Stepanić V, Gall TK, Lučić B, Marković Z, Amić D (2013) Bond dissociation free energy as a general parameter for flavonoid radical scavenging activity. Food Chem 141(2):1562–1570

[59] Syahir AZ, Zulkifli NWM, Masjuki HH, Kalam MA, Alabdulkarem A, Gulzar M, Khuong LS, Harith MH (2017) A review on bio-based lubricants and their applications. J Clean Prod 168(1):997–1016

[60] Wright JS, Johnson ER, DiLabio GA (2001) Predicting the activity of phenolic antioxidants: theoretical method, analysis of substituent effects, and application to major families of antioxidants. J Am Chem Soc 123(6):1173–1183

[61] Zhang H-Y (1999) Theoretical methods used in elucidating activity differences of phenolic antioxidants. J Am Oil Chem Soc 76(6):745–748

[62] Zhao H, Feng J, Zhu J, Yu H, Liu Y, Shi P, Wang S, Liu S (2020) Synthesis and application of highly efficient multifunctional vegetable oil additives derived from biophenols. J Clean Prod 242(1):1–9

CHAPTER 2 – ANTIOXIDANT ACTIVITY OF EUGENOL AND ITS ACETYL AND NITRODERIVATIVES: THE ROLE OF QUINONE INTERMEDIATES—A DFT APPROACH OF DPPH TEST[2]

RESUMO

Este trabalho investigou o potencial antioxidante de derivados de eugenol acetilados e nitrados por meio de análise estrutural e o mecanismo de transferência atômica de hidrogênio (HAT) pela teoria do funcional da densidade (DFT). As estruturas foram otimizadas pelo funcional híbrido M06-2X com conjunto de bases 6–31 + G(d,p), e o mecanismo HAT foi avaliado com radicais HO, HOO, CH 3O, DPPH. De acordo com dados experimentais de estudos anteriores, duas etapas de transferência de hidrogênio foram testadas. Os dados termodinâmicos mostraram que há necessidade de duas etapas de transferência atômica de hidrogênio a partir de antioxidantes, seguidas da formação de p-quinometanos (27, 28 e 29) para tornar a reação espontânea com o DPPH. Além disso, dados cinéticos teóricos mostraram que o sítio antioxidante preferido depende da instabilidade do radical atacante e confirmaram o perfil antioxidante para eugenol (1,4-alilbenzeno-1,2-diol) e nitroderivado 7 (5-alil- 3-nitrobenzeno-1,2-diol) no ensaio DPPH. Por fim, este estudo mostrou que o composto nitro 6 (4-alil-2-metoxi-6-nitrofenol) também possui atividade antirradicalar contra radicais menores, mas não é observado no experimento devido às características estruturais e quimiosseletividade do DPPH.

Palavras-Chave: Eugenol · Acetil e nitroderivados · DFT ·DPPH · Mecanismos de Transferências de Hidrogênio Atômico.

[2] Article published in the Journal of Molecular Modeling entitled "Antioxidant activity of eugenol and its acetyl and nitroderivatives: the role of quinone intermediates—a DFT approach of DPPH test," available at: https://doi.org/10.1007/s00894-022-05120-z

Antioxidant activity of eugenol and its acetyl and nitroderivatives: the role of quinone intermediates—a DFT approach of DPPH test

ABSTRACT

This work investigated the antioxidant potential of acetylated and nitrated eugenol derivatives through structural analysis and the mechanism of hydrogen atomic transfer (HAT) by density functional theory (DFT). The structures were optimized by the hybrid functional M06-2X with basis set 6–31 + G(d,p), and the HAT mechanism was evaluated with HO, HOO, CH_3O, DPPH radicals. In agreement with experimental data from previous studies, two steps of hydrogen transfer were tested. The thermodynamic data showed the need for two hydrogen atomic transfer steps from antioxidants, followed by the formation of *p*-quinomethanes (**27**, **28**, and **29**) to make the reaction spontaneous with DPPH. Furthermore, theoretical kinetic data showed that the preferred antioxidant site depends on the instability of the attacking radical and confirmed the antioxidant profile for eugenol (**1**, 4-allyl-2-methoxyphenol), and nitro-derivative **7** (5-allyl-3-nitrobenzene-1,2-diol) in the DPPH assay. Finally, this study showed that nitro compound **6** (4-allyl-2-methoxy-6-nitrophenol) also has anti-radical activity with smaller radicals but is not observed in the experiment due to structural characteristics and chemoselectivity of DPPH.

Keywords: Eugenol · Acetyl and nitro derivatives · Antioxidant · DFT · DPPH · Hydrogen atomic transfer mechanism

+

INTRODUCTION

In the last 600 million years, since the great oxidative event generated by cyanobacteria about 3.5 billion years ago, we have been constantly adapting to the oxidative environment that surrounds us through antioxidant mechanisms that aim to inhibit the primitive changes generated by oxygen free radicals present in the atmosphere. Oxidation inhibition modification of their physicochemical properties due to oxidation by reactive oxygen species (ROS), affecting performance and generating possible engine damage [1–3].

In turn, as a result of our evolutionary process, our body balances antioxidant and reactive oxidant species. However, as we age, excess reactive oxidant species alter this balance, resulting in the condition known as oxidative stress. This condition is associated with thrombosis, heart attacks, strokes, depression, and cancer [4]. Therefore, the search and development of new compounds with antioxidant properties are of interest to researchers in materials and health.

Eugenol (**1**), a well-known bioactive phenolic compound present in clove (*Syzygium aromaticum*), has different activity profiles as an analgesic, gastroprotective, anti-inflammatory, antibacterial, antifungal, antiviral, and anticancer [5]. During the metabolism of **1**, there is the formation of a *p*-quinomethane (**2**) which has an alpha, betaunsaturated system known as Michael acceptor, which is the toxicophoric group of this metabolite (Fig. 1). Inactivation of metabolite **2** occurs by adding glutathione (GSH) to the beta position of the *p*-quinomethane [6, 7].

Fig. 1 Structures of eugenol (**1**), *p*-quinomethane metabolite (**2**), and capsaicin (**3**)

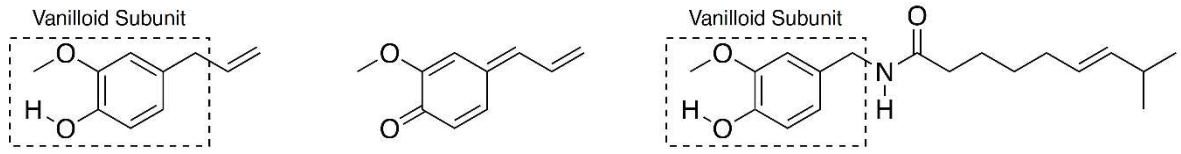

1: eugenol **2:** *p*-quinomethane **3:** capsaicin

Source: Prepared by authors. Reproduced with permission of Springer Nature.

However, as GSH is the most abundant antioxidant for the inactivation of free radicals, its decrease or depletion makes organs and tissues vulnerable to the action of reactive oxygen species (ROS) [8–11]. This toxicity profile led to studies of modified eugenol derivatives aiming to reduce the formation of **2**. In this context, studies carried out with the insertion of nitro groups (NO_2) in the aromatic ring and acetyl (CH_3CO) in the phenolic

hydroxyl groups showed the loss of antioxidant activity in the tests with 1,1-diphenyl-2-picrylhydrazyl radical (DPPH$^{\bullet}$) assay [12].

Additionally, studies of the antioxidant activity of capsaicin (**3**) (Fig. 1), a vanilloid compound such as eugenol showed the relevance of the benzyl radical in the antioxidant profile of this compound. Density functional theory (DFT) calculations in the gas phase revealed that the benzyl site of **3** is 3.3 kcal mol^{-1}, more stable than the phenoxyl site [13]. Furthermore, when the implicit solvation model was applied, the benzyl radical was 0.2 more stable than the phenoxyl radical [14].

The presence of the vanilloid subunit in **1** and **3**, in principle, equates to their phenoxyl and benzyl antioxidant sites. However, the possibility of benzyl-allylic radical formation at **1** is even more stable than the benzyl radical at **3,** suggesting that the oxidation mechanism by hydrogen atomic transfer (HAT) should occur at this site [13]. Nevertheless, this is not observed experimentally since acetylated eugenol derivatives do not show antioxidant activity in the DPPH test [12].

In turn, the kinetic parameters obtained by DFT studies for capsaicin (**3**) showed that the phenoxyl radical formation reaction is faster than that of the benzylic radical. This trend increases the higher the solvent polarity and the lower the reactivity of the sequestered radical, which may explain the non-antioxidant profile of some of these derivatives [12, 14].

Most computational chemistry studies address the use of bond dissociation energy (BDE) to assess antioxidant activity. However, in the case of reactivity studies by the HAT mechanism, a single-step reaction with simple radicals such as hydroxyl (HO$^{\bullet}$) and peroxyl (HOO$^{\bullet}$) has been the approach used [13–18]. However, there is evidence that a single hydrogen transfer is not sufficient to describe the antioxidant mechanism for eugenol.

The first clue is that the stoichiometry of the eugenol-DPPH reaction is approximately 1:2 [19]. The second is that the in vitro oxidation of eugenol by silver oxide leads to *p*-quinomethane (**2**) [8]. Third, the main eugenol metabolite excreted in human urine has the SH group added at position 5 of the saturated eugenol aromatic ring [10]. This kind of product is commonly formed via Michael's addition to the *p*-quinomethane intermediate.

Although the BDE analysis is efficient in some studies, it does not consider the radical structure that will react with the antioxidant molecule. The use of simple radicals does not describe the interaction of the substituent groups of the reactants well, as in the case of DPPH $^{\bullet}$, which is a bulky radical, neglecting both a steric hindrance and electrostatic repulsion effects.

In this work, we revisit the work of Hidalgo *et al*. [12], using DFT to assess the antioxidant activity of eugenol and its derivatives. Unlike other studies, a two-step HAT mechanism was considered to evaluate the role of quinone formation in the thermodynamic stabilization of the reaction. For this simulation, radicals of different volumes and reactivities such as HO $^{\bullet}$, HOO$^{\bullet}$, $CH_3O^{\bullet}$, and DPPH $^{\bullet}$ were used to evaluate the stereo and chemoselectivity of the antioxidant sites in the eugenol derivatives studied by Hidalgo et al., [12] (Fig. 2).

Fig. 2 Structures of eugenol (1) and its derivatives 4–8

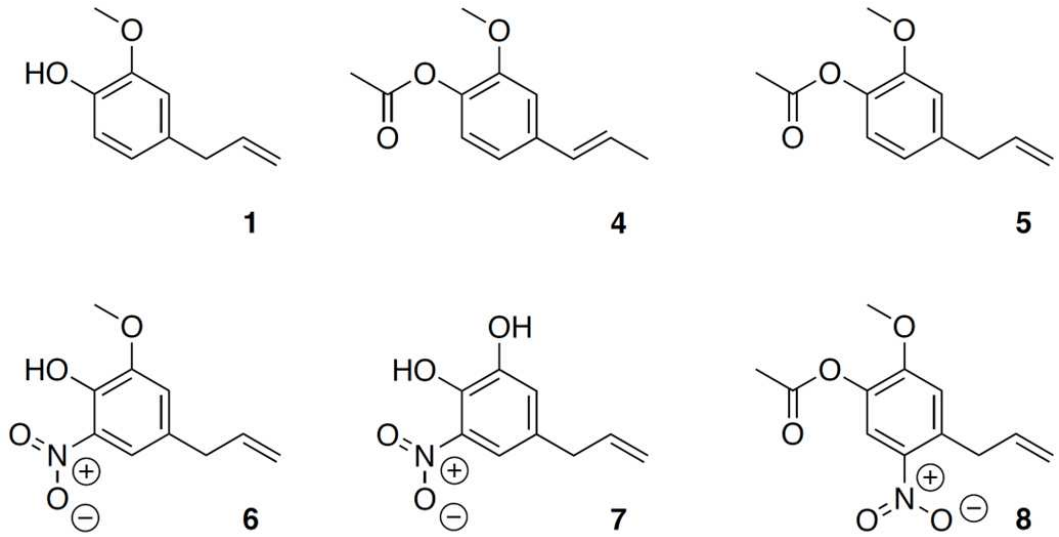

Source: Prepared by authors. Reproduced with permission of Springer Nature

MATERIALS AND METHODS

Conformational Analysis

Conformational analysis was performed in two steps. In the first, the 10 lowest energy structures were obtained using the Conformers Plugin with the MMFF94 force field present in ChemAxon's Marvin Sketch V. 18.1.0. Structures with an energy difference of 0.2 kJ mol $^{-1}$ were considered identical, only structures with an energy difference greater than this diversity range. The optimization limit used was "very strict."

In the second step, the structures obtained were reoptimized using the DFT-M06-2X [20] method with the 6–31 + G(d,p) [21, 22] basis set using Gaussian 09 program from Gaussian INC. This function has better accuracy than the well-known B3LYP for obtaining energy barriers for transition states [20]. The calculations were performed in the gas phase and at 298.15 K, using the tight convergence criterion. Frequency calculations were made to confirm

the correct minimization of the structures through the absence of imaginary frequencies. Only the minimum energy structure (with the lowest Gibbs free energy – G) of each compound was used for the next calculation steps in this work.

Thermodynamic analysis

Reaction spontaneity was evaluated using the Free Energy of Reaction ($\Delta_r G$) data for the HAT mechanism. Hydroxyl ($HO^{\bullet}$), peroxyl ($HOO^{\bullet}$), methoxyl ($CH_3O^{\bullet}$), and DPPH ($DPPH^{\bullet}$) radicals were used. In addition, phenolic, benzylic, and allylic sites were evaluated as atomic hydrogen donors. In the first step, the antioxidant (ArXH) transferred a single atomic hydrogen to the free radical ($R^{\bullet}$), forming a more stable pair of radical ($ArX^{\bullet}$) and molecule (RH) (Eq. 1). $\Delta_r G$ was obtained by subtracting G of the reactants from G of the products (Eq. 2),

$$\mathrm{ArXH} + \mathrm{R}^{\bullet} \rightarrow \mathrm{ArX}^{\bullet} + \mathrm{RH} \quad (1)$$

$$\Delta_r \mathrm{G} = \mathrm{G(RH)} + \mathrm{G(ArX}^{\bullet}) - \mathrm{G(R}^{\bullet}) - \mathrm{G(ArXH)} \quad (2)$$

where X could be oxygen for phenolic sites or carbon for both methoxyl, benzyl-allilyc, and allylic sites. The quinone formation overall reaction was also considered for the compounds **1**, **6,** and **7** structures (Eq. 3). The formation of *p*-quinomethane for the three structures and *ortho*-benzoquinone for **7** was considered. In addition, the $\Delta_r G$ for the formation of quinones (QN) was computed (Eq. 4).

$$\mathrm{ArXH} + 2\mathrm{R}^{\bullet} \rightarrow \mathrm{QN} + 2\mathrm{RH} \quad (3)$$

$$\Delta_r \mathrm{G} = 2\mathrm{G(RH)} + \mathrm{G(QN)} - 2\mathrm{G(R}^{\bullet}) - \mathrm{G(ArXH)} \quad (4)$$

Kinetics analysis

Reaction kinetics were evaluated from activation-free energy ($\Delta G^{\ddagger}$) and rate constant (k) at 298.15 K. Transition states (TS) were obtained using the QST3 algorithm [23, 24] of Gaussian 09 and confirmed by frequency analysis, based on the existence of only one imaginary frequency associated to a vibration in the direction of proton transfer (bonding stretching or bending) [25, 26]. For the first HAT step, $\Delta G^{\ddagger}$ was obtained by subtracting G of the reactants from G of TS (Eq. 5).

$$\Delta G^{\ddagger} = G(TS) - G(AOH) - G(R^{\bullet}) \quad (5)$$

For the second HAT step, the attacking radical ($R^{\bullet}$) receives a hydrogen atom from the radical ($ArX^{\bullet}$), producing a quinone. In this step, $\Delta G^{\ddagger}$ was obtained following Eq. 6:

$$\Delta G^{\ddagger} = G(TS) - G(ArX^{\bullet}) - G(R^{\bullet}) \quad (6)$$

Rate constants (k) for bimolecular reaction were computed from values of $\Delta G^{\ddagger}$ through the Eyring equation (Eq. 7) [27],

$$k = \frac{k_B T}{h} e^{-\Delta G^{\ddagger}/RT} \quad (7)$$

where k_B is Boltzmann constant, T is absolute temperature, *h* is Planck constant, and R is perfect gas constant. For this study, a temperature of 298.15 K was considered.

Data analysis

Data analysis was performed by multiple linear regression using Microsoft ® Excel's ® proj.lin function. The *ln*(C_0/Ct) values after 30 min in the DPPH test were used as the response variable [12]. The absence and presence of functional groups, as well as reaction data and activation free energy, in addition to the rate constant, were used as regressors. For the models obtained, residue (b) was considered equal to zero. In the absence of specific functional groups for the HAT mechanisms, the molecule should not have antioxidant activity ($y = 0$).

Natural bond order

NBO (natural bond order) analysis [28] was used to determine Wiberg bonding orders [28] and identify electronic factors that contributed to the stabilization of free radical reactants. During the formation of the radical, the transfer of atomic hydrogen and the presence of unpaired electrons cause a change in the geometry of the molecule seen by the alteration of the values of bond length and angles. In this case, the incentive to make a connection indicates mesomeric or hyperconjugative effects.

RESULTS AND DISCUSSION

Part A. Thermodynamics of radical formation

The first part of the study aimed to obtain the free energy values of the reaction of antioxidants with HO $^{\bullet}$, HOO$^{\bullet}$, and $CH_3O^{\bullet}$ e DPPH$^{\bullet}$.

Stability of the tested radicals

The regular radical stability (RS) was calculated by the difference of energy between free energies of formation of free radical R$^{\bullet}$ and the molecule formed by capture of atomic hydrogen from antioxidant (HR) as described by Eq. 8.

$$RS = G(R^{\bullet}) - G(HR) \quad (8)$$

The lower the value of RS, the more stable the radical and the more selective the hydrogen abstraction (Table 1). RS values were normalized to compare the stability among radicals.

Table 1 Regular (RS) and relative stabilities (ΔRS) of radicals

Radical	RS (kcal mol^{-1})	ΔRS (kcal mol^{-1})
HO$^{\bullet}$	427.7	39.1
$CH_3O\bullet$	412.7	24.1
HOO$^{\bullet}$	395.7	7.1
DPPH$^{\bullet}$	388.6	0.0

Source: Prepared by authors. Reproduced with permission of Springer Nature

For this calculation, the value of RS for DPPH$^{\bullet}$ was considered zero, and a value of relative stability of the radical (ΔRS) was obtained through Eq. 9.

$$\Delta RS = RS - RS(DPPH) \quad (9)$$

These values show HO$^{\bullet}$ as the most unstable radical. Both HOO $^{\bullet}$ and $CH_3O^{\bullet}$ are less reactive than hydroxyl radicals due to the hyperconjugation effect. Table 2 shows the Wiberg analysis of bond order (WBO) for molecules and their respective radicals.

Table 1 Regular (RS) and relative stabilities (ΔRS) of radicals

Bond	HR	WBO	R•	WBO
O–O	HOOH	1.0130	HOO•	1.2031
C–O	CH_3OH	0.9483	CH_3O•	1.0649

Source: Prepared by authors. Reproduced with permission of Springer Nature

The increase of WBO of the O–O bond from 1.0130 to 1.2031 shows the higher stabilization of HOO• by hyperconjugation, which implies a less reactivity of this radical than CH_3O•. The DPPH• is the most stable radical due to the mesomeric effect by conjugating the nitrogen radical with the tri-nitrated ring.

Selectivity of antioxidant sites

Δ_rG values for reactions between eugenol and its derivatives with HO •, HOO•, CH_3O•, and DPPH• are shown in Table 3. These results show the trends for hydrogen loss of the functional groups studied: Benzyl-Allyl (BnAll) ~ allyl (All) > phenoxyl (PhO) > methoxyl (MeO) > acetyl (Ac) (Fig. 3).

Fig. 3 Antioxidant sites for **1** and its derivatives **4**–**8**

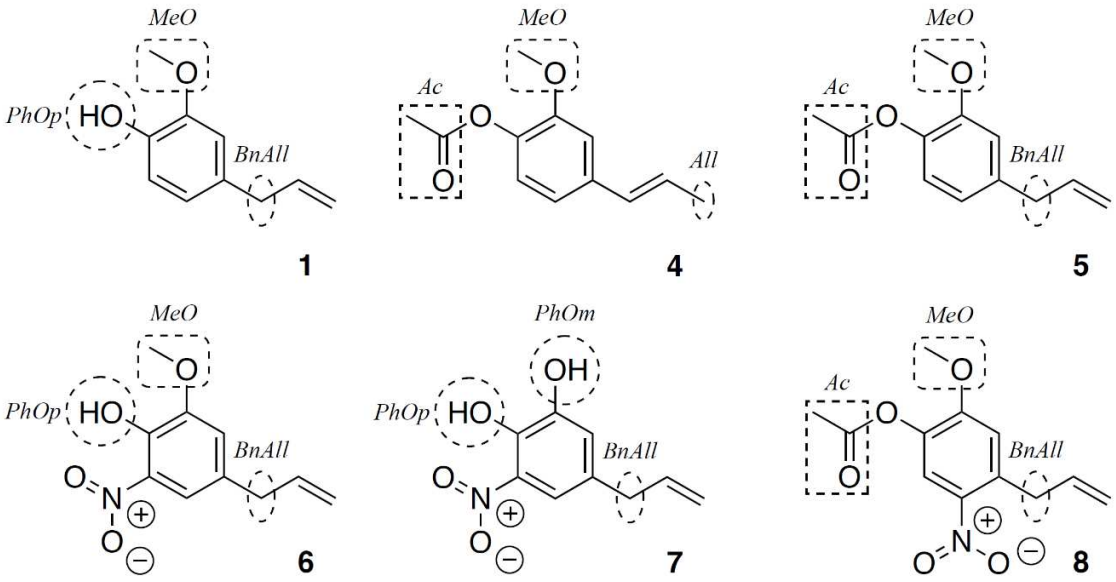

Source: Prepared by authors (2022). Reproduced with permission of Springer Nature.

The higher selectivity of the allylic and benzylic radicals is due to the isoenergetic resonance of the unpaired electron with the π* orbitals of the allyl group and the aromatic ring, which allow better dispersion of the unpaired electron density by the structure, leading to a more stable radical.

Among the antioxidants evaluated, eugenol (**1**) proved to be the most favorable molecule to transfer atomic H in the first step of reaction showing more negative $\Delta_r G$ of − 38.9 kcal mol^{-1} with the HO • radical through the BnAll site.

The **6** and **7** structures have stronger hydrogen bonds (OH---ON) than those present in **1** (OH---OCH_3) due to the more significant electrostatic attraction between the phenolic OH and the nitro group. This more robust binding increases $\Delta_r G$ from 4.0 to **6** and 3.1 kcal mol^{-1} for **7** for the phenolic site compared to eugenol (**1**). The nitro group also influences the formation of the benzyl-allyl radicals (BnAll), increasing $\Delta_r G$ by approximately1.0 kcal mol^{-1} for **6**, **7,** and **8**. The presence of the acetyl group destabilizes the BnAll radical of **5** increasing the value of $\Delta_r G$ by 0.9 kcal mol^{-1} concerning **1**.

Radical selectivity for hydrogen abstraction

The reactions with the HO• radical showed negative values for the free energy of the reaction, showing that any H atom of the evaluated antioxidant sites can be spontaneously transferred to this radical (Fig. 4).

Fig. 4 Possible theoretical radicals (**9–26**) formed from the abstraction of hydrogen by the HO• radical.

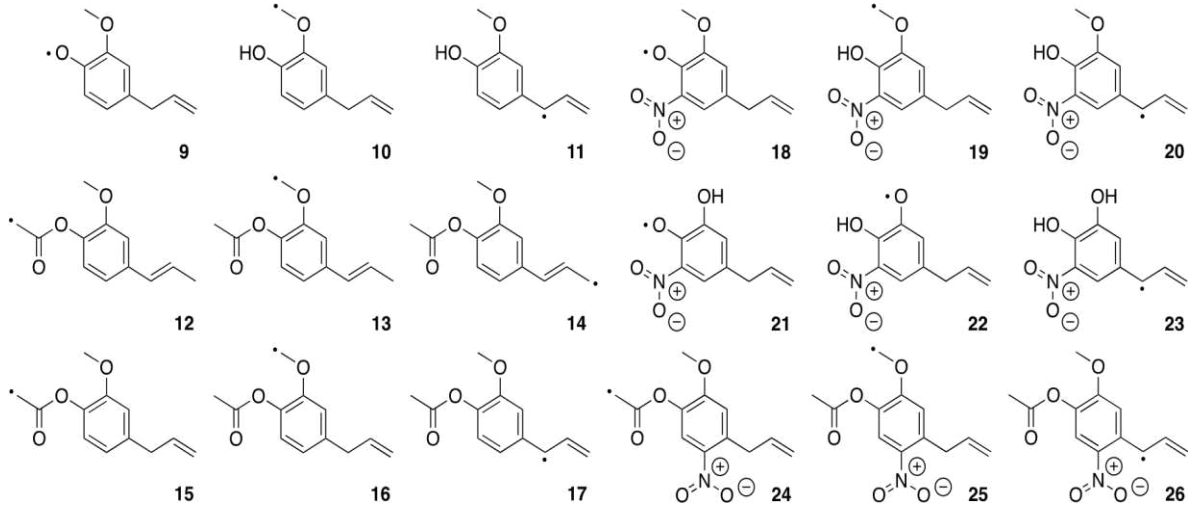

Source: Prepared by authors (2022). Reproduced with permission of Springer Nature

$CH_3O^{\bullet}$ accepted hydrogen from almost all assessed sites, except for the formation of the eugenol methylenoxyl radical ($^{\bullet}CH_2O$), which presented a positive reaction-free energy change of 1.2 kcal mol^{-1}. The $HOO^{\bullet}$ radical proved to be quite selective, reacting only with allylic and benzylic sites due to its lower reactivity. None of the sites showed a spontaneous reaction with $DPPH^{\bullet}$.

The literature indicates that the reaction of DPPH with eugenol (**1**) follows a 1:2 reaction stoichiometry, corroborating the formation of quinone excreted as a metabolite of **1** in human urine.

Part B. Kinetics of radical formation

In general, the less stable the attacking radical, the lower the free energy of activation. In this sense, we evaluated the influence of reactive radical stability through their activation of free energies and rate constants (Table 4).

Table 4 Gibbs free energies of activation ($\Delta G^{\ddagger}$) and rate constants (k) for the first hydrogen atom transfer at 298.15 K

Compound	Site	$HO^{\bullet}$		$CH_3O^{\bullet}$		$HOO^{\bullet}$	
		$\Delta G^{\ddagger a}$	k^b	$\Delta G^{\ddagger a}$	k^b	$\Delta G^{\ddagger a}$	k^b
9	PhO*p*	6.3	$1.5 \cdot 10^{8}$	10.6	$1.1 \cdot 10^{5}$	17.1	1.8
10	MeO	7.2	$3.5 \cdot 10^{7}$	14.2	$2.4 \cdot 10^{2}$	25.0	$2.9 \cdot 10^{-6}$
11	BnAll	6.4	$1.2 \cdot 10^{8}$	12.5	$4.1 \cdot 10^{3}$	20.0	$1.4 \cdot 10^{-2}$
12	Ac	9.2	$1.1 \cdot 10^{6}$	18.2	$3.0 \cdot 10^{-1}$	28.4	$1.0 \cdot 10^{-8}$
13	MeO	7.8	$1.3 \cdot 10^{7}$	15.8	$1.6 \cdot 10^{1}$	21.3	$1.5 \cdot 10^{-3}$
14	All	8.3	$5.3 \cdot 10^{6}$	13.8	$5.0 \cdot 10^{2}$	23.1	$7.2 \cdot 10^{-5}$
15	Ac	10.7	$9.6 \cdot 10^{4}$	18.7	$1.3 \cdot 10^{-1}$	28.6	$7.0 \cdot 10^{-9}$
16	MeO	7.9	$1.1 \cdot 10^{7}$	15.4	$3.3 \cdot 10^{1}$	24.7	$5.1 \cdot 10^{-6}$
17	BnAll	7.5	$2.0 \cdot 10^{7}$	12.8	$2.4 \cdot 10^{3}$	20.9	$3.0 \cdot 10^{-3}$
18	PhO*p*	11.0	$5.1 \cdot 10^{4}$	14.8	$8.5 \cdot 10^{1}$	19.0	$7.2 \cdot 10^{-2}$
19	MeO	8.0	$9.1 \cdot 10^{6}$	15.5	$2.8 \cdot 10^{1}$	24.8	$4.3 \cdot 10^{-6}$
20	BnAll	7.5	$1.9 \cdot 10^{7}$	12.8	$2.5 \cdot 10^{3}$	20.6	$5.0 \cdot 10^{-3}$
21	PhO*p*	12.5	$4.2 \cdot 10^{3}$	15.6	$2.3 \cdot 10^{1}$	24.6	$6.2 \cdot 10^{-6}$
22	PhO*m*	8.2	$6.3 \cdot 10^{6}$	13.9	$3.8 \cdot 10^{2}$	23.5	$3.4 \cdot 10^{-5}$
23	BnAll	8.4	$4.6 \cdot 10^{6}$	14.2	$2.6 \cdot 10^{2}$	21.3	$1.4 \cdot 10^{-3}$
24	Ac	10.5	$1.2 \cdot 10^{5}$	18.2	$2.7 \cdot 10^{-1}$	32.8	$5 \cdot 10^{-12}$
25	MeO	2.9	$4.6 \cdot 10^{10}$	10.6	$1.1 \cdot 10^{5}$	24.1	$1.2 \cdot 10^{-5}$
26	BnAll	5.7	$3.9 \cdot 10^{8}$	12.3	$5.5 \cdot 10^{3}$	20.4	$6.6 \cdot 10^{-3}$

Source: Prepared by authors (2022). Reproduced with permission of Springer Nature

In all evaluated sites, the $HO^{\bullet}$ showed to be the fastest to abstract the atomic H, showing lower values of $\Delta G^{\ddagger}$. The only exception found was the formation of BnAll radical (**20**), where the lowest energy barrier found was for the attack of the $CH_3O^{\bullet}$ radical. The presence of the nitro group does not allow the methoxy group to be in the same plane as the ring, which aids the formation of a stable 6-membered ring intermediate.

Influence of radical reactivity

The reaction of eugenol (1) with $HO^{\bullet}$ showed $\Delta G^{\ddagger}$ value of 6.3 kcal mol^{-1} for the formation of the phenoxyl radical (9) and 6.4 kcal mol^{-1} for the benzylic (11) ones. In turn, in

the reactions with HOO $^{\bullet}$ and $CH_3O^{\bullet}$, as the radical becomes more stable, 1 showed a kinetic preference to oxidize the phenolic group concerning the benzylic. Structurally, nitro derivatives **6** and **7** differ in the substitution pattern at the *meta* position of their aromatic rings by the presence of methoxy (MeO) and hydroxy (OH) groups, respectively. Thus, **7** presents an additional hydrogen abstraction site to form a second phenoxyl radical (**22**, PhO*m*).

The nitro groups at **6** and **7** showed an increase in the free energy of activation for the formation of PhO*p* (**18** and **21**) due to the strong hydrogen bond with the hydroxyl, which makes the hydrogen transfer process difficult. In turn, Bn$^{\bullet}$All formation is kinetically favored for **6** (**20**, $\Delta G^{\ddagger}$ 7.5 kcal mol^{-1}) but destabilized at **7** due to the effect of the meta hydroxyl group (**23**).

Thus, the formation of the PhO*m* (**22**) is preferred with a better $\Delta G^{\ddagger}$ value of 8.2 kcal mol $^{-1}$. Separately, thermodynamic and kinetic data for a single transferred atomic hydrogen show that the antioxidant activity of eugenol (**1**) is better than that of its derivatives **4**–**8**. However, these results appear inconsistent with the literature data, where **7** has a higher antioxidant capacity than **1**, and **6** has no activity in the DPPH assay [12].

Part C. Thermodynamics of quinone formation

The first hydrogen transfer did not provide satisfactory answers to justify the reactivity or not of eugenol (**1**) and its derivatives **4**–**8**. In addition, none were spontaneous with the DPPH radical considering 1:1 stoichiometry. This observation encouraged us to investigate the second abstraction to explain the literature data. Only structures **1**, **6**, and **7** can form *para*-quinomethane, and only **7** can generate an *ortho*-benzoquinone (Fig. 5).

Fig. 5 Quinones **27**–**30** generated from derivatives **1**, **6**, and **7**

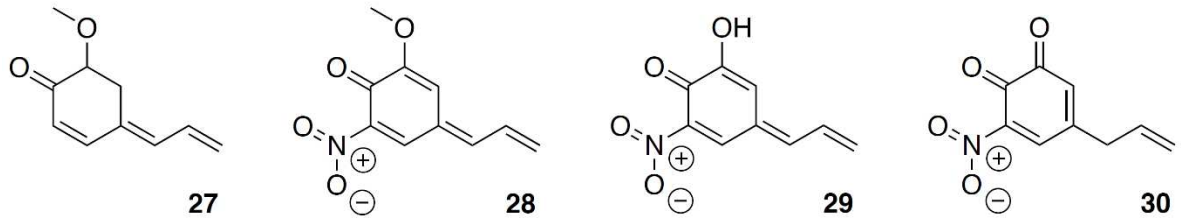

Source: Prepared by authors (2022). Reproduced with permission of Springer Nature

We evaluated thermodynamics of quinone formation by comparing the $\Delta_r G$ for the reaction between ArXH and two equivalents of R$^{\bullet}$. Table 5 shows the values of $\Delta_r G$ with radicals for two consecutive HAT steps.

Table 5. Free energies of reaction ($\Delta_r G$) for the formation of quinones

Compound	Quinone	$HO^{\bullet}$	$CH_3O^{\bullet}$	$HOO^{\bullet}$	$DPPH^{\bullet}$
			$\Delta_r G$ (kcal mol^{-1})[a]		
27	*p*QM	–91.4	–61.4	–27.5	–13.2
28	*p*QM	–85.0	–54.9	–21.1	–6.8
29	*p*QM	–86.9	–56.9	–23.0	–8.7
30	*o*BQ	–69.9	–39.9	–6.0	+ 8.3

*Isolated Reactants; a. 298.15 K; Abbreviations: *p*QM, *para*-Quinomethane; *o*BQ, *ortho*-Benzoquinone

Source: Prepared by authors (2022). Reproduced with permission of Springer Nature

The results show that the less stable the reactive radical, the more spontaneous is the formation of quinones. Furthermore, *p*-quinomethanes (**27**–**29**, *p*QM) formation was more spontaneous than *o*-benzoquinone (**30**, *o*BQ), probably due to electrostatic repulsion between lone pairs at the three oxygen centers in **30** (Scheme 1).

The structures that have the higher tendency to form *p*-quinomethane are **1** (− 91.4 kcal mol^{-1}), **7** (− 6.9 kcal mol^{-1}), and **6** (− 86.6 kcal mol^{-1}), where the one formed from **6** is only 0.3 kcal mol^{-1} less stable than the one from **7**.

For the three structures analyzed, the formation of the *p*-quinomethanes (*p*QM) showed spontaneous reaction with $DPPH^{\bullet}$. The formation of *ortho*-quinone (*o*BQ) presented $\Delta_r G$ of + 8.3 kcal mol^{-1}, suggesting that this mechanistic route is the least favorable to occur. The structural inability to form *p*QM may explain the negative result of antioxidant activity of the derivatives **4**, **5**, and **8** (Fig. 2) in the DPPH assay. However, the experimental data for **6** is still nuclear.

Part D. Kinetics of quinone formation

Obtaining the transition state for the formation of quinones was performed from the most stable radical of each structure. For compounds **1** and **7**, we used the phenoxyl radicals PhO*p* (**9**) and PhO*m* (**22**), while for **6** and **7**, their respective benzyl-allyl radicals (**20** and **23**) (Scheme 1). Table 6 shows the values of $\Delta G^{\ddagger}$ and k for quinone formation.

Scheme 1 Formation of the *p*-quinomethanes (**27**-–**29**) and o-benzoquinone (**30**)

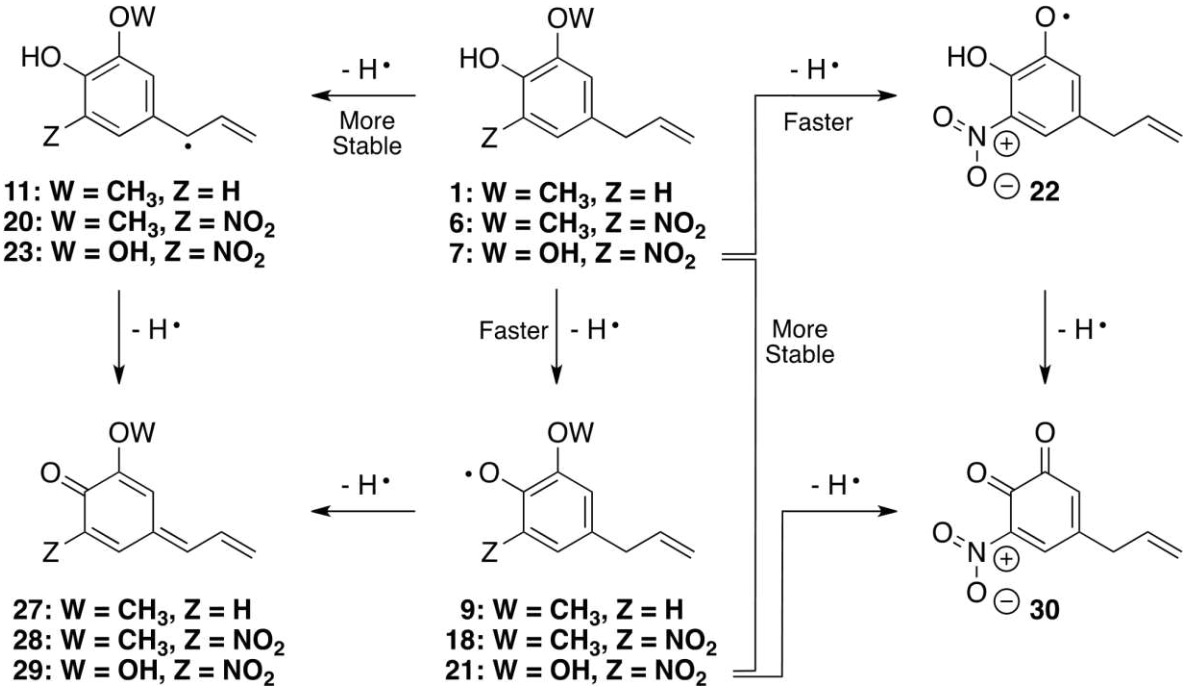

Source: Prepared by authors (2022). Reproduced with permission of Springer Nature

Likewise, as for the transition state of the first HAT, the free energy of activation for the second HAT is lower the less stable the attacking radical. The value of $\Delta G^{‡}$ is 7.3 kcal mol^{-1} in reaction of **1** with HO$^{\bullet}$ and shows only hydrogen transfer, as expected. However, the second transfer to **6** and **7** proceeds differently.

Table 6. Gibbs free energies of activation ($\Delta G^{‡}$) and rate constants (k) in for quinone formation at 298.15 K

Compound	Quinone	HO$^{\bullet}$		$CH_3O^{\bullet}$		HOO$^{\bullet}$	
		$\Delta G^{‡a}$	k^b	$\Delta G^{‡a}$	k^b	$\Delta G^{‡a}$	k^b
27	*p*QM	7.3	$2.9\cdot10^{7}$	11.5	$2.3\cdot10^{4}$	18.6	$1.5\cdot10^{-1}$
28	*p*QM	–3.3	$1.6\cdot10^{15}$	10.0	$2.7\cdot10^{5}$	24.9	$3.3\cdot10^{-6}$
29	*p*QM	7.3	$3.0\cdot10^{7}$	11.3	$3.2\cdot10^{4}$	17.2	1.5
30	*o*BQ	5.5	$5.9\cdot10^{8}$	19.5	$3.1\cdot10^{-2}$	38.0	$8\cdot10^{-16}$

*Isolated Reactants; *p*QM, para-quinomethane; *o*BQ, ortho-benzoquinone

Source: Prepared by authors (2022). Reproduced with permission of Springer Nature

Scheme 2 shows possible radical intermediates to form quinones in compounds **1**, **6**, and **7**.

Scheme 2 Sequence of intermediates for the formation of quinones.

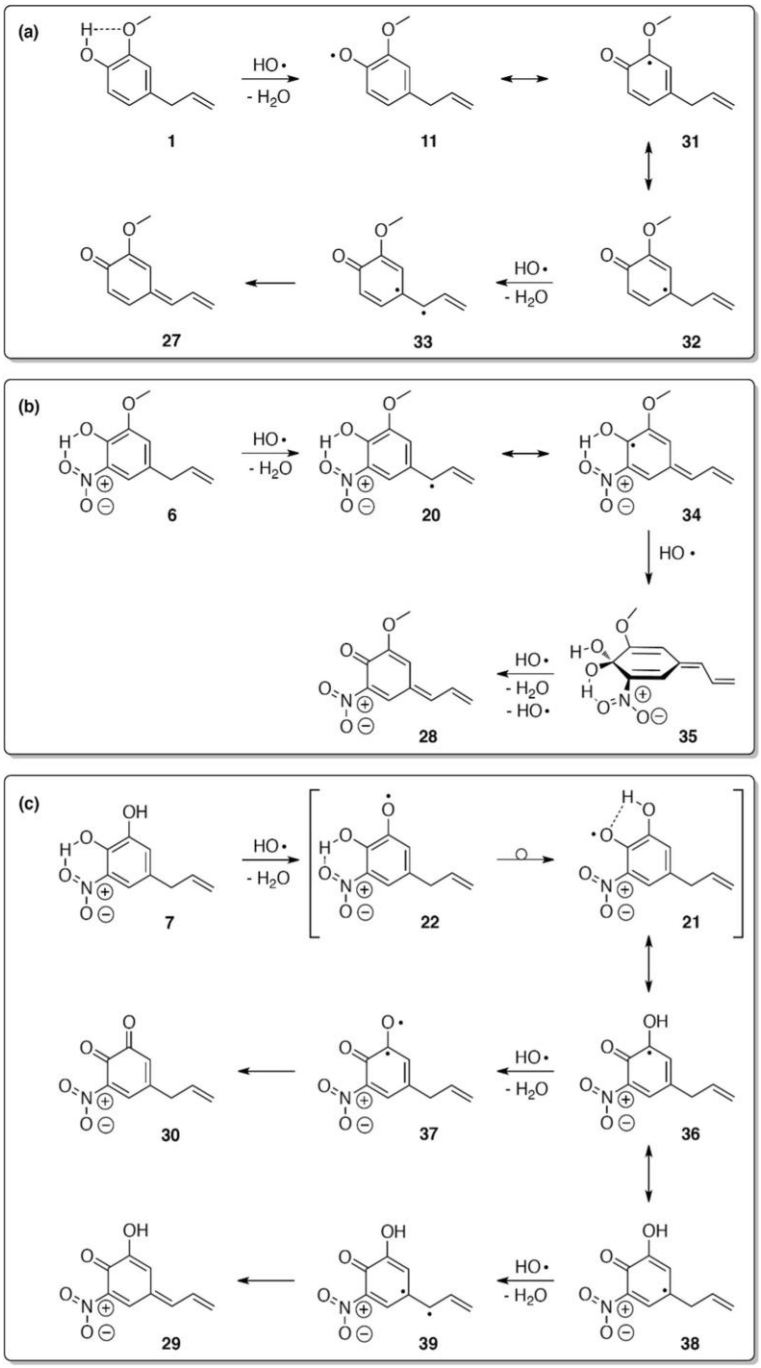

a compound **1**, via radical PhO*p* (**9**), to form *p*-quinomethane **27**; **b** compound **6**, via radical BnAll (**20**), to form *p*-quinomethane **28**; **c** compound **7,** via radical PhO*m* (**22**) followed rearrangement to radical PhO*p* (**21**), to form *p*-quinomethane **29** and *o*-benzoquinone **30.**

Source: Prepared by authors (2022). Reproduced with permission of Springer Nature.

For compound **1** (a), which presents intramolecular hydrogen bonding (HBi) between the 4-OH (hydrogen bond donor—HBD) and 3-OMe (hydrogen bond acceptor—HBA) groups, the first hydrogen abstraction occurs at the 4-OH group leading to the PhO*p* radical (**11**). In turn, electron delocalization from radical **11** leads to cyclohexadienone radicals **31** and **32**. The second hydrogen abstraction from **32** generates the diradical **33**, forming *p*-quinomethane **27**.

Considering compound **6** (b), in the face of HBi between the hydrogen of the 4-OH group and the 5-NO_2 group, the formation of the BnAll radical (**20**) occurs first, followed by electron delocalization generating the radical intermediate **34**. In turn, **34** undergoes the addition of the $HO^{\bullet}$ radical to form ketal **35**, stabilized by intramolecular hydrogen bonds.

The calculation of the IRC in the gas phase showed a concerted mechanism with the transfer of phenolic hydrogen (4-OH) and elimination of water to form p-quinomethane **28**. However, as this transfer presents a 4-membered transition state with polar characteristics, we consider the participation of a third $HO^{\bullet}$ radical. In this sense, the $HO^{\bullet}$ could work as a catalyst to abstract hydrogen from the 4-OH group while forming **28** and releasing the $HO^{\bullet}$ added in the previous step.

Finally, compound **7** has the possibility of forming two types of quinones: o-benzoquinone and *p*-quinomethane. For **7**, which presents similar HBi compound **6**, the first abstraction of hydrogen occurs on the 3-OH group forming the kinetically favored PhO*m* radical (**22**). Then, an intramolecular hydrogen abstraction (IHA) rearrangement generates the thermodynamically more stable PhO*p* (**21**) radical.

In turn, electron delocalization of orthosemiquinone **21** yields cyclodienone **36** with the radical at carbon 3 that contains a phenolic group 3-OH restored after IHA. Then, the second hydrogen abstraction at the phenolic group 3-OH leads to the diradical **37** to form *o*-benzoquinone **30**. On the other hand, electronic delocalization of intermediate **36** produces cyclodienone **38** with the radical at the *ipso* carbon. Then, the second hydrogen abstraction at the benzyl-allyl methylene group leads to the diradical **39** to finally form *p*-quinomethane **29**.

The calculations also showed that structure **34** is susceptible to adding $HOO^{\bullet}$ and $CH_3O^{\bullet}$ radicals to carbon 4, forming 4- and 5-membered rings, 4-OH---$^{\bullet}OCH_3$ and 4-OH---$^{\bullet}OOH$, respectively. The formation of these intermediates is responsible for lowering the activation energy for the second stage HAT with $HO^{\bullet}$ and $CH_3O^{\bullet}$ radicals with the nitrated derivatives concerning the first stage.

On the other hand, the second hydrogen transfer step from the reaction of the derivatives **6** and **7** with $HOO^{\bullet}$ proved to be slower than the first step. These results suggest that the less stable the radical, the greater the ease of forming *p*-quinomethanes in nitrated derivatives.

As DPPH$^{\bullet}$ is more stable than HOO $^{\bullet}$, it is expected to be kinetically more susceptible to quinone formation in the reaction with eugenol (**1**) than with **6** and **7**. However, as structural analysis shows the formation of *p*-quinomethanes as the key to the results of the DPPH test, the better profile for compound **7** may be associated with the amount of hydrogen abstraction sites and the possibility of forming an additional ortho-benzoquinone.

Part E. Analysis of structure, thermochemistry, and reactivity

For a better understanding of the system, from the data obtained, linear regressions were performed with the data: (a) structural, (b) thermodynamic, and (c) kinetic of the molecules.

Structural aspects

For the structural analysis, multiple linear regression was performed to correlate the antioxidant activity with specific functional groups. For this, we assigned values 1 for the presence or 0 for the absence of a functional groups in the antioxidant structure.

Having the allyl group as the ipso reference carbon, we used seven variables for regression analysis: (i) presence of a phenol group at position 4 (4-OH); (ii) the presence of the phenol group at position 3 (3-OH); (iii) the presence of a nitro group at position 5 (5-NO_2); (iv) the presence of a nitro group at position 6 (6-NO_2); v) the possibility of formation of benzyl-allyl radicals (BnAll); (vi) possibility of *p*-quinomethane (*p*QM), and (vii) possibility of *o*-benzoquinone formation (*o*BQ).

For example, according to Fig. 3, it is possible to identify that eugenol (**1**) has a phenolic group at position 4 (4-OH), which can form benzyl-allyl radicals (BnAll) and is capable of generating *p*-quinomethane (*p*QM). In this sense, the value 1 must be assigned for all these structural attributes. On the other hand, structure **1** does not have a phenolic group at position 3 (3-OH) and, therefore, cannot form *o*-benzoquinones (*o*BQ), being assigned 0 values for these variables.

Finally, antioxidant activity (AA), defined as ln(C_0/Ct) from the results of Hidalgo et al. [12], was used as a response variable for multiple linear regression studies (Table 7). As expected, the results reinforce the relevance of phenolic sites in antioxidant activity, where forming a hydrogen bond (HB) between DPPH and phenol seems to be necessary before H transfer. We highlight compound **6**, differing from **1** due to a nitro group with relative steric hindrance, which shows an additional intramolecular HB between the 4-OH and 5-NO_2 groups (Scheme 2).

Table 7. Structural analysis for antioxidant profile

Compound	4-OH	3-OH	5-NO_2	6-NO_2	BnAll	*p*QM	*o*BQ	AA
1	1	0	0	0	1	1	0	0.71
4	0	0	0	0	0	0	0	0.00
5	0	0	0	0	1	0	0	0.00
6	1	0	1	0	1	1	0	0.00
7	1	1	1	0	1	1	1	1.85
8	0	0	0	1	1	0	0	0.00

Source: Prepared by authors (2022). Reproduced with permission of Springer Nature

Multiple linear regression showed a structure–activity relationship according to Eq. 10.

$$AA = 0.71 \times(4 - OH) + 1.85 \times(3 - OH) - 0.71 \times(5 - NO_2) \quad (10)$$

This new feature may reflect the difficulty of H abstraction by DPPH and converges for the absence of antioxidant activity **6**. Furthermore, a second phenolic site (3-OH), as seen in compound **7**, is responsible for the 61.6% increase in antioxidant activity even with the nitro group. Therefore, once the 4-OH group maintains the HB with the 3-OH or 5-NO_2 groups, the abstraction will occur in the accessible 3-OH group to form HB with $DPPH^{\bullet}$.

Finally, the absence of antioxidant activity for compounds **4**, **5**, and **8** corroborates the relevance of phenols as antioxidant sites.

Thermodynamics aspects

In the second analysis, we used the free energy released from the reaction of the $HO^{\bullet}$ radical (Tables 3 and 5) to form phenolic radicals (PhO*p* and PhO*m*), benzyl-allyl radicals (BnAll), and quinones (*p*QM and *o*BQ).

Table 8 shows the $\Delta_r G$ data for the main reactive sites. When the structure does not have a specific site for the reaction, the value 0 was assigned to the free energy of the reaction.

Table 8 Free energies of reactions and antioxidant profile

Compound	PhOp	PhOm	BnAll	*p*QM	*o*BQ	AA
1	-30.6	0	-38.9	-91.4	0	0.71
4	0	0	0	0	0	0.00
5	0	0	-38.0	0	0	0.00
6	-26.6	0	-37.9	-85.0	0	0.00
7	1	-26.8	-37.8	-86.9	-69.9	1.85
8	0	0	-37.6	0	0	0.00

Source: Prepared by authors (2022). Reproduced with permission of Springer Nature.

The linear regression for the evaluated dataset originated the relationship between the energy of the sites and the antioxidant activity represented by Eq. 11.

$$AA = -0.356 \times \Delta_r G(PhO_p) + 0.111 \times \Delta_r G({}_pQM) - 0.0249 \times \Delta_r G({}_oQ) \quad (11)$$

According to this equation, the more negative the free energy of the reaction for the formation of the phenoxyl radical (PhO*p*) and the *o*-benzoquinone (*o*BQ), the greater the antioxidant activity. The positive coefficient of $\Delta_r G$ (*p*QM) for *p*-quinomethane (*p*QM) formation may suggest that greater stability of *p*QM may decrease the antioxidant activity in the DPPH test. Considering eugenol (**1**), this possibility can be explained by the secondary reaction between two radicals PhO*p* (**9**), via disproportionation reaction, to form *p*-quinomethane (**27**) with DPPH-independent regeneration of **1**. In this sense, this reaction would compete with the reaction between DPPH and the benzyl-allyl site, delaying the change in the DPPH absorption band at 515 nm.

Kinetics aspects

In the third analysis, we used the free energy of activation from the reaction of the $HO^{\bullet}$ radical (Tables 4 and 6) to form phenolic radicals (PhO*p* and PhO*m*), benzyl-allyl radicals (BnAll), and quinones (*p*QM and *o*BQ).

Table 9 shows the $\Delta G^{\ddagger}$ values for the formation of PhO*p*, PhO*p*, BnAll, *p*QM, and *o*BQ using the antioxidant activity (AA) results of the DPPH test [12]. Similar to Table 8, we assign a value of 0 to the free energy of activation for structures that do not have a specific site for the reaction.

Table 9 Free energies of activation and antioxidant profile

Compound	PhOp	PhOm	BnAll	*p*QM	*o*BQ	AA
1	6.3	0	6.4	7.3	0	0.71
4	0	0	0	0	0	0.00
5	0	0	7.5	0	0	0.00
6	11.0	0	7.5	-3.1	0	0.00
7	12.5	8.2	8.4	-1.7	5.5	1.85
8	0	0	5.7	0	0	0.00

Source: Prepared by authors (2022). Reproduced with permission of Springer Nature.

From the data analysis in Table 9, we obtained Eq. 12 that correlates the kinetic data with the antioxidant activity.

$$AA = 0.0220 \times \Delta G^{\ddagger}(PhO_p) + 0.2082 \times \Delta G^{\ddagger}(PhO_m) + 0.0782 \times \Delta G^{\ddagger}({}_pQM) \quad (12)$$

This equation shows that activation barriers influence antiradical activity to form PhO*p*, *p*QM, and mainly PhO*m* species. For compound 7, the results suggest that the presence of PhO*m* helps in the reaction kinetics, while the thermodynamics of the antioxidant activity depends on the PhO*p* site.

Part F. Reaction rates with radical DPPH

To understand the inactivity of **6** and the greater reactivity of **7**, when compared to **1**, we obtained the transition states for the reaction among these three antioxidants with DPPH$^{\bullet}$. In this case, they were used as phenolic sites for H transfer, discarding the BnAll ones in the study. Table 10 shows the value of $\Delta G^{\ddagger}$ and k for these reactions.

The DPPH$^{\bullet}$ activation free energy data show $\Delta G^{\ddagger}$ values of 20.6 kcal mol^{-1} for PhO*p* at **1** In comparison, its BnAll site showed a value of 24.0 kcal mol^{-1} (data not shown), following the observed trend that the greater the stability of the radical, the greater the preference of reaction with the phenolic site.

Table 10 Kinetics data for reaction of phenolic sites with DPPH•

Compound	Site	$\Delta G^{\ddagger}$ kcal mol^{-1}	K L mol^{-1} s^{-1}
1	4-OH	20.6	$4.9 \cdot 10^{-3}$
6	4-OH	29.4	$1.6 \cdot 10^{-9}$
7	4-OH	22.6	$1.6 \cdot 10^{-4}$
	3-OH	21.1	$2.2 \cdot 10^{-3}$

Source: Prepared by authors (2022). Reproduced with permission of Springer Nature

Data for compound **6**, a 5-nitro-analogue of **1** (Scheme 2) reveal that the HB between the 4-OH and 5-NO_2 groups drastically influences the energy and kinetics of formation to obtain the PhO*p* of compound **6**. The $\Delta G^{\ddagger}$ for reaction with **6** is 29.4 kcal mol^{-1}, which makes this reaction almost 106 slower than with **1**. Together with the volume around the 4-OH site and additional HB with the NO_2 group, this data could explain why **6** did not show antioxidant profile over time of the DPPH test.

In turn, compound **7** presents identical HB to **6**, making the 3-OH site the second most reactive with $\Delta G^{\ddagger}$ of 21.1 kcal mol^{-1} and the second-best kinetics. Furthermore, since the phenolic group 3-OH is also a hydrogen bond donor (HBD), unlike the 3-OMe group of **1** (only HBA), there is the possibility of new HB between the phenolic groups, where 4-OH would act as BHA and 3-OH as HBD, leading to the formation of the PhO*p* radical (**21**) as the third-best result.

It is worth noting that this difference in the energy barrier suggests that the reaction is approximately 300 times faster with the phenolic site, which would justify that O-acetyl derivatives **4**, **5**, and **8**, masking the phenolic groups, do not show antiradical activity during the analysis time in the DPPH assay.

Part G. Studies on transition states for HAT to DPPH radical

To show the characteristics of the transition states for hydrogen transfer from the phenolic sites of compounds **1**, **6**, and **7** to the DPPH•, we performed a SCAN calculation approximating the nitrogen radical of the DPPH to the respective phenolic groups.

Therefore, phenol hydrogen was positioned at an initial distance of 2.0 angstroms from the N-DPPH, performing ten approximation steps of 0.1 angstroms each, allowing structural relaxation. Finally, we performed the energy minimization calculation to obtain the TS at the

highest energy point of the trajectory. Figure 6 shows the transitions states of hydrogen transfer from phenolic sites to DPPH$^{\bullet}$ of **1**, **6**, and **7**.

Fig. 6 Transitions states for DPPH reactions with: **1** (**a**), **6** (**b**), **7**-PhO*p* (**c**), and **7**-PhO*m* (**d**)

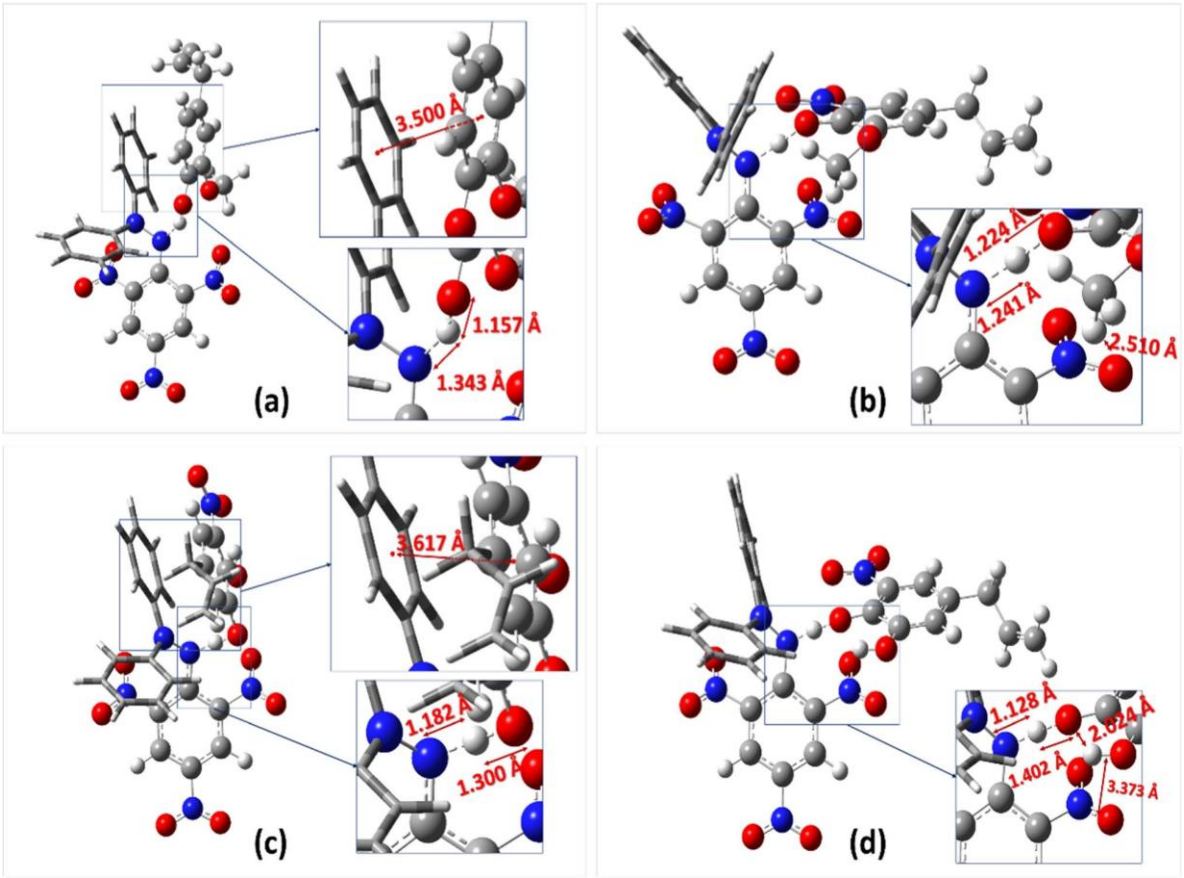

Source: Prepared by authors (2022). Reproduced with permission of Springer Nature

For compound **1**, the nearly parallel arrangement of the aromatic rings suggests that a π stacking interaction facilitates the reaction. In turn, nitro groups at **6** and **7** create a repulsive force that prevents the aromatic rings from stacking up. We observed that only the 4-OH in **1** and the 3-OH in **7** were appropriate arrangements due to lacking nitro group in **1** and the considerable distance between the *meta* (3-OH) and *para* (4-OH) hydroxyl groups. In this sense, the distance between the centroids of the aromatic rings is 3.500 Å for **1** (a) and 3.617 Å for the PhOm radical (c) at compound **7**, respectively.

From this perspective, the second phenol group (3-OH) in the structure must act in two different ways: (i) as an amplifier of the reactive surface area, once the two sites of **7** have nearby free activation energies; or (ii) a kinetic facilitator of the reaction as shown in Scheme 3.

Considering the direct path, the hydrogen abstraction reaction of the 4-OH site leading to the radical PhO*p* (**21**) occurs in a one-step only (a), which is about ten times slower than the

step of the 3-OH site by indirect path (b), showing the characteristics of the thermodynamic and kinetic products.

The indirect route of formation of PhO*p* (**21**) has three steps: (a) the HAT of **7** to the radical DPPH producing PhO*m* (**22**) with a $\Delta G^{\ddagger}$ value of 21.1 kcal mol^{-1}; (b) twist rotation of HOCC forming an OH---$^{\bullet}$O hydrogen bond (**40**) with a rotation $\Delta G^{\ddagger}$ value of 11.3 kcal mol^{-1}; and (c) internal transfer of H producing **21**with $\Delta G^{\ddagger}$ value of 6.5 kcal mol^{-1}.

The indirect route presented two particularities. The value of rotation $\Delta G^{\ddagger}$ is high, and the **40** rotamer formed in step c is isoenergetic with **21**. These factors led us to investigate a third two-step route, where **22** is formed, followed by solvent-mediated prototropism to form **21**. Figure 7 shows the schematic solvent-assisted transformation of PhO*m* (**22**) to PhO*p* (**21**).

Fig. 7 Solvent-assisted prototropism of PhO*m* (**22**)

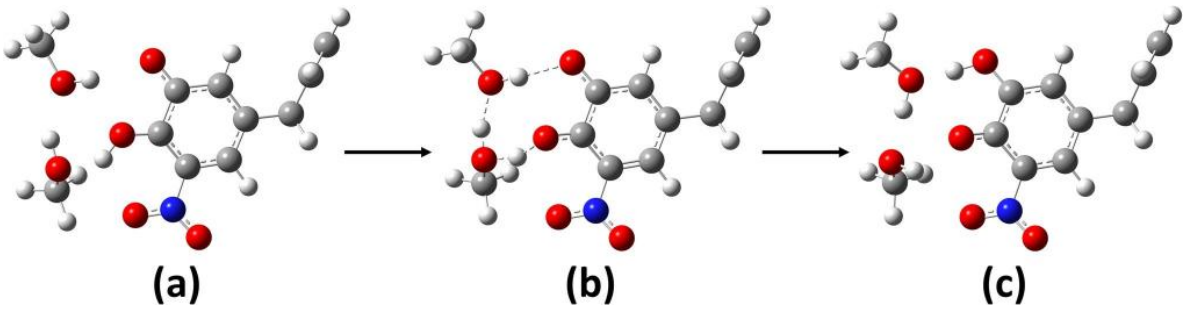

(a) 22 bonded to two methanol molecules; **(b)** transition state; and **(c)** PhO*p* (**21**) bonded to two methanol molecules

Source: Prepared by authors (2022). Reproduced with permission of Springer Nature

For this last step, methanol was used as a solvent similar to the DPPH test. The number of solvent molecules used was equal to two, the minimum amount capable of connecting the DPPH radical with the 3-OH phenolic site (a) by hydrogen bonding. The transition state (b) presented a $\Delta G^{\ddagger}$ value of 2.3 kcal mol^{-1}. These results suggest that the third solvent-mediated mechanistic route is the most favorable to occur.

CONCLUSIONS

The computational method used allowed a better understanding of the antioxidant mechanism of eugenol (**1**) and its derivatives (**4**–**8**). Additionally, the free energies of the reaction data showed that the benzyl-allyl radical is the most stable to be formed by the HAT mechanism in the gas phase. Furthermore, the transfer of only one hydrogen atom appears to be non-spontaneous towards the DPPH radical.

The formation of quinones (*p*-quinomethane and *ortho*quinone) plays an essential key for the antioxidant activity in the DPPH assay since the second atomic hydrogen transfer releases more energy than the first. Thus, the formation of quinones presented negative values of $\Delta_r G$ for the global reaction of **1**, **6**, and **7** with two DPPH equivalents, which corroborates the data in the literature.

Except for eugenol (**1**), kinetic data showed that the more stable the attacking radical, the greater the kinetic affinity for the phenolic sites. The nitro group affected the antioxidant activity of derivatives of **1**, being kinetically unfavorable for the 4-OH group of **6** and **7**, and at the same time, favorable for the 3-OH site of **7**, explaining the results of these three compounds in the DPPH test.

REFERENCES

[1] Esmaeili H, Karami A, Maggi F (2018) Essential oil composition, total phenolic and flavonoids contents, and antioxidant activity of Oliveria decumbens Vent. (Apiaceae) at different phenological stages. J Clean Prod 198:91–95. https://doi.org/10.1016/j.jclepro.2018.07.029

[2] Kleinberg MN, Rios MAS, Buarque HLB, Parente MMV, Cavalcante CL, Luna FMT (2019) Influence of synthetic and natural antioxidants on the oxidation stability of beef tallow before biodiesel production. Waste Biomass Valoriz 10(4):797–803. https://doi.org/10.1007/s12649-017-0120-x

[3] Maia FJN, Ribeiro FWP, Rangel JHG, Lomonaco D, Luna FMT, Lima-Neto P, Mazzetto SE (2015) Evaluation of antioxidant action by electrochemical and accelerated oxidation experiments of phenolic compounds derived from cashew nut shell liquid. Ind Crops Prod 67:281–286. https://doi.org/10.1016/j.indcrop.2015.01.034

[4] Barreiros ALBS, David JM, David JP (2006) Oxidative stress: relations between the formation of reactive species and the organism's defense. Quim Nova 29(1):113–123. https://doi.org/10.1590/s0100-40422006000100021

[5] Pramod K, Ansari SH, Ali J (2010) Eugenol: a natural compound with versatile pharmacological actions. Nat Prod Commun 5(12):1999–2006. https://doi.org/10.1177/1934578x1000501236

[6] Boobis AR, Fawthrop DJ, Davies DS (1989) Mechanisms of cell death. Trends Pharmacol Sci 10(7):275–280. https://doi.org/10.1016/0165-6147(89)90027-8

[7] Nelson SD, Pearson PG (1990) Covalent and noncovalent interactions in acute lethal cell injury caused by chemicals. Annu Rev Pharmacol Toxicol 30:169–195. https://doi.org/10.1146/annurev.pa.30.040190.001125

[8] Bolton JL, Comeau E, Vukomanovic V (1995) The influence of 4-alkyl substituents on the formation and reactivity of 2-methoxy-quinone methides: evidence that extended π-conjugation dramatically stabilizes the quinone methide formed from eugenol. Chem Biol Interact 95(3):279–290. https://doi.org/10.1016/0009-2797(94)03566-Q

[9] Bolton JL, Dunlap T (2017) Formation and biological targets of quinones: cytotoxic versus cytoprotective effects. Chem Res Toxicol 30(1):13–37. https://doi.org/10.1021/acs.chemrestox.6b00256

[10] Fischer IU, Von Unruh GE, Dengler HJ (1990) The metabolism of eugenol in man. Xenobiotica 20(2):209–222. https://doi.org/10.3109/00498259009047156

[11] Thompson DC, Constantin-Teodosiu D, Moldéus P (1991) Metabolism and cytotoxicity of eugenol in isolated rat hepatocytes. Chem Biol Interact 77(2):137–147. https://doi.org/10.1016/0009-2797(91)90069-J

[12] Hidalgo ME, De La Rosa C, Carrasco H, Cardona W, Gallardo C, Espinoza L (2009) Antioxidant capacity of eugenol derivatives. Quim Nova 32(6):1467–1470. https://doi.org/10.1590/S0100-40422009000600020

[13] Kogure K, Goto S, Nishimura M, Yasumoto M, Abe K, Ohiwa C, Sassa H, Kusumi T, Terada H (2002) Mechanism of potent antiperoxidative effect of capsaicin. Biochim Biophys Acta Gen Subj 1573(1):84–92. https://doi.org/10.1016/S0304-4165(02)00335-5

[14] Galano A, Martínez A (2012) Capsaicin, a tasty free radical scavenger: mechanism of action and kinetics. J Phys Chem B 116(3):1200–1208. https://doi.org/10.1021/jp211172f

[15] Okada Y, Tanaka K, Sato E, Okajima H (2010) Kinetics and antioxidative sites of capsaicin in homogeneous solution. JAOCS J Am Oil Chem Soc 87(12):1397–1405. https://doi.org/10.1007/s11746-010-1628-4

[16] Joshi R (2018) Nature of transients produced on hydrogen atom transfer from capsaicin. J Theor Comput Chem 17(5). https://doi.org/10.1142/S0219633618500360

[17] Yancheva DY, Stoyanov SS, Velcheva EA, Stamboliyska BA, Smelcerovic A (2019) DFT study on the radical scavenging capacity of apocynin with different free radicals. Bul Chem Commun 49:137–144.

[18] Paula RSF, Vieira RS, Luna FMT, Cavalcante-Júnior CL, Figueredo IM, Candido-Júnior JR, Silva LP, Marinho ES, LimaNeto P, Lomonaco D, Mazzetto SE, Rios MAS (2020) A potential bio-antioxidant for mineral oil from cashew nutshell liquid: an experimental and theoretical approach. Braz J Chem Eng 37:369–381. https://doi.org/10.1007/s43153-020-00031-z

[19] Bortolomeazzi R, Verardo G, Liessi A, Callea A (2010) Formation of dehydrodiisoeugenol and dehydrodieugenol from the reaction of isoeugenol and eugenol with DPPH radical and their role in the radical scavenging activity. Food Chem 118(2):256–265. https:// doi. org/10 . 1016/j. foodc hem. 2009. 04. 115

[20] Zhao Y, Truhlar DG (2008) The M06 suite of density functionals for main group thermochemistry, thermochemical kinetics, noncovalent interactions, excited states, and transition elements: two new functionals and systematic testing of four M06-class functionals and 12 other functionals. Theoret Chem Acc 120(1– 3):215–241.

https://doi.org/10.1007/s00214-007-0310-x

[21] Hehre WJ, Ditchfield R, People JA (1972) Self—consistent molecular orbital methods. XII. Further extensions of Gaussian—type basis sets for use in molecular orbital studies of organic molecules. J Chem Phys 56:2257–2261. https://doi.org/10.1063/1.1677527

[22] Clark T, Chandrasekhar J, Spitznagel GW, Schleyer PVR (1983) Efficient diffuse function-augmented basis sets for anion calculations. III. The 3–21+G basis set for first-row elements, Li–F. J Comput Chem 4(3):294–301. https://doi.org/10.1002/jcc.540040303

[23] Peng C, Schlegel HB (1993) Combining synchronous transit and quasi-Newton methods for finding transition states. Israel J Chem 33:449–454. https://doi.org/10.1002/ijch.199300051

[24] Peng C, Ayala PY, Schlegel HB, Frisch MJ (1996) Using redundant internal coordinates to optimize equilibrium geometries and transition states. J Comput Chem 17: 49-56. https://doi.org/10.1002/(SICI)1096-987X(19960115)17:1<49::AID-JCC5>3.0.CO;2-0

[25] Fukui K (1981) The path of chemical-reactions – The IRC approach. Acc Chem Res 14(12):363–368. https://doi.org/10.1021/ar00072a001

[26] Hratchian HP, Schlegel HB (2005) Finding minima, transition states, and following reaction pathways on ab initio potential energy surfaces. In: Dykstra C, Frenking G, Kim K, Scuseria G (eds) Theory and Applications of Computational Chemistry, 1st edn. Elsevier, Amsterdan, pp 243–249

[27] McQuarrie DA, Simon JD (1997) Physical Chemistry: A Molecular Approach, The key equation number 28.72, 1137–1180, University Science Books, United States of America

[28] Glendening ED, Reed AE, Carpenter JE, Weinhold F, Wiberg KB (1968) Application of the pople-santry-segal CNDO method to the cyclopropylcarbinyl and cyclobutyl cation and to bicyclobutane. Tetrahedron 24(3):1083–1096. https://doi.org/10.1016/0040-4020(68)88057-3

4 CONCLUSIONS

The quantum descriptors and the reaction simulation showed efficacy to justify the experimental results of the antioxidant activities of cardanols and eugenol and their derivatives.

Theoretical calculations for cardanols showed that HAT was the best presented mechanism, as expected since these mechanisms this mechanism is predominant in non-polar systems. The study showed that increasing the number of unsaturations present in the cardanol chain increases the global reactivity of the structure. Nevertheless, cardanol monoene was shown to have the best antioxidant profile.

The cardanol mixture showed applicability to act as an antioxidant in naphthenic mineral oil. The effectiveness of the quantum descriptor method proved to be interesting for application testing in possible derivatizations of cardanol to improve its antioxidant activity to compete with synthetic antioxidants such as BHT.

In the second work, the computational method used allowed a better understanding of the antioxidant mechanism of eugenol (1) and its derivatives (4–8). The Capsaicin-Eugenol paradox was elucidated, showing that the allyl-benzyl is the most stable radical, but the reaction with DPPH is dependent on two HAT steps, which explains the lack of activity in non-phenolic derivatives.

The formation of quinones (*p*-quinomethane and orthoquinone) plays an essential key for the antioxidant activity in the DPPH assay since the second atomic hydrogen transfer releases more energy than the first. Thus, the formation of quinones presented negative values of $\Delta_r G$ for the global reaction of 1, 6, and 7 with two DPPH equivalents, which corroborates the data in the literature.

The results show that the kinetic data have a greater influence on the experimental results and that the preferred site for hydrogen transfer changes according to the radical reactivity, which is not possible to perceive only with the use of chemical descriptors. This mechanism method would be used to test novel eugenol derivatives to try improve antioxidant profile and reduce its cytotoxicity.

REFERENCES

AMERICAN SOCIETY FOR TESTING AND MATERIALS, ASTM E1970-16 (2016) Standard test method for statistical treatment of thermoanalytical data, ASTM International.

AMERICAN SOCIETY FOR TESTING AND MATERIALS, ASTM E2041-18 (2018) Standard test method for estimating kinetic parameters by differential scanning calorimeter using the Borchardt and Daniels, ASTM International.

AMERICAN SOCIETY FOR TESTING AND MATERIALS, ASTM E537-12 (2012) Standard test method for the thermal stability of chemicals by differential scanning calorimetry, ASTM International.

AMERICAN SOCIETY FOR TESTING AND MATERIALS, ASTM E698-18 (2018) Standard test method for Arrhenius kinetic constants for thermally unstable materials using differential scanning calorimetry and the Flynn/Wall/Ozawa Method, ASTM International.

ARAÚJO, S. V. *et al.* A rapid method for evaluation of the oxidation stability of castor oil FAME: influence of antioxidant type and concentration. **Fuel Processing Technology**, Amsterdam, v. 90, n. 10, p. 1272–1277, 2009.

ATTIA, A. K.; ABDEL-MOETY, M. M.; ABDEL-HAMID, S. G. Thermal analysis study of antihypertensive drug doxazosin mesylate. **Arabian Journal of Chemistry**, Amsterdam, v. 10, n. 1, p. S334–S338, 2017.

BARREIROS, A. L. B. S.; DAVID, J. M.; DAVID, P. J. Estresse oxidativo: relação entre geração de espécies reativas e defesa do organismo. **Química Nova**, São Paulo, v. 29, p. 113–123, 2006.

BARTMESS, J. E. Thermodynamics of the electron and the proton. **The Journal of Chemical Physics**, Melville, v. 98, n. 25, p. 6420–6424, 1994.

BECKE, A. D. Density-functional thermochemistry. III. The role of exact exchange. **The Journal of Chemical Physics**, Melville, v. 98, n. 7, p. 5648–5652, 1993. DOI: https://doi.org/10.1063/1.464913

CAILLOL, S. Cardanol: a promising building block for biobased polymers and additives. **Current Opinion in Green and Sustainable Chemistry**, Amsterdam, v. 14, p. 26–32, 2018. DOI: https://doi.org/10.1016/j.cogsc.2018.05.002

CASHOL RESIBRAS. Materiais. Disponível em: https://cashol.com.br/2017/#materiais Acesso em: 19 abr. 2020.

DIMOVA, S.; HOET, P. H.; NEMERY, B. Paracetamol (acetaminophen) cytotoxicity in rat type II pneumocytes and alveolar macrophages *in vitro*. **Biochemical Pharmacology**, Amsterdam, v. 59, n. 11, p. 1467–1475, 2000. DOI: https://doi.org/10.1016/S0006-2952(00)00257-4

DWIVEDI, G.; VERMA, P.; SHARMA, M. P. Optimization of storage stability for Karanja biodiesel using Box–Behnken design. **Waste and Biomass Valorization**, Dordrecht, v. 9, n. 4, p. 645–655, 2018.

EDDY, N. O.; ITA, B. I. QSAR, DFT and quantum chemical studies on the inhibition potentials of some carbozones for the corrosion of mild steel in HCl. **Journal of Molecular Modeling**, Berlin, v. 17, n. 2, p. 359–376, 2011.

ESMAEILI, H.; KARAMI, A.; MAGGI, F. Essential oil composition, total phenolic and flavonoids contents, and antioxidant activity of *Oliveria decumbens* Vent. (Apiaceae) at different phenological stages. **Journal of Cleaner Production**, Amsterdam, v. 198, p. 91–95, 2018.

FERREIRA, A. L. A.; MATSUBARA, L. S. Radicais livres: conceitos, doenças relacionadas, sistema de defesa e estresse oxidativo. **Revista da Associação Médica Brasileira**, São Paulo, v. 43, p. 61–68, 1997. DOI: https://doi.org/10.1590/S0104-42301997000100014

FOOD AND AGRICULTURE ORGANIZATION OF THE UNITED NATIONS. **FAOSTAT – Statistics Database.** Disponível em: https://www.fao.org/faostat/en/#data/QC. Acesso em: 19 abr. 2020.

FOX, N. J.; STACHOWIAK, G. Vegetable oil based lubricants: a review of oxidation. **Tribology International**, Oxford, v. 40, n. 7, p. 1035–1046, 2007.

FREITAS, A. R. *et al*. Green methodology for synthesis of alkylated cardanol based on the green chemical principles. **Progress in Industrial Ecology – An International Journal**, Genève, v. 9, n. 3, p. 312–325, 2015.

GALANO, A.; ALVAREZ-IDABOY, J. R. A computational methodology for accurate predictions of rate constants in solution: application to the assessment of primary antioxidant activity. **Journal of Computational Chemistry**, Hoboken, v. 34, n. 28, p. 2430–2445, 2013.

GENENA, Aziza Kamal. **Extração e caracterização do extrato de alecrim (Rosmarinus officinalis L.): estudo de sua ação antioxidante**. 2005. Dissertação (Mestrado em Engenharia de Alimentos) – Centro Tecnológico, Universidade Federal de Santa Catarina, Florianópolis, 2005.

HALLIWELL, Barry; GUTTERIDGE, John M. C. **Free radicals in biology and medicine**. 4. ed. New York: Oxford University Press, 2006.

HEHRE, W. J.; DITCHFIELD, R.; POPLE, J. A. Self-consistent molecular orbital methods. XII. Further extensions of Gaussian-type basis sets for use in molecular orbital studies of organic molecules. **The Journal of Chemical Physics**, Melville, v. 56, n. 5, p. 2257–2261, 1972.

HIDALGO, M. E. *et al*. Antioxidant capacity of eugenol derivatives. **Química Nova**, São Paulo, v. 32, n. 6, p. 1467–1470, 2009. DOI: https://doi.org/10.1186/s13065-018-0407-4

ILYAS, S. U.; PENDYALA, R.; NARAHARI, M. Stability and thermal analysis of MWCNT-thermal oil-based nanofluids. **Colloids and Surfaces A: Physicochemical and Engineering Aspects**, Amsterdam, v. 527, p. 11–22, 2017.

XIE, J.; SCHAICH, K. M. Re-evaluation of the 2,2-diphenyl-1-picrylhydrazyl free radical (DPPH) assay for antioxidant activity. **Journal of Agricultural and Food Chemistry**, Washington, DC, v. 62, p. 4251–4260, 2014. DOI: https://doi.org/10.1021/jf500180u

JENSEN, F. **Introduction to computational chemistry.** 2. ed. Chichester: John Wiley & Sons, 2007.

JOSEPHY, P. D.; MANNERVIK, B. Molecular toxicology. 2. ed. New York: Oxford University Press, 2006. 589 p.

KAJIYAMA, T.; OHKATSU, Y. Effect of meta-substituents of phenolic antioxidants—proposal of secondary substituent effect. **Polymer Degradation and Stability**, Amsterdam, v. 75, n. 3, p. 535–542, 2002.

KARELSON, M.; LOBANOV, V. S. Quantum-chemical descriptors in QSAR/QSPR studies. **Chemical Reviews**, Washington, DC, v. 96, p. 1027–1043, 1996. DOI: https://doi.org/10.1021/cr950202r

.

KLEINBERG, M. N. *et al*. Influence of synthetic and natural antioxidants on the oxidation stability of beef tallow before biodiesel production. **Waste and Biomass Valorization**, Dordrecht, v. 10, n. 4, p. 797–803, 2017.

KOGURE, K. *et al*. Mechanism of potent antiperoxidative effect of capsaicin. **Biochimica et Biophysica Acta**, Amsterdam, v. 1573, n. 1, p. 84–92, 2002. DOI: https://doi.org/10.1016/S0304-4165(02)00335-5

KOOPMANS, T. Über die Zuordnung von Wellenfunktionen und Eigenwerten zu den einzelnen Elektronen eines Atoms. Physica, Amsterdam, v. 1, n. 1–6, p. 104–113, 1934.

KÖK, M. V.; VARFOLOMEEV, M. A.; NURGALIEV, D. K. Crude oil characterization using TGA-DTA, TGA-FTIR and TGA-MS techniques. Journal of Petroleum Science and Engineering, Amsterdam, v. 154, p. 537–542, 2017.

LEE, C. Y. *et al*. Computational study of ortho-substituent effects on antioxidant activities of phenolic dendritic antioxidants. **Antioxidants**, Basel, v. 9, p. 189, 2020. DOI: https://doi.org/10.3390/antiox9030189

LEOPOLDINI, M.; RUSSO, N.; TOSCANO, M. The molecular basis of working mechanisms of natural polyphenolic antioxidants. **Food Chemistry,** Oxford, v. 125, n. 2, p. 288–306, 2011.

LOMONACO, D.; MAIA, F. J. N.; MAZZETTO, S. E. Thermal evaluation of cashew nutshell liquid as new bioadditives for poly(methyl methacrylate). **Journal of Thermal Analysis and Calorimetry**, Dordrecht, v. 111, p. 619–626, 2013.

LOPES, A. A. S. *et al*. Study of antioxidant property of a thiosphosphorated compound derived from cashew nut shell liquid in hydrogenated naphthenic oils. **Brazilian Journal of Chemical Engineering**, São Paulo, v. 25, n. 1, p. 119–127, 2008.

LU, T.; CHEN, F. Multiwfn: a multifunctional wavefunction analyzer. **Journal of Computational Chemistry**, Hoboken, v. 33, n. 5, p. 580–592, 2012a.

LU, T.; CHEN, F. Quantitative analysis of molecular surface based on improved Marching Tetrahedra algorithm. **Journal of Molecular Graphics and Modelling**, Amsterdam, v. 38, p. 314–322, 2012b.

LUNA, F. M. T. *et al*. Assessment of biodegradability and oxidation stability of mineral, vegetable and synthetic oil samples. **Industrial Crops and Products**, Amsterdam, v. 33, n. 3, p. 579–583, 2011.

MAZZETTO, S. E. Evaluation of antioxidant action by electrochemical and accelerated oxidation experiments of phenolic compounds derived from cashew nut shell liquid. Industrial Crops and Products, Amsterdam, v. 67, p. 281–286, 2015. DOI: https://doi.org/10.1016/j.indcrop.2015.01.034

MAIA, F. J. N. *et al*. Evaluation of antioxidant action by electrochemical and accelerated oxidation experiments of phenolic compounds derived from cashew nut shell liquid. **Industrial Crops and Products**, Amsterdam, v. 67, p. 281–286, 2015.

MARTÍNEZ-MONTEAGUDO, S. I.; SALDAÑA, M. D. A.; KENNELLY, J. J. Kinetics of non-isothermal oxidation of anhydrous milk fat rich in conjugated linoleic acid using differential scanning calorimetry. **Journal of Thermal Analysis and Calorimetry**, Dordrecht, v. 107, n. 3, p. 973–981, 2012.

MASOUD, M. S.; GHAREEB, D. A.; AHMED, S. S. Synthesis, characterization, spectral, thermal analysis and computational studies of thiamine complexes. **Journal of Molecular Structure**, Amsterdam, v. 1137, p. 634–648, 2017.

MICIĆ, D. M. *et al*. Kinetics of blackberry and raspberry seed oils oxidation by DSC. **Thermochimica Acta**, Amsterdam, v. 601, p. 39–44, 2015.

MOHAMMED, M. N. *et al*. Characterization of Hemp (Cannabis sativa L.) biodiesel blends with euro diesel, butanol and diethyl ether using FT-IR, UV–Vis, TGA and DSC techniques. **Waste and Biomass Valorization**, Dordrecht, p. 1–17, 2018.

MOREIRA, R.; ORSINI, R. R.; VAZ, J. M.; PENTEADO, J. C. Production of biochar, bio-oil and synthesis gas from cashew nut shell by slow pyrolysis. **Waste and Biomass Valorization**, Dordrecht, v. 8, n. 1, p. 217–224, 2017.

MOTHÉ, C. G.; VIEIRA, C. R.; MOTHÉ, M. G. Thermal and surface study of phenolic resin from cashew nut shell liquid cured by plasma treatment. **Journal of Thermal Analysis and Calorimetry**, Dordrecht, v. 114, n. 2, p. 821–826, 2013.

NEESE, F. Software update: the ORCA program system, version 4.0. **WIREs Computational Molecular Science**, Hoboken, v. 8, n. 1, 2017. https://doi.org/10.1002/wcms.1327

NENADIS, N.; TSIMIDOU, M. Z. Contribution of DFT computed molecular descriptors in the study of radical scavenging activity trend of natural hydroxybenzaldehydes and corresponding acids. **Food Research International**, Oxford, v. 48, n. 2, p. 538–543, 2012.

NEUMANN, A.; JEBENS, T.; WIERZBICKI, V. A method for determining oxidation stability of petrodiesel, biodiesel, and blended fuels. **American Laboratory**, Shelton, v. 40, n. 4, p. 22–26, 2008.

NWANKWO, H. U.; OLASUNKANMI, L. O.; EBENSO, E. E. Experimental, quantum chemical and molecular dynamic simulations studies on the corrosion inhibition of mild steel by some carbazole derivatives. **Scientific Reports**, London, v. 7, p. 1–18, 2017.

OLIVEIRA, M. A.; YOSHIDA, M. I.; GOMES, E. C. L. Análise térmica aplicada a fármacos e formulações farmacêuticas na indústria farmacêutica. **Química Nova**, São Paulo, v. 34, p. 1224–1230, 2011.

OSORIO, E. *et al*. Why is quercetin a better antioxidant than taxifolin? Theoretical study of mechanisms involving activated forms. **Journal of Molecular Modeling**, Berlin, v. 19, p. 2165–2172, 2013.

PAIVA, G. M. S. *et al*. Kinetic and thermal stability study of hydrogenated cardanol and alkylated hydrogenated cardanol. **Journal of Thermal Analysis and Calorimetry**, Dordrecht, v. 120, n. 3, p. 1617–1625, 2015.

PARKER, V. D. Homolytic bond (H–A) dissociation free energies in solution. Applications of the standard potential of the ($H^+/H\cdot$) couple. **Journal of the American Chemical Society**, Washington, DC, v. 114, n. 19, p. 7458–7462, 1992.

PARR, R. G.; YANG, W. Density functional approach to the frontier-electron theory of chemical reactivity. **Journal of the American Chemical Society**, Washington, DC, v. 106, n. 14, p. 4049–4050, 1984.

PRAMOD, K.; ANSARI, S. H. Eugenol: a natural compound with versatile pharmacological actions. **Natural Product Communications**, Thousand Oaks, v. 5, n. 12, p. 1999–2006, 2010. DOI: https://doi.org/10.1177/1934578X1000501236

PRETSCH, E.; BÜHLMANN, P.; BADERTSCHER, M. **Structure determination of organic compounds: tables of spectral data**. 4. ed. Heidelberg: Springer, 2009.

RANG, H. P. *et al*; **Farmacologia**. Tradução da 6. ed. Rio de Janeiro: Elsevier, 2007.

Reda SY (2011) Avaliação da estabilidade de antioxidantes por análise térmica e seu efeito protetor em óleo vegetal aquecido. Food Sci Technol 31(2):475–480

RIMARČÍK, J.; LUKEŠ, V.; KLEIN, E.; ILČIN, M. Study of the solvent effect on the enthalpies of homolytic and heterolytic N–H bond cleavage in p-phenylenediamine and tetracyano-p-phenylenediamine. **Journal of Molecular Structure (Theochem)**, Amsterdam, v. 952, p. 25–30, 2010.

RIOS, M. A. S.; FREITAS, A. R. **Processo para preparação de alquilfenóis a partir do cardanol hidrogenado para utilização deste como aditivos em biodieseis e óleos.** Depositante: Rios, M. A. S.; Freitas, A. R. BR n. 10 2014 032181-0 A2. Depósito: 11 jul. 2017.

RIOS, M. A. F. *et al*. Evaluation of antioxidant properties of a phosphorated cardanol compound on mineral oils (NH10 and NH20). **Fuel**, Amsterdam, v. 86, n. 15, p. 2416–2421, 2007.

RIOS, M. A. S.; MAZZETTO, S. E. Thermal behavior of phosphorus derivatives of hydrogenated cardanol. **Fuel Processing Technology**, Amsterdam, v. 96, p. 1–8, 2012.

RIOS, M. A. S. *et al*. Antioxidative activity of 5-n-pentadecyl-2-tert-butylphenol stabilizers in mineral lubricant oil. **Energy & Fuels**, Washington, DC, v. 24, n. 5, p. 3285–3291, 2010.

RIOS, M. A. S. *et al*. Evaluation of antioxidants on the thermo-oxidative stability of soybean biodiesel. **Journal of Thermal Analysis and Calorimetry**, Dordrecht, v. 112, p. 921–927, 2013.

SANTOS, Francisco Francielle Pinheiro dos. **Avaliação de antioxidantes aplicados à produção de biodiesel.** 2013. 152 f. Tese (Doutorado em Engenharia Química) – Departamento de Engenharia Química, Universidade Federal do Ceará, Fortaleza, 2013.

SANTOS, M. H. *et al*. Influência do processamento e da torrefação sobre a atividade antioxidante do café (Coffea arabica). **Química Nova**, São Paulo, v. 30, p. 604–610, 2007. DOI: https://doi.org/10.1590/S0100-40422007000300020

SILVA, G.; NAKAMURA, N. M.; ILHA, K. Estudo cinético da decomposição térmica do pentaeritritol-tetranitrado (PETN). **Química Nova**, São Paulo, v. 31, p. 2060–2064, 2008.

SILVA, G. A. M. *et al*. Physico-chemical, spectroscopical and thermal characterization of biodiesel obtained by enzymatic route as a tool to select the most efficient immobilized lipase. **Brazilian Journal of Chemical Engineering**, São Paulo, v. 29, n. 1, p. 39–47, 2012.

SOUSA RIOS, M. A.; MAZZETTO, S. E. Effect of organophosphate antioxidant on the thermo-oxidative degradation of a mineral oil. **Journal of Thermal Analysis and Calorimetry**, Dordrecht, v. 111, p. 553–559, 2013.

SOUSA, S. F.; FERNANDES, P. A.; RAMOS, M. J. General performance of density functional. **The Journal of Physical Chemistry A**, Washington, DC, v. 111, p. 10439–10452, 2007. DOI: https://doi.org/10.1021/jp0734474

.

SPEYER, R. F. **Thermal analysis of materials**. New York: CRC Press, 1993.

SRIVASTAVA, S. *et al*. One pot synthesis of curcumin-NSAIDs prodrug, spectroscopic characterization, conformational analysis, chemical reactivity, intramolecular interactions and first order hyperpolarizability by DFT method. **Journal of Molecular Structure**, Amsterdam, v. 117, n. 5, p. 173–180, 2016.

STEPANIĆ, V. *et al*. Bond dissociation free energy as a general parameter for flavonoid radical scavenging activity. **Food Chemistry**, Oxford, v. 141, n. 2, p. 1562–1570, 2013.

SYAHIR, A. Z. *et al*. A review on bio-based lubricants and their applications. **Journal of Cleaner Production**, Amsterdam, v. 168, n. 1, p. 997–1016, 2017.

SZELĄG, M.; MIKULSKI, D.; MOLSKI, M. Quantum-chemical investigation of the structure and the antioxidant properties of α-lipoic acid and its metabolites. **Journal of Molecular Modeling**, Berlin, v. 18, p. 2907–2916, 2012. DOI: https://doi.org/10.1007/s00894-011-1306-y

TREVISAN, M. T. S. *et al*. Characterization of alkyl phenols in cashew (Anacardium occidentale) products and assay of their antioxidante capacity. **Food and Chemical Toxicology**, Oxford, v. 44, p. 188–196, 2006. DOI: https://doi.org/10.1016/j.fct.2005.06.012

THOMPSON, D. C. *et al*. Biological and toxicological consequences of quinone methide formation. **Chemico-Biological Interactions**, Amsterdam, v. 86, n. 2, p. 129–162, 1993. DOI: https://doi.org/10.1016/0009-2797(93)90117-H

VOLLHARDT, K. P. C.; SCHORE, N. E. **Organic chemistry: structure and function**. New York: W. H. Freeman and Company, 2011.

WASSERMAN, David; CAPLAN, Solomon. **4-amino cardanol as an antioxidant for mineral hydrocarbon oil.** Depositante: The Harvel Corporation (US). US n. 2,571,330. Depósito: 21 ago. 1948. Concessão: 16 out. 1951. Disponível em: https://patentimages.storage.googleapis.com/c7/00/d5/fc2a71e6243cd5/US2571092.pdf

WANG, L. *et al.* Quantum chemical descriptors in quantitative structure–activity relationship models and their applications. **Chemometrics and Intelligent Laboratory Systems**, Amsterdam, v. 217, p. 104384, 2021. DOI: https://doi.org/10.1016/j.chemolab.2021.104384

WRIGHT, J. S.; JOHNSON, E. R.; DILABIO, G. A. Predicting the activity of phenolic antioxidants: theoretical method, analysis of substituent effects, and application to major families of antioxidants. **Journal of the American Chemical Society**, Washington, DC, v. 123, n. 6, p. 1173–1183, 2001.

ZHANG, H.-Y. Theoretical methods used in elucidating activity differences of phenolic antioxidants. **Journal of the American Oil Chemists' Society**, Hoboken, v. 76, n. 6, p. 745–748, 1999.

ZHAO, H. *et al.* Synthesis and application of highly efficient multifunctional vegetable oil additives derived from biophenols. **Journal of Cleaner Production**, Amsterdam, v. 242, p. 1–9, 2020.

ZHAO, Y.; TRUHLAR, D. G. The M06 suite of density functionals for main group thermochemistry, thermochemical kinetics, noncovalent interactions, excited states, and transition elements: two new functionals and systematic testing of four M06-class functionals and 12 other functionals. **Theoretical Chemistry Accounts**, Berlin, v. 120, n. 1–3, p. 215–241, 2008. DOI: https://doi.org/10.1007/s00214-007-0310-x

CHEMAXON. **ChemAxon.** Disponível em: https://www.chemaxon.com. Acesso em: 2 dez. 2019.

FEDERAÇÃO DAS INDÚSTRIAS DO ESTADO DE SÃO PAULO. **Notícia.** Disponível em: https://www.fiesp.com.br/mobile/noticia/?id=239879. Acesso em: 2 dez. 2019.

APÊNDICE A – DADOS CURRICULARES DO AUTOR

Currículo **Lattes**

Imprimir currículo

José Roberval Cândido Júnior

Endereço para acessar este CV: **http://lattes.cnpq.br/6247235731527552**

Última atualização do currículo em 06/06/2022

Resumo informado pelo autor

Tem experiência na área de Química, com ênfase em Química, atuando principalmente nos seguintes temas: antioxidantes, elucidação de estruturas, modelagem molecular de compostos bioinorgânicos com potencial aplicação farmacológica, DFT.
(Texto informado pelo autor)

Nome civil

Nome José Roberval Cândido Júnior

Dados pessoais

Filiação José Roberval Cândido e Kátia Cristiane Romeiro Cândido

Nascimento 19/03/1984 - Recife/PE - Brasil

Carteira de Identidade 98002168953 SSP - CE - 24/04/1998

CPF 003.541.893-10

Formação acadêmica/titulação

2016 Doutorado em Química.
Universidade Federal do Ceará, UFC, Fortaleza, Brasil
Título: COMPOSTOS FENÓLICOS: UM ESTUDO TEÓRICO-COMPUTACIONAL DA CAPACIDADE ANTIOXIDANTE

Orientador: Pedro de Lima Neto
Co-orientador: Luiz Antônio Soares Romeiro

Doutorado interrompido(a) em Química.
Universidade Federal do Ceará, UFC, Fortaleza, Brasil
Título: COMPOSTOS FENÓLICOS: UM ESTUDO TEÓRICO-COMPUTACIONAL: DA CAPACIDADE ANTIOXIDANTE À SUA APLICAÇÃO FARMACOLÓGICA EM SISTEMAS ENZIMÁTICOS

Orientador: Pedro de Lima Neto
Co-orientador: Luiz Antônio Soares Romeiro
Bolsista do(a): Conselho Nacional de Desenvolvimento Científico e Tecnológico
Ano de interrupção: 2016

2009 - 2010 Mestrado em Química.
Universidade Federal do Ceará, UFC, Fortaleza, Brasil
Título: CISTEÍNA: DAS PROPRIEDADES BÁSICAS À AÇÃO ANTI-CORROSIVA, Ano de obtenção: 2011

Orientador: Pedro de Lima Neto
Bolsista do(a): Conselho Nacional de Desenvolvimento Científico e Tecnológico

2009 - 2013 Graduação em Licenciatura em Química.
Universidade Estadual do Ceará, UECE, Fortaleza, Brasil
Título: Eugenol: Estudo Computacional da Atividade Antioxidante
Orientador: Márcia Rodrigues de Sousa

2005 - 2008 Graduação em Bacharelado em Química.
Universidade Federal do Ceará, UFC, Fortaleza, Brasil
Bolsista do(a): Fundação Cearense de Apoio ao Desenvolvimento Científico e Tecnológico

2000 - 2002 Ensino Médio (2o grau) .
Colégio Militar de Fortaleza, CMF, Brasil

1996 - 1999 Ensino Fundamental (1o grau) .
Colégio Militar de Fortaleza, CMF, Brasil

Formação complementar

2010 - 2010 Curso de curta duração em Workshop - Interfaces entre a Química e a Biologia.
Sociedade Brasileira de Química, SBQ, Sao Paulo, Brasil

2010 - 2010 Curso de curta duração em Predição de Estruturas de Proteínas. (Carga horária: 6h).
Laboratório Nacional de Computação Científica, LNCC, Petropolis, Brasil

2010 - 2010 Curso de curta duração em Planejamento de candidatos à novos fármacos. (Carga horária: 6h).
Sociedade Brasileira de Química, SBQ, Sao Paulo, Brasil

2010 - 2010 Curso de curta duração em Simulação de Proteínas de Biomembranas. (Carga horária: 6h).
Laboratório Nacional de Computação Científica, LNCC, Petropolis, Brasil

Producão

Produção bibliográfica

Artigos completos publicados em periódicos

1. doi **CANDIDO JÚNIOR, JOSÉ ROBERVAL**; ROMEIRO, LUIZ ANTONIO SOARES; MARINHO, EMMANUEL SILVA; MONTEIRO, NORBERTO DE KÁSSIO VIEIRA; DE LIMA-NETO, PEDRO
Antioxidant activity of eugenol and its acetyl and nitroderivatives: the role of quinone intermediates-a DFT approach of DPPH test. JOURNAL OF MOLECULAR MODELING (ONLINE). JCR, v.28, p.133 - , 2022.

2. doi PAULA, RUBEM S. F.; VIEIRA, RODRIGO S.; LUNA, F. MURILO T.; CAVALCANTE, CÉLIO L.; FIGUEREDO, IGOR M.; **CANDIDO, JOSÉ R.**; SILVA, LEONARDO P.; MARINHO, EMMANUEL S.; DE LIMA-NETO, PEDRO; LOMONACO, DIEGO; MAZZETTO, SELMA E.; RIOS, MARIA A. S.
A potential bio-antioxidant for mineral oil from cashew nutshell liquid: an experimental and theoretical approach. BRAZILIAN JOURNAL OF CHEMICAL ENGINEERING. JCR, v.37, p.369 - 381, 2020.

3. doi GOMES, AKENATON O.C.V.; BRITO, MARIA V.; MARQUES, RICARDO A.; LIMA, LEANDRO B.; CAVALCANTE, IGOR M.; VIEIRA, TELLIN D.N.; NUNES, FÁTIMA M.; LIMA, MARY A.S.; UCHÔA, DANIEL E.; LIMA, CRISTIANO S.; SILVA, GISELE S.; **CANDIDO-JÚNIOR, JOSÉ R.**; LIMA-NETO, PEDRO; MATTOS, MARCOS C.; DE OLIVEIRA, FRANCISCO L.S.; ZANATTA, GEANCARLO; OLIVEIRA, MARIA C.F.
Multi-step bioconversion of annonalide by Fusarium oxysporum f. sp. tracheiphilum and theoretical investigation of the decarboxylase pathway. JOURNAL OF MOLECULAR STRUCTURE. JCR, v.1204, p.127514 - , 2020.

4. doi NASCIMENTO, RAIMUNDO R. G.; PIMENTA, ANTÔNIA T. A.; LIMA NETO, PEDRO DE; **CÂNDIDO JÚNIOR, JOSÉ ROBERVAL**; COSTA-LOTUFO, LETÍCIA V.; FERREIRA, ELTHON G.; TINOCO, LUZINEIDE W.; BRAZ-FILHO, RAIMUNDO; SILVEIRA, EDILBERTO R.; LIMA, MARY A. S.
New Alkaloids from *Margaritopsis carrascoana* (Rubiaceae). Journal of the Brazilian Chemical Society (Impresso). JCR, v.26, p.1152 - 1159, 2015.

5. doi **Cândido-Júnior, J.R.**; Sales, F.A.M.; Costa, S.N.; de Lima-Neto, P.; Azevedo, D.L.; Caetano, E.W.S.; Albuquerque, E.L.; Freire, V.N.
Monoclinic and orthorhombic cysteine crystals are small gap insulators. Chemical Physics Letters (Print). JCR, v.512, p.208 - 210, 2011.

Trabalhos publicados em anais de eventos (resumo)

1. RODRIGUES, F. W. S.; **Cândido-Júnior, J.R.**
ADSORÇÃO DE ATRAZINA EM COMPLEXO POLIELETROLÍTICO DE QUITOSANA E ALGINATO: UMA ABORDAGEM COMPUTACIONAL In: VIII SEMIC – Semana de Iniciação Científica e Tecnológica do IFCE, 2019, QUIXADÁ.
Anais da VIII SEMIC IFCE. , 2019.

2. OLIVEIRA, B. M. M.; **Cândido-Júnior, J.R.**
ESTUDO COMPUTACIONAL DA ISONIAZIDA E DOS SEUS DERIVADOS: O USO DE UM PRÓ-FARMACO PARA TRATAMENTO DA TUBERCULOSE In: VIII SEMIC – Semana de Iniciação Científica e Tecnológica do IFCE, 2018, Quixadá.
Anais da VII SEMIC IFCE. , 2018.

3. BESSA, A. S.; **Cândido-Júnior, J.R.**; Mendonça, G. L. F.; Lima Neto, P.; Azevedo, D. L.; ROMEIRO, L. A. S.; FREIRE, V. N.
A Theoretical Study of the Role of Solvent on the Antioxidant Activity of Eugenol In: XVI Simpósio Brasileiro de Química Teórica – SBQT 2011, 2011, Ouro Preto.
Anais do XVI Simpósio Brasileiro de Química Teórica – SBQT 2011. , 2011.

4. **Cândido-Júnior, J.R.**; Mendonça, G. L. F.; Lima Neto, P.; Azevedo, D. L.; FREIRE, V. N.
Mircrosolvation of Cysteine – a pH-dependency Study of Thermodynamic and Vibrational Properties In: XVI Simpósio Brasileiro de Química Teórica – SBQT 2011, 2011, Ouro Preto.
Anais do XVI Simpósio Brasileiro de Química Teórica – SBQT 2011. , 2011.

Trabalhos publicados em anais de eventos (resumo expandido)

1. LIMA, D. M. V.; **Cândido-Júnior, J.R.**
DESENVOLVIMENTO DE AMINODERIVADOS DOCARDANOL: DESIGN COMPUTACIONAL, SÍNTESE E APLICAÇÃO COMO ANTIOXIDANTE EMBIODÍESEL DE SOJA In: VIII SEMIC – Semana de Iniciação Científica e Tecnológica do IFCE, 2018, Quixadá.
Anais da VII SEMIC IFCE. , 2018.

2. SILVA, A. C. C. Q.; **Cândido-Júnior, J.R.**
ESTUDO COMPUTACIONAL DO PERFIL ANTIOXIDANTE DO GINGEROL E SHOGAOL: IDENTIFICAÇÃO DO SÍTIO ATIVO E OS PAPÉIS DO SOLVENTE E ÍONS METÁLICOS In: VIII SEMIC – Semana de Iniciação Científica e Tecnológica do IFCE, 2018, Quixadá.
Anais da VII SEMIC IFCE. , 2018.

3. FIRMINO, E. S.; ARAUJO, V. P.; MELO, E. J.; **Cândido-Júnior, J.R.**; LIMA, A. E. O.
Adsorção de CO2 em estruturas metalorgânicas previsto por simulação de Monte Carlo In: 39ª Reunião Anual da Sociedade Brasileira de Química, 2016, Goiânia - GO.
Anais da 39ª Reunião Anual da Sociedade Brasileira de Química. , 2016.

4. MELO, E. J.; ARAUJO, V. P.; TEIXEIRA, J. B.; FIRMINO, E. S.; Lima Neto, P.; LIMA, A. E. O.; ROMEIRO, L. A. S.; **Cândido-Júnior, J.R.**
Estudo cinético teórico do perfil antioxidante do Eugenol, 4-alil-2-metóxi-6-nitrofenol e 5-alil-3-nitrobenzeno-1,2-diol In: 39ª Reunião Anual da Sociedade Brasileira de Química, 2016, Goiânia - GO.
Anais da 39ª Reunião Anual da Sociedade Brasileira de Química. , 2016.

5. ARAUJO, V. P.; MELO, E. J.; FIRMINO, E. S.; Lima Neto, P.; ROMEIRO, L. A. S.; **Cândido-Júnior, J.R.**
Estudo do perfil antioxidante de complexos de Fe(II)-isoeugenol utilizando métodos computacionais In: 39ª Reunião Anual da Sociedade Brasileira de Química, 2016, Goiânia - GO.
Anais da 39ª Reunião Anual da Sociedade Brasileira de Química. , 2016.

6. OLIVEIRA, S. J.; SILVA, M. M.; LAVOR, M. B.; OLIVEIRA, R. T.; OLIVEIRA, A. M.; FERREIRA, J. L.; ANDRADE, M. B.; **Cândido-Júnior, J.R.**; PINHEIRO, A. I.; SILVA, A. W.
A contextualização e o Ensino de Química: Concepções dos discentes da disciplina Físico-química do curso de Licenciatura em Química do Instituto Federal de Educação, ciências e Tecnologia (IFCE)-Campus Iguatu. In: 55° Congresso Brasileiro de Química, 2015, Goiânia-GO.
TRABALHOS APROVADOS E APRESENTADOS. , 2015.

7. FIRMINO, E. S.; LEMOS, A. R. P.; **Cândido-Júnior, J.R.**; LIMA, A. E. O.
Desenvolvimento do híbrido Cu-BTC/DEA e aplicação em adsorção de gases através de simulação molecular. In: 38ª Reunião Anual da Sociedade Brasileira de Química, 2015, Águas de Lindóia.
38ª Reunião Anual da Sociedade Brasileira de Química - Luz, Química, Ação.. , 2015.

8. MELO, E. J.; ARAUJO, V. P.; SILVA, A. W.; ROMEIRO, L. A. S.; LIMA NETO, PEDRO DE; LIMA, A. E. O.; **Cândido-Júnior, J.R.**
Estudo computacional da influência do grupo nitro na propriedade antioxidante do Eugenol. In: 38ª Reunião Anual da Sociedade Brasileira de Química, 2015, Águas de Lindóia-SP.
38ª Reunião Anual da Sociedade Brasileira de Química - Luz, Química, Ação.. , 2015.

9. LEMOS, A. R. P.; FIRMINO, E. S.; **Cândido-Júnior, J.R.**; LIMA, A. E. O.
Estudo teórico da adsorção CO2 na sílica mesoporosa MCM-41 modificada com alcanolaminas. In: 38ª Reunião Anual da Sociedade Brasileira de Química, 2015, Águas de Lindóia-SP.
38ª Reunião Anual da Sociedade Brasileira de Química - Luz, Química, Ação.. , 2015.

10. ARAUJO, V. P.; MELO, E. J.; SILVA, A. W.; LIMA NETO, PEDRO DE; ROMEIRO, L. A. S.; LIMA, A. E. O.; **Cândido-Júnior, J.R.**
Estudo Teórico do Perfil Antioxidante de Complexos de Fe(II) e Eugenol In: 38ª Reunião Anual da Sociedade Brasileira de Química, 2015, Águas de Lindóia-SP.
38ª Reunião Anual da Sociedade Brasileira de Química - Luz, Química, Ação.. , 2015.

11. BESSA, A. S.; **Cândido-Júnior, J.R.**; Mendonça, G. L. F.; Lima Neto, P.; ROMEIRO, L. A. S.
Estudo computacional da atividade antioxidante da N-vanilil-acetamida e da Zingerona In: 36ª Reunião Anual da Sociedade Brasileira de Química, 2013, Águas de Lindóia.
Anais da 36ª Reunião Anual da Sociedade Brasileira de Química. , 2013.

12. **Cândido-Júnior, J.R.**; BESSA, A. S.; Mendonça, G. L. F.; Lima Neto, P.; ROMEIRO, L. A. S.
Estudo computacional do mecanismo antioxidante do alfa-tocoferol, eugenol e isoeugenol In: 36ª Reunião Anual da Sociedade Brasileira de Química, 2013, Águas de Lindóia.
Anais da 36ª Reunião Anual da Sociedade Brasileira de Química. , 2013.

13. AMORIM, L.; Mendonça, G. L. F.; **Cândido-Júnior, J.R.**; Lima Neto, P.; Caetano, E.W.S.; FREIRE, V. N.
Adsorção lateral da LDOPA em nanotubos de carbono de parede simples: um estudo computacional. In: 35ª Reunião Anual da Sociedade Brasileira de Química, 2012, Águas de Lindóia.
Anais da 35ª Reunião Anual da Sociedade Brasileira de Química. , 2012.

14. Costa, S. N.; SALES, F. A.; **CÂNDIDO JÚNIOR, J. R.**; Lima Neto, P.; FREIRE, V. N.
Estudos comparativos dos espectros vibracionais experimentais e teóricos da treonina com variação do pH In: 34ª Reunião Anual da Sociedade Brasileira de Química, 2011, Florianópolis.
Anais da 34ª Reunião Anual da Sociedade Brasileira de Química. , 2011.

15. **Cândido-Júnior, J.R.**; Mendonça, G. L. F.; Lima Neto, P.; Correia, A. N.; FREIRE, V. N.; Azevedo, D. L.
O papel do hidrogênio tiólico nas propriedades estruturais, eletrônicas e ópticas do cristal ortorrômbico da cisteína In: 34ª Reunião Anual da Sociedade Brasileira de Química, 2011, Florianópolis.
Anais da 34ª Reunião Anual da Sociedade Brasileira de Química. , 2011.

16. **Cândido-Júnior, J.R.**; Mendonça, G. L. F.; Correia, A. N.; Lima Neto, P.; FREIRE, V. N.; Azevedo, D. L.; ROMEIRO, L. A. S.
Um estudo computacional do papel dos hidrogênio benzílico e fenólico no caráter antioxidante do eugenol In: 34ª Reunião Anual da Sociedade Brasileira de Química, 2011, Florianópolis.
Anais da 34ª Reunião Anual da Sociedade Brasileira de Química. , 2011.

17. **Cândido-Júnior, J.R.**; Mendonça, G. L. F.; Lima Neto, P.; Correia, A. N.; FREIRE, V. N.; Azevedo, D. L.
Cisteína Monoclínica: propriedades estruturais, eletrônicas e óptica. In: 33ª Reunião Anual da Sociedade Brasileira de Química, 2010, Águas de Lindóia.
Anais da 33ª Reunião Anual da Sociedade Brasileira de Química. , 2010.

18. **Cândido-Júnior, J.R.**; Penha, C. S.; Nascimento, J. M.; Lima Neto, P.; Oliveira, J. T.
Da cozinha para a sala de aula: atividade antioxidante de chás e temperos In: 33ª Reunião Anual da Sociedade Brasileira de Química, 2010, Águas de Lindóia.
Anais da 33ª Reunião Anual da Sociedade Brasileira de Química. , 2010.

19. Penha, C. S.; **Cândido-Júnior, J.R.**; Mendonça, G. L. F.; Lima Neto, P.; Correia, A. N.; FREIRE, V. N.
O papel dos hidrogênios benzílicos na capacidade antioxidante da N-Vanilil-Acetamida (NVA). In: 33ª Reunião Anual da Sociedade Brasileira de Química, 2010, Águas de Lindóia.
Anais da 33ª Reunião Anual da Sociedade Brasileira de Química. , 2010.

20. Mendonça, G. L. F.; GOMES, R. A.; **Cândido-Júnior, J.R.**; FREIRE, V. N.; FARIAS, A. M.; Azevedo, D. L.; Correia, A. N.; Lima Neto, P.
Serina, cisteína e metionina como inibidores de corrosão do aço carbono em meio ácido. In: 33ª Reunião Anual da Sociedade Brasileira de Química, 2010, Águas de Lindóia.
Anais da 33ª Reunião Anual da Sociedade Brasileira de Química. , 2010.

21. **Cândido-Júnior, J.R.**; ROMEIRO, L. A. S.
Determinação de Distâncias Entre Grupos Funcionais em Moléculas Bidimensionais em Excel: A Matemática Sob um Olhar Químico In: 32ª Reunião Anual da Sociedade Brasileira de Química, 2009, Fortaleza.
Anais da 32ª Reunião Anual da Sociedade Brasileira de Química. , 2009.

Produção técnica

Demais produções técnicas

1. CÂNDIDO JÚNIOR, J. R.; SANTOS, S. J. M.; CAVALCANTE, R. F.
Apostila de Química do Projeto Novo Vestibular, 2008. (Desenvolvimento de material didático ou instrucional)

2. CÂNDIDO JÚNIOR, J. R.; ALMEIDA, R. F.
Aula Experimental de Química, 2008. (Extensão, Curso de curta duração ministrado)

3. **CÂNDIDO JÚNIOR, J. R.**
Curso de Férias de Específica de Química, 2008. (Extensão, Curso de curta duração ministrado)

4. CÂNDIDO JÚNIOR, J. R.; SANTOS, S. J. M.
Química do Meio Ambiente, 2008. (Extensão, Curso de curta duração ministrado)

Orientações e Supervisões

Orientações e supervisões

Orientações e supervisões concluídas

Trabalhos de conclusão de curso de graduação

1. Francisco Wallis Sousa Rodrigues. **Estudo Computacional da Adsorção de Atrazina em Quitosana: Influência de íons SO_4^{2-}, $Cℓ^-$, Fe^{3+}, Fe^{2+} e Zn^{2+}.**. 2022. Curso (Química) - Instituto Federal do Ceará - Reitoria
2. Ana Clara Correia Queiroz da Silva. **ANÁLISE DA ATIVIDADE ANTIOXIDANTE DO GINGEROL, SHOGAOL E ZINGERONA UMA ABORDAGEM COMPUTACIONAL**. 2021. Curso (Química) - Instituto Federal do Ceará - Reitoria
3. Dhagilla Maria Viana Lima. **Desenvolvimento de derivados de cardanol e cardol: design computacional e aplicação como antioxidante em biodiesel de soja**. 2019. Curso (Licenciatura em Química) - Instituto Federal do Ceará
4. Eduardo da Silva Firmino. **Estudo computacional adsorção de CO2 na MOF Cu-BTC**. 2017. Curso (Licenciatura em Química) - Instituto Federal de Educação, Ciência e Tecnologia - Campus Iguatu
5. Adelaide de Souza Bessa. **CONSCIENTIZAÇÃO DO USO DE MEDICAMENTOS: UMA ABORDAGEM AOS OLHOS DA QUÍMICA PARA O ENSINO MÉDIO**. 2015. Curso (Química) - Universidade Federal do Ceará
6. Antônio Weslley da Silva. **ESTUDO COMPUTACIONAL DA ATIVIDADE ANTIOXIDANTE DO BHT E DO CARDANOL: PLANEJAMENTO REACIONAL DE ANTIOXIDANTES DERIVADOS DO CARDANOL APLICADOS A BIOCOMBUSTÍVEIS**. 2015. Curso (Química) - Instituto Federal do Ceará - Reitoria
7. Carlos André da Silva. **Uso da tecnologia no colégio Pólos de Iguatu : um estudo sobre a inclusão dos novos recursos tecnológicos, pelos docentes, no processo ensino-aprendizagem**. 2015. Curso (Química) - Instituto Federal do Ceará - Reitoria
8. Francisca Erisvânia da Silva Barroso. **O Uso de aulas práticas e multimídias para a contextualização do ensino da química e uma aprendizagem significativa no 1º ano do ensino médio**. 2014. Curso (Química) - Instituto Federal do Ceará - Reitoria
9. Juliana Borges Trigueiro de Souza. **Sistema de liberação controlada de fármacos à base de quitosana : estudo computacional do efeito do pH e da solubilidade sobre a matriz polimérica e o fármaco diclofenaco de sódio**. 2014. Curso (Química) - Instituto Federal do Ceará - Reitoria

Iniciação científica

1. DJONATA BRUNO MACEDO SILVA. **Estudo Computacional de Metalocomplexos Derivados da Isoniazida: Relação Estrutura-Atividade Aplicada no Design de Fármacos Antituberculose.**. 2020. Iniciação científica (Química) - Instituto Federal do Ceará - Reitoria
2. SABRINA LORRAINE FREITAS MENEZES. **Estudo Computacional do Perfil Antioxidante e Hepatotóxico de Compostos Análogos da Capsaicina**. 2020. Iniciação científica - Instituto Federal do Ceará
3. Dhagilla Maria Viana Lima. **DESENVOLVIMENTO DE AMINODERIVADOS DOCARDANOL: DESIGN COMPUTACIONAL, SÍNTESE E APLICAÇÃO COMO ANTIOXIDANTE EMBIODÍESEL DE SOJA**. 2018. Iniciação científica (Licenciatura em Química) - Instituto Federal do Ceará
4. Ana Clara Correia Queiroz da Silva. **ESTUDO COMPUTACIONAL DO PERFILANTIOXIDANTE DO GINGEROL E SHOGAOL: IDENTIFICAÇÃO DO SÍTIO ATIVO E OS PAPÉIS DOSOLVENTE E ÍONS METÁLICOS**. 2018. Iniciação científica (Licenciatura em Química) - Instituto Federal do Ceará
5. Virna Pereira de Araújo. **Estudo computacional do perfil antioxidante do eugenol e isoeugenol: identificação do sítio ativo e os papéis do solvente e íons metálicos.**. 2014. Iniciação científica (Química) - Instituto Federal do Ceará - Reitoria

Orientações e supervisões em andamento

Trabalhos de conclusão de curso de graduação

1. Mikaely Silva Lima. **RPG e o Ensino de Química: Criação e aplicação de jogo RPG digital como ferramenta metodológica para o ensino de química ambiental na EEMTI Assis Bezerra no Município de Quixeramobim - CE**. 2021. Curso (Química) - Instituto Federal do Ceará - Reitoria

Página gerada pelo sistema Currículo Lattes em 06/06/2022 às 22:12:40.

APPENDIX B - Supplementary Material – Chapter 1

Fukui functions

$$f(\boldsymbol{r}) = \left[\frac{\partial \rho(r)}{\partial N}\right]_{\upsilon(r)} \quad (20)$$

$$f^{+}(\boldsymbol{r}) = \left[\frac{\partial \rho(\boldsymbol{r})}{\partial N}\right]^{+}_{\upsilon(\boldsymbol{r})} \approx \rho_{N+1(\boldsymbol{r})} - \rho_{N(\boldsymbol{r})} \quad (21)$$

$$f^{-}(\boldsymbol{r}) = \left[\frac{\partial \rho(\boldsymbol{r})}{\partial N}\right]^{-}_{\upsilon(\boldsymbol{r})} \approx \rho_{N(\boldsymbol{r})} - \rho_{N-1(\boldsymbol{r})} \quad (22)$$

$$f^{\circ}(r) = \left[\frac{\partial \rho(r)}{\partial N}\right]^{\circ}_{\upsilon(r)} \approx \rho_{N+1(r)} - \rho_{N-1(r)} \quad (23)$$

Hirshfeld charges

$$f_k^{+}(\boldsymbol{r}) = [q_k(N+1) - q_k(N)] \quad (24)$$

$$f_k^{-}(\boldsymbol{r}) = [q_k(N) - q_k(N-1)] \quad (25)$$

$$f_k{}^{\circ}(r) = \frac{1}{2}[q_k(N+1) - q_k(N-1)] \quad (26)$$

Table S1 - Enthalpies (kcal.mol^{-1}) of radicals and BDE calculations for the cardanol monoene molecule

Molecule	Radical enthalpy	H˙ enthalpy	Neutral enthalpy	BDE
Saturated	-561876.679	-311.370	-562269.380	81.331
Monoene	-561119.253		-561511.944	81.321
Diene	-560363.795		-560756.539	81.373
Triene	-559604.958		-559997.689	81.361

Table S2 - Values of the Fukui function considering Hirshfelf charges for individual atoms of the cardanol monoene

Atom number	*f*+ value	*f*– value	Δ*f* value	*f*° value
0 C	0.039	**0.079**	**-0.041**	**0.059**
1 C	**0.097**	**0.038**	**0.059**	**0.068**
2 C	**0.106**	**0.088**	0.018	**0.097**
3 C	**0.089**	**0.059**	0.029	**0.074**
4 C	**0.043**	**0.116**	**-0.072**	**0.080**
5 C	**0.100**	**0.046**	**0.054**	**0.073**
6 O	0.028	**0.119**	**-0.091**	**0.073**

7 H	**0.051**	**0.043**	0.008	**0.047**
8 H	**0.047**	0.033	0.015	**0.040**
9 C	0.019	0.010	0.009	0.014
10 H	0.034	**0.047**	-0.013	**0.040**
11 H	**0.052**	0.036	0.017	**0.044**
12 H	0.024	**0.040**	-0.016	0.032
13 H	0.026	0.021	0.006	0.024
14 C	0.009	0.011	-0.002	0.010
15 H	0.024	0.018	0.006	0.021
16 H	0.009	0.004	0.005	0.007
17 H	0.008	0.006	0.002	0.007
18 C	0.006	0.009	-0.003	0.007
19 H	0.010	0.007	0.003	0.009
20 C	0.002	0.006	-0.005	0.004
21 H	0.009	0.007	0.002	0.008
22 H	0.005	0.003	0.002	0.004
23 H	0.005	0.003	0.002	0.004
24 C	0.001	0.006	-0.004	0.004
25 H	0.004	0.004	0.001	0.004
26 C	0.000	0.004	-0.004	0.002
27 H	0.005	0.003	0.001	0.004
28 H	0.003	0.001	0.002	0.002
29 H	0.004	0.001	0.003	0.003
30 C	0.001	0.005	-0.005	0.003
31 H	0.004	0.003	0.001	0.003
32 C	-0.001	0.005	-0.006	0.002
33 H	0.003	0.002	0.000	0.002
34 C	0.004	0.011	-0.008	0.007
35 C	0.001	0.006	-0.005	0.003
36 H	0.002	0.007	-0.005	0.005
37 H	0.004	0.004	-0.001	0.004
38 H	0.001	0.001	0.000	0.001
39 C	0.004	0.005	-0.001	0.004
40 H	0.008	0.003	0.005	0.006

41 H	0.007	0.003	0.003	0.005
42 C	0.005	0.007	-0.002	0.006
43 H	0.009	0.002	0.007	0.006
44 C	0.005	0.008	-0.003	0.006
45 H	0.008	0.002	0.006	0.005
46 H	0.010	0.005	0.005	0.008
47 H	0.009	0.003	0.006	0.006
48 C	0.004	0.009	-0.005	0.006
49 H	0.009	0.013	-0.004	0.011
50 C	0.007	0.004	0.003	0.005
51 H	0.008	0.003	0.005	0.006
52 H	0.011	0.007	0.004	0.009
53 H	0.008	0.003	0.005	0.005
54 H	0.006	0.002	0.003	0.004
55 H	0.005	0.009	-0.004	0.007

Figure S1 – Typical DSC Curve with Exothermic event and Thermal parameters

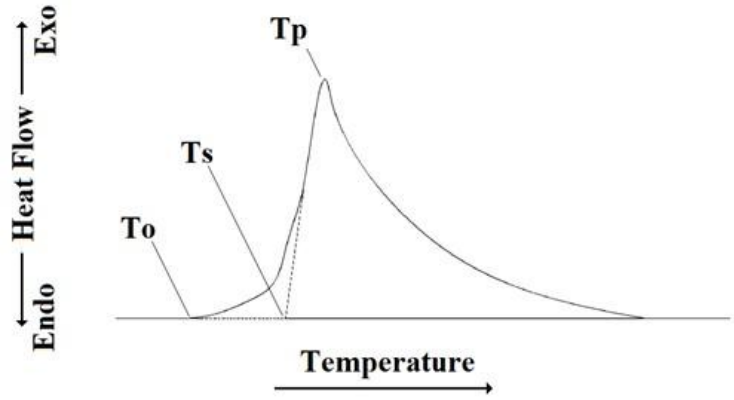

Figure S2 – Idealized DSC Curve: Borchardt and Daniels method (ASTM E2041-18)

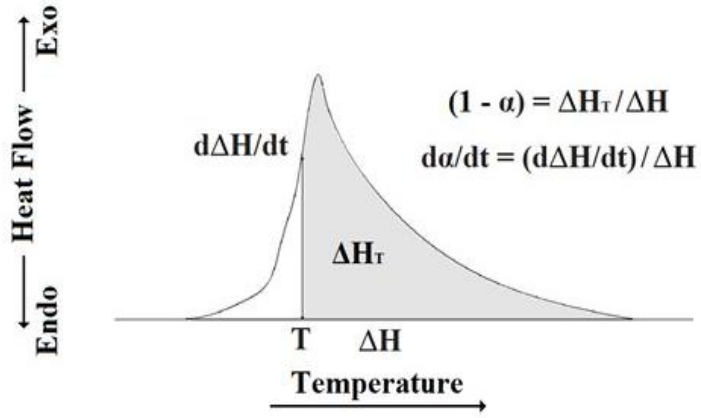

Figure S3 - Cardanol monoene - numbered atoms

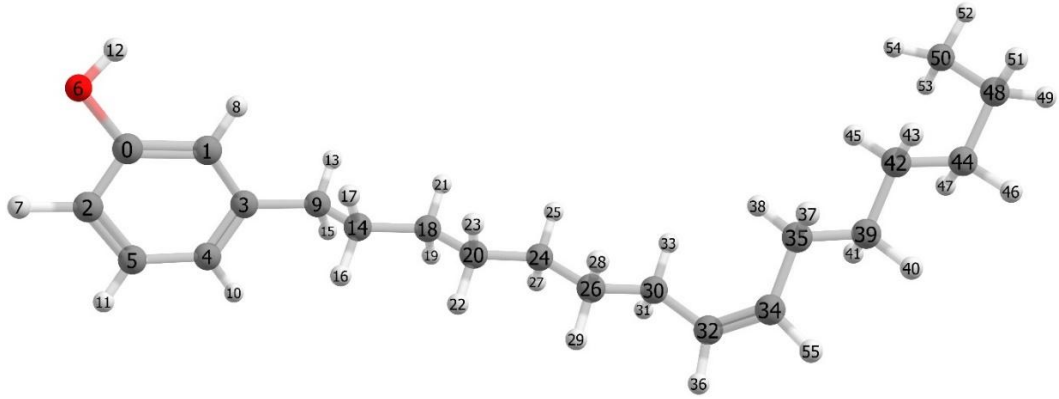

APPENDIX C - Supplementary Material – Chapter 2

Supplementary Information The online version contains supplementary material available at https://doi.org/10.1007/s00894-022-05120-z .

ANNEX – LICENCE TO PUBLISH – SPRINGER NATURE

Licence to Publish

SPRINGER NATURE

Licensee:	Springer-Verlag GmbH, DE	(the 'Licensee')
Journal Name:	Journal of Molecular Modeling	(the 'Journal')
Manuscript Number:	JMMO-D-21-01001R1	
Proposed Title of Article:	Antioxidant activity of eugenol and its acetyl and nitroderivatives: the role of quinone intermediates—a DFT approach of DPPH test	(the 'Article')
Author(s) [Please list all named Authors]:	José Roberval Candido Júnior, Luiz Antonio Soares Romeiro, Emmanuel Silva Marinho, Norberto de Kássio Viera Monteiro, Pedro de Lima-Neto	(the 'Author')
Corresponding Author Name:	José Roberval Candido Júnior	

1 Grant of Rights

a) For good and valuable consideration, the Author hereby grants to the Licensee the perpetual, exclusive, world-wide, assignable, sublicensable and unlimited right to: publish, reproduce, copy, distribute, communicate, display publicly, sell, rent and/ or otherwise make available the article identified above, including any supplementary information and graphic elements therein (e.g. illustrations, charts, moving images) (the "Article") in any language, in any versions or editions in any and all forms and/or media of expression (including without limitation in connection with any and all end-user devices), whether now known or developed in the future. Without limitation, the above grant includes: (i) the right to edit, alter, adapt, adjust and prepare derivative works; (ii) all advertising and marketing rights including without limitation in relation to social media; (iii) rights for any training, educational and/or instructional purposes; (iv) the right to add and/or remove links or combinations with other media/works; and (v) the right to create, use and/or license and/or sublicense content data or metadata of any kind in relation to the Article (including abstracts and summaries) without restriction. The above rights are granted in relation to the Article as a whole or any part and with or in relation to any other works.

b) Without limiting the rights granted above, Licensee is granted the rights to use the Article for the purposes of analysis, testing, and development of publishing- and research-related workflows, systems, products, projects, and services; to confidentially share the Article with select third parties to do the same; and to retain and store the Article and any associated correspondence/files/forms to maintain the historical record, and to facilitate research integrity investigations. The grant of rights set forth in this clause (b) is irrevocable.

c) The Licensee will have the right, but not the obligation, to exercise any or all of the rights granted herein. If the Licensee elects not to publish the Article for any reason, all publishing rights under this Agreement as set forth in clause 1.a) above will revert to the Author.

2 Copyright

Ownership of copyright in the Article will be vested in the name of the Author. When reproducing the Article or extracts from it, the Author will acknowledge and reference first publication in the Journal.

3 Use of Article Versions

a) For purposes of this Agreement: (i) references to the "Article" include all versions of the Article; (ii) "Submitted Manuscript" means the version of the Article as first submitted by the Author; (iii) "Accepted Manuscript" means the version of the Article accepted for publication, but prior to copy-editing and typesetting; and (iv) "Version of Record" means the version of the Article published by the Licensee, after copy-editing and typesetting. Rights to all versions of the Manuscript are granted on an exclusive basis, except for the Submitted Manuscript, to which rights are granted on a non-exclusive basis.

b) The Author may make the Submitted Manuscript available at any time and under any terms (including, but not limited to, under a CC BY licence), at the Author's discretion. Once the Article has been published, the Author will include an acknowledgement and provide a link to the Version of Record on the publisher's website: "This preprint has not undergone peer review (when applicable) or any post-submission improvements or corrections. The Version of Record of this article is published in [insert journal title], and is available online at https://doi.org/[insert DOI]".

c) The Licensee grants to the Author (i) the right to make the Accepted Manuscript available on their own personal, self-maintained website immediately on acceptance, (ii) the right to make the Accepted Manuscript available for public release on any of the following twelve (12) months after first publication (the "Embargo Period"): their employer's internal website; their institutional and/or

funder repositories. Accepted Manuscripts may be deposited in such repositories immediately upon acceptance, provided they are not made publicly available until after the Embargo Period.

The rights granted to the Author with respect to the Accepted Manuscript are subject to the conditions that (i) the Accepted Manuscript is not enhanced or substantially reformatted by the Author or any third party, and (ii) the Author includes on the Accepted Manuscript an acknowledgement in the following form, together with a link to the published version on the publisher's website: "This version of the article has been accepted for publication, after peer review (when applicable) but is not the Version of Record and does not reflect post-acceptance improvements, or any corrections. The Version of Record is available online at: http://dx.doi.org/[insert DOI]. Use of this Accepted Version is subject to the publisher's Accepted Manuscript terms of use https://www.springernature.com/gp/open-research/policies/accepted-manuscript-terms". Under no circumstances may an Accepted Manuscript be shared or distributed under a Creative Commons or other form of open access licence.

d) The Licensee grants to the Author the following non-exclusive rights to the Version of Record, provided that, when reproducing the Version of Record or extracts from it, the Author acknowledges and references first publication in the Journal according to current citation standards. As a minimum, the acknowledgement must state: "First published in [Journal name, volume, page number, year] by Springer Nature".

   i. to reuse graphic elements created by the Author and contained in the Article, in presentations and other works created by them;

   ii. the Author and any academic institution where they work at the time may reproduce the Article for the purpose of course teaching (but not for inclusion in course pack material for onward sale by libraries and institutions);

   iii. to reuse the Version of Record or any part in a thesis written by the same Author, and to make a copy of that thesis available in a repository of the Author(s)' awarding academic institution, or other repository required by the awarding academic institution. An acknowledgement should be included in the citation: "Reproduced with permission from Springer Nature"; and

   iv. to reproduce, or to allow a third party to reproduce the Article, in whole or in part, in any other type of work (other than thesis) written by the Author for distribution by a publisher after an embargo period of 12 months.

4 Warranties & Representations

Author warrants and represents that:

a)

   i. the Author is the sole copyright owner or has been authorised by any additional copyright owner(s) to grant the rights defined in clause 1,

   ii. the Article does not infringe any intellectual property rights (including without limitation copyright, database rights or trade mark rights) or other third party rights and no licence from or payments to a third party are required to publish the Article,

   iii. the Article has not been previously published or licensed, nor has the Author committed to licensing any version of the Article under a licence inconsistent with the terms of this Agreement,

   iv. if the Article contains materials from other sources (e.g. illustrations, tables, text quotations), Author has obtained written permissions to the extent necessary from the copyright holder(s), to license to the Licensee the same rights as set out in clause 1 but on a non-exclusive basis and without the right to use any graphic elements on a stand-alone basis and has cited any such materials correctly;

b) all of the facts contained in the Article are according to the current body of research true and accurate;

c) nothing in the Article is obscene, defamatory, violates any right of privacy or publicity, infringes any other human, personal or other rights of any person or entity or is otherwise unlawful and that informed consent to publish has been obtained for any research participants;

d) nothing in the Article infringes any duty of confidentiality owed to any third party or violates any contract, express or implied, of the Author;

e) all institutional, governmental, and/or other approvals which may be required in connection with the research reflected in the Article have been obtained and continue in effect;

f) all statements and declarations made by the Author in connection with the Article are true and correct; and

g) the signatory who has signed this agreement has full right, power and authority to enter into this agreement on behalf of all of the Authors.

5 Cooperation

a) The Author will cooperate fully with the Licensee in relation to any legal action that might arise from the publication of the Article, and the Author will give the Licensee access at reasonable times to any relevant accounts, documents and records within the power or control of the Author. The Author agrees that any Licensee affiliate through which the Licensee exercises any rights or performs any obligations under this Agreement is intended to have the benefit of and will have the right to enforce the terms of this Agreement.

b) Author authorises the Licensee to take such steps as it considers necessary at its own expense in the Author's name(s) and on their behalf if the Licensee believes that a third party is infringing or is likely to infringe copyright in the Article including but not limited to initiating legal proceedings.

6 Author List

Changes of authorship, including, but not limited to, changes in the corresponding author or the sequence of authors, are not permitted after acceptance of a manuscript.

7 Post Publication Actions

The Author agrees that the Licensee may remove or retract the Article or publish a correction or other notice in relation to the Article if the Licensee determines that such actions are appropriate from an editorial, research integrity, or legal perspective.

8 Controlling Terms

The terms of this Agreement will supersede any other terms that the Author or any third party may assert apply to any version of the Article.

9 Governing Law

This Agreement will be governed by, and construed in accordance with, the laws of the Federal Republic of Germany. The courts of Berlin, Germany will have exclusive jurisdiction.

Signed for and on behalf of the Author(s)
Corresponding Author: José Roberval Candido Júnior
Email: junior.candido@ifce.edu.br
IP Address: 177.37.132.97

Time Stamp: 2022-04-25 10:41:09

ANNEX – PERMISSION TO REUSE SPRINGER NATURE CONTENT

Springer

Permissions

Get permission to reuse Springer Nature content

Springer Nature is partnered with the Copyright Clearance Center to meet our customers' licensing and permissions needs.

Copyright Clearance Center's RightsLink® service makes it faster and easier to secure permission for the reuse of Springer Nature content to be published, for example, in a journal/magazine, book/textbook, coursepack, thesis/dissertation, annual report, newspaper, training materials, presentation/slide kit, promotional material, etc.

Simply visit SpringerLink and locate the desired content;

Go to the article or chapter page you wish to reuse content from. (Note: permissions are granted on the article or chapter level, not on the book or journal level). Scroll to the botton of the page, or locate via the side bar, the "Reprints and Permissions" link at the end of the chapter or article.

Select the way you would like to reuse the content;

Complete the form with details on your intended reuse. Please be as complete and specific as possible ao as not to delay your permission request;

Create an account if you haven't already. A RightsLink account is different than a SpringerLink account, and is necessary to receive a licence regardless of the permission fee. You will receive your licence via the email attached to your RightsLink receipt;

Accept the terms and conditions and you're done!

For questions about using the RightsLink service, please contact Customer Support at Copyright Clearance Center via phone +1-855-239-3415 or +1-978-646-2777 or email springernaturesupport@copyright.com.

How to obtain permission to reuse Springer Nature content not available online on SpringerLink

Requests for permission to reuse content (e.g. figure or table, abstract, text excerpts) from Springer Nature publications currently not available online must be submitted in writing. Please be as detailed and specific as possible about what, where, how much, and why you wish to reuse the content.

Your contacts to obtain permission for the reuse of material from:

- books: bookpermissions@springernature.com
- journals: journalpermissions@springernature.com

Author reuse

Please check the Copyright Transfer Statement (CTS) or Licence to Publish (LTP) that you have signed with Springer Nature to find further information about the reuse of your content.

Authors have the right to reuse their article's Version of Record, in whole or in part, in their own thesis. Additionally, they may reproduce and make available their thesis, including Springer Nature content, as required by their awarding academic institution. Authors must properly cite the published article in their thesis according to current citation standards.
Material from: 'AUTHOR, TITLE, JOURNAL TITLE, published [YEAR], [publisher - as it appears on our copyright page]'

If you are any doubt about whether your intended re-use is covered, please contact journalpermissions@springernature.com for confirmation.

Self-Archiving

- Journal authors retain the right to self-archive the final accepted version of their manuscript. Please see our self-archiving policy for full details: